Natural genetic variation and underlying ecophysiological factors in photosynthetic induction in rice

2023

Kazuki Taniyoshi

Contents

Summary

Crop productivity is needed to be increased with growing world population. Leaf photosynthesis is a fundamental process in plant biomass production and regarded as an important trait for enhancement of crop productivity. The majority of previous researches have focused on light-saturating CO_2 assimilation rate (A_{sat}) for improvement of leaf photosynthesis. Plants grown under the field environment are subjected to changing environmental factors. These variable environmental factors influence leaf photosynthesis, and thus plants cannot always perform their maximum photosynthetic activity. Especially, the light intensity in the crop canopy fluctuates drastically due to cloud movement, self-shading or wind, which has a great effect to leaf photosynthesis. When light intensity increases stepwise from low to high, CO_2 assimilation rate (A) rises gradually and it takes a significant time to approach a new steady state. This process is termed as photosynthetic induction and the lag leads to loss of potential carbon gain. Therefore, improvements in both of A_{sat} and photosynthetic induction would contribute to enhancement of carbon gain and ultimately crop productivity under the field environment. Exploiting the natural genetic variation among untapped genetic resources can contribute to developing effective breeding programs for photosynthetic induction. Based on the above, I aimed to clarify the natural genetic variation, room of improvement, and related ecophysiological factors in photosynthetic induction in rice.

At first, I demonstrated the natural genetic variation in photosynthetic induction in World Rice Core Collection (WRC) and two reference cultivars; Koshihikari and Takanari. WRC is a powerful tool to investigate the potential variation of genetic traits in rice. Koshihikari is a popular rice cultivar and Takanari is a high-yielding rice cultivar in Japan. To quantify the speed of photosynthetic induction, I calculated the cumulative CO_2 fixation during the first 10 minutes of the photosynthetic induction (CCF_{10}). An *indica* genotype, ARC 11094, showed the

highest value of CCF_{10}, which was approximately 4.0 and 1.2 fold greater than those of Koshihikari and Takanari, respectively. This suggests that there is a large natural genetic variation and substantial room of improvement in photosynthetic induction in rice. The genotypes with a rapid photosynthetic induction showed efficient CO_2 diffusion from the atmosphere into the carboxylation site and CO_2 fixation in the carboxylation site during photosynthetic induction. In addition, the underlying mechanisms were thought to be different between photosynthetic induction and A_{sat} because there is no significant correlation between CCF_{10} and A_{sat}. Besides, *temperate japonica* showed low CCF_{10}, which implies that *temperate japonica* would have a slower photosynthetic induction compared with *indica* or *tropical japonica*.

Next, I analyzed the underlying physiological factors on the rapid photosynthetic induction in ARC 11094, comparing with Koshihikari and Takanari. I confirmed the reproducibility of the rapid photosynthetic induction, and efficient CO_2 diffusion and CO_2 fixation in ARC 11094 and Takanari. The dynamics of the maximum carboxylation rate (V_{Cmax}), ribulose 1,5-bisphosphate carboxylase/oxygenase (Rubisco) contents and chlorophyll contents were evaluated as related traits to CO_2 fixation, but there was no apparent difference in these traits between three rice genotypes. Stomatal morphology, root activity and stomatal behaviour under water stress were evaluated as related traits to CO_2 diffusion. Consequently, the efficient CO_2 diffusion in Takanari was attributable to its high stomatal density, small guard cell length and great root activity due to extensive root mass. The efficient CO_2 diffusion in ARC 11094 was attributable to its high stomatal conductance per stoma and stomatal opening in leaves with insufficient water (i.e., anisohydric stomatal behaviour).

Subsequently, I measured photosynthetic induction in Rice Core Collection of Japanese Landraces (JRC), and investigated the difference between rice subspecies; *indica*,

temperate japonica and *tropical japonica*, from the results in WRC and JRC. A_{sat} was not different between rice subspecies, whereas CCF_{10} was significantly lower in *temperate japonica* than in *indica* and *tropical japonica*. The slow photosynthetic induction in *temperate japonica* resulted in less carbon gain, but its water loss was also less, compared with *indica* or *tropical japonica*. The rice genotypes in *temperate japonica* may put importance to reduce water loss rather than to increase carbon gain under fluctuating light conditions. The speed of photosynthetic induction may be related to the ecological significance or genetic bottleneck for the plant adaptation to growth environments.

Additionally, I evaluated photosynthetic induction in 166 *temperate japonica* rice cultivars developed in Japan, and its relationship with release year of the cultivars. Photosynthetic induction have not been accelerated, or rather deaccelerated gradually during the rice modern breeding in Japan since 1800s. Besides, Koshihikari would have inherited the slow photosynthetic induction from its ancestors; Shinriki, Aikoku, Ginbouzu or Kyoto-asahi, which were widely cultivated in Japan during its Meiji to Taisho Era and used as parents of popular cultivars. These imply that the factors related to the slow photosynthetic induction have been inherited from Shinriki, Aikoku, Ginbouzu or Kyoto-asahi to Koshihikari and its relatives, and spread throughout Japan so far.

Through the present study, I elucidated the large natural genetic variation and substantial room of improvement in photosynthetic induction in rice. Subsequently, I determined the characteristics underlying on the rapid photosynthetic induction and that these were different depending on each rice genotype. In addition, skewed distribution of slow photosynthetic induction in *temperate japonica* implies that the ecological significance are related to the speed of photosynthetic induction. In near future, the causal quantitative trait loci (QTL) or gene will be revealed. Further and comprehensive understanding of leaf

photosynthesis in response to fluctuating light conditions through these analysis will be required to optimize the photosynthetic dynamics under field environments for enhancement of crop productivity.

Chapter 1

General Introduction

1.1 Attempts for improvement of rice productivity

The world population is 7.9 billion in 2021 and estimated to reach 9.7 billion in 2050 (United Nations, 2022). In order to feed increasing population, crop production is needed to be enhanced. Rice is a staple cereal in the most part of Asia and Africa, and the rice production in Asia and Africa is approximately 94% (7.1×10^8 t year^{-1}) of world rice production in 2020 (FAO, 2022). Rice yield increased 0.67% per year from 2010 (4.3 t ha^{-1}) to 2020 (4.6 t ha^{-1}) (FAO, 2022) although population growth rate in Asia or Africa from 2020 to 2050 is estimated to be 1.0% per year (United Nations, 2018). Therefore, further increase in rice production, notably rice yield per unit area, has to be achieved within the near future.

One of the limiting factors in crop productivity is the yield potential, which is termed as 'the yield of a cultivar when grown in environments to which it is adapted, with nutrients and water non-limiting, and with pests, diseases, weeds, lodging and other stresses effectively controlled' (Evans & Fischer, 1999). Yield potential is determined by 1) the total incident solar radiation across the growing season, 2) the efficiency with which that radiation is intercepted by the crop (light interception efficiency), 3) the efficiency with which the intercepted radiation is converted into biomass (conversion efficiency or radiation use efficiency) and 4) the efficiency with biomass is partitioned into the harvested product (partitioning efficiency or harvest index) (Monteith, 1977; Long *et al*., 2006; Zhu *et al*., 2010). The management of the total incident solar radiation is very difficult because it largely depends on the climate and/or topography. The enhancement of rice productivity has mainly been resulted from the

improvement of plant structure related to light interception efficiency and/or harvest index. A steep increase in the yields of wheat or rice during the 1960s, i.e. Green Revolution, was led by the genetic mutation to the gibberellin response modulators (Peng *et al*., 1999; Sasaki *et al*., 2002). These mutants show dwarf plant structure and higher harvest index, which enables the plant to resist lodging and thus allows higher fertilizer application (Yoshida, 1972; Hedden, 2003; Peng & Khushg, 2003). After the Green Revolution, hybrid rice has been developed. Hybrid rice cultivars have characteristics of a rapid growth rate, great biomass and very large sink (Laza *et al*., 2001; Peng & Khushg, 2003; Yang *et al*., 2007; Yuan, 2017). Following dwarf or hybrid rice cultivars, the rice cultivars with erect panicle became focused as a new ideotype in Northeast China. Erect panicle rice shows efficient light interception throughout canopy, large grain number per panicle, great grain filling and high harvest index (Wang *et al*., 2009; Li *et al*., 2010; Tang *et al*., 2017; Hirooka *et al*., 2018). The light interception efficiency and partitioning efficiency have been approached the upper limit through these attempts and there seems to be few room for further improvement. On the other hand, the conversion efficiency from solar energy into biomass have been far from the theoretical maximum efficiency and remained a challenge. Leaf photosynthesis is the one of the key targets for improvement of the conversion efficiency and crop productivity (Long *et al*., 2006; Zhu *et al*., 2010).

1.2 Photosynthetic dynamics under field environments

Photosynthetic capacity (the CO_2 assimilation rate under optimized condition, e.g. light intensity, ambient CO_2 concentration or relative humidity) has large natural genetic variation in major crops: rice (Kanemura *et al*., 2007; Jahn *et al*., 2011; Qu *et al*., 2017), soybean (Sakoda *et al*. 2016), wheat (Carmo-Silva *et al*., 2017) and maize (Choquette *et al*., 2019). Related physiological and/or genetical factors have been determined and these effects on

photosynthetic capacity and/or crop productivity have been evaluated (Adachi *et al*., 2011, 2014, 2017a, 2019a; Takai *et al*., 2013; Hirotsu *et al*., 2017; Sakoda *et al*. 2020a; Wang *et al*., 2020; Shamim *et al*., 2022). Significant progress has been made in manipulation of photosynthetic capacity by utilizing genetic resources. Parallelly, we should consider that the crops do not always perform their photosynthetic capacity under field environment because leaf photosynthesis is affected by various abiotic factors.

Environment surrounding the crops grown under the field consistently vary and is not optimized for photosynthetic capacity. Especially, light intensity subjected by leaves fluctuates every seconds or minutes due to cloud cover, wind or self-shading (Reifsnyder *et al*., 1971; Norman *et al*., 1971; Burgess *et al*. 2016), which has great effects on leaf photosynthesis (Slattery *et al*. 2018; Wang *et al*., 2020). When light intensity increases suddenly, the CO_2 assimilation rate (A) rises gradually and approaches a new steady state. This process is termed as photosynthetic induction (Chazdon & Pearcy, 1986) and takes significant time to complete (Pearcy, 1990; Yamori, 2016). Taylor & Long (2017) and Tanaka *et al*. (2019) estimated photosynthetic induction could loss 21% of a potential daily CO_2 assimilation under fluctuating light conditions. Therefore, both of photosynthetic capacity and induction are important to increase amounts of carbon gain in crops under field environment. Previous studies showed that improvement of photosynthetic response to fluctuating light resulted in enhancement of crop productivity under field environment using transgenic plants (Kromdijk *et al*. 2016; De Souza *et al*. 2022). Differences of photosynthetic induction between interspecies (Kursar & Coley, 1993; Naumburg & Ellsworth, 2000; Urban *et al*., 2007; Tomimatsu & Tang, 2012; McAusland *et al*., 2016; Wachendorf & Küppers, 2017a; Meinzer *et al*., 2017; Xiong *et al*., 2018, Zhang *et al*., 2019; Acevedo-Siaca *et al*., 2021a; Sakoda *et al*., 2021, 2022a; Zhang *et al*., 2022) or intraspecies (Qu *et al*., 2016; Soleh *et al*., 2016, 2017; Faralli *et al*., 2019a; Adachi *et al*, 2019b;

Salter *et al*., 2019, 2020; Ohkubo *et al*., 2020; De Souza *et al*., 2020; Acevedo-Siaca *et al*., 2020, 2021b) have been demonstrated, however, the natural genetic variation and underlying factors remain to be elucidated for the improvement of photosynthetic induction by utilizing genetic resources.

1.3 The objectives in the present thesis

The objective in the present study was to investigate the natural genetic variation, the room of improvement and the underlying factors in photosynthetic induction in rice for the future breeding with utilizing the photosynthetic response to fluctuating light.

In Chapter 2, the natural genetic variation in photosynthetic induction in rice was examined by using World Rice Core Collection (WRC). WRC was selected to cover a wide range of DNA polymorphism or phenotypic diversity in a small number of genotypes (Kojima *et al*., 2005) and is archived at the genebank in the National Institute of Agrobiological Sciences (NIAS).

An *indica* rice genotype 'ARC 11094' showed the most rapid photosynthetic induction in WRC 57 genotypes (Chapter 2). Therefore, in Chapter 3, the physiological factors underlying on the rapid photosynthetic induction of ARC 11094 were analyzed. Photosynthetic induction is typically limited by two process: CO_2 diffusion from the atmosphere into the carboxylation site and CO_2 fixation by ribulose 1,5-bisphosphate carboxylase/oxygenase (Rubisco). CO_2 diffusion and CO_2 fixation of ARC 11094 during photosynthetic induction were evaluated, comparing with two reference genotypes, Koshihikari and Takanari. Furthermore, stomatal characteristics and root activity were evaluated as the related traits to CO_2 diffusion, and maximum rate of carboxylation and electron transport, and biochemical characteristics were evaluated as the related traits to CO_2 fixation.

In Chapter 4, difference of photosynthetic induction among rice subspecies (*indica*, *temperate japonica* and *tropical japonica*) was evaluated by additional investigation using Rice Core Collection of Japanese Landraces (JRC). JRC was selected from Japanese accessions stored in the NARO genebank and developed as a suitable population for understanding rice adaptation in northern areas (Ebana *et al*., 2007). Evaluation of the difference of photosynthetic induction among rice subspecies was conducted including the results of measurement in WRC (Chapter 2). In addition, I mentioned about the varietal differences of photosynthetic induction in 166 *temperate japonica* rice cultivars developed in Japan.

Finally, I discussed the natural genetic variation in photosynthetic induction in rice from the views of agronomy, physiology or ecology. The perspectives of the study, including ongoing genetic analyses such as genome wide association study (GWAS), quantitative trait loci (QTL) mapping or QTL-seq, were also stated.

Chapter 2

Natural genetic variation of photosynthetic induction in rice

2.1 Introduction

The response of leaf photosynthesis to a stepwise increase in light intensity, which is termed as photosynthetic induction, is a key trait for enhancement of crop productivity (Taylor & Long, 2017; Tanaka *et al*., 2019). Exploiting the natural genetic variation among untapped genetic resources can contribute to improve photosynthetic induction and crop productivity (Sakoda *et al*., 2022b). There are the large natural genetic variation of photosynthetic induction in some crops: soybean (*Glycine max* (L.) Merrill; Soleh *et al*., 2016, 2017), wheat (*Triticum aestivum* L.; Faralli *et al*., 2019a; Salter *et al*., 2019) and barley (*Hordeum vulgare* L.; Salter *et al*., 2020). Previous reports have demonstrated that rice (*Oryza sativa* L.) shows the varietal difference of photosynthetic induction, and it is mainly limited by both of CO_2 diffusion from the atmosphere into the carboxylation site (Adachi *et al*., 2019b; Xiong *et al*., 2022a) and CO_2 fixation in carboxylation site (Sun *et al*., 2016; Adachi *et al*., 2019b; Ohkubo *et al*., 2020; Acevedo-Siaca *et al*., 2020, 2021; Xiong *et al*., 2022b). But, these could not completely cover the potential variation of photosynthetic induction in rice due to a limited number of genotypes or populations.

Kojima *et al*. (2005) developed World Rice Core Collection (WRC), which is consist of 69 worldwide rice genotypes. WRC is selected based on the origin, restricted fragment length polymorphism (RFLP) marker analysis and several morphological traits from approximately 37,000 genotypes, suggesting that it is a powerful tool to investigate the potential variation of genetic traits in rice (Kojima *et al*., 2005). The natural genetic variations of WRC have been

elucidated in many traits, e.g. photosynthetic capacity (Kanemura *et al*., 2007), stomatal traits (Ohsumi *et al*., 2007), root characteristics (Uga *et al*., 2009) and response to pathogen attack (Kariya *et al*., 2019, 2020). Therefore, investigation of the natural genetic variation in photosynthetic induction among WRC would provide a novel insight into the strategy of optimizing photosynthetic dynamics under various environmental conditions.

In Chapter 2, I measured the photosynthetic response to a stepwise increase in light intensity and related traits with WRC and two reference cultivars: Koshihikari and Takanari, to identify the natural genetic variation and the room of improvement in photosynthetic induction in rice. Additionally, I assessed the relationship between photosynthetic induction and other related traits.

2.2 Materials and Methods

2.2.1 Plant materials and cultivation procedures

I used 57 genotypes of WRC, which were able to reach maturity in Kyoto, Japan, with two reference cultivars: Koshihikari and Takanari. The 57 genotypes of WRC was consist of 35 *indica*, 2 *temperate japonica* and 10 *tropical japonica*. Tanaka *et al*. (2020a) classified the WRC into seven subpopulations based on a phylogenetic tree from a set of 2,315 representative single nucleotide polymorphisms (SNPs). WRC was divided into three major groups, corresponding to *japonica*, *indica* and *aus*. Among these three groups, the *indica* group was further divided into four subgroups (I-1, I-2, I-3 and I-4) and the *aus* group was further divided into two subgroups (A-1 and A-2). Koshihiakri is a popular cultivar in Japan and classified into *temperate japonica*. Takanari is a high-yielding rice cultivar and classified into *indica*, and has superior photosynthetic response to fluctuating light than Koshihikari (Adachi *et al*., 2019b; Ohkubo *et al*., 2020). Seeds of all genotypes were sown in nursery boxes on 23 April 2018 and

seedlings were transplanted into 2 L plastic pots filled with alluvial loam soil on 18 May 2018. Four plants of each genotype were grown at an experimental field in the Graduate School of Agriculture, Kyoto University, Japan. Slow-release fertilizer (ECOLONG413-100, JCAM AGRI. CO., Tokyo, Japan; volume and composition: 0.25 g N, 0.19 g P_2O_5 and 0.23 g K_2O) was applied to each pot to provide a baseline fertility level. Afterwards, 0.1 g N (in the form of ammonium sulfate) and more slow-release fertilizer (ECOLONG413-40, JCAM AGRI. CO., Tokyo, Japan; volume and composition: 0.16 g N, 0.13 g P_2O_5 and 0.15 g K_2O) were applied to each pot one week before measurements. The water level of pots was maintained at approximately 3 cm above the soil surface to avoid drought.

2.2.2 Gas exchange rate and chlorophyll fluorescence measurements

Gas exchange rate and chlorophyll fluorescence were measured simultaneously with three portable gas exchange analyzers, LI-6800 (Li-Cor Biosciences, Lincoln, NE, USA) in the morning at 66-70 days after sowing. The uppermost fully expanded leaf was selected from four plants per genotype for the measurement of photosynthetic induction and capacity. To observe the photosynthetic induction, plants were placed into the dark room from the previous evening until the measurement. Condition of the leaf chamber was set to air temperature (T_{air}) of 30°C, reference CO_2 concentration (CO_2R) of 400 μmol mol^{-1} and relative humidity (RH) of 55-70%. The photosynthetic photon flux density (PPFD) was set to 50 μmol photons m^{-2} s^{-1} (low light) for the first four minutes, and was changed to 1500 μmol photons m^{-2} s^{-1} (high light) for the following 10 minutes. The following photosynthetic parameters were recorded every two minutes: A, stomatal conductance (g_s), intercellular CO_2 concentration (C_i), normalized CO_2 assimilation rate to a C_i of 300 μmol mol^{-1} (A^*), transpiration rate (T), water use efficiency (WUE), photosynthetic electron transport rate around photosystem II (PSII) (ETR) and non-

photochemical quenching (*NPQ*). A^* was used to account for the effects of differences in C_i among genotypes. A^*, *WUE*, *ETR* and *NPQ* were calculated as follows;

$$A^* = A \times 300/C_i \quad (2\text{-}1)$$

$$WUE = A/T \quad (2\text{-}2)$$

$$ETR = \Phi PSII \times 0.5 \times 0.84 \times PPFD \quad (2\text{-}3)$$

$$\Phi PSII = (F_m{}' - F_s)/F_m{}' \quad (2\text{-}4)$$

$$NPQ = (F_m - F_m{}')/F_m{}' \quad (2\text{-}5)$$

where $\Phi PSII$ is the quantum yield of PSII, F_s is the steady state fluorescence intensity in the light-adapted state, F_m' is the maximum fluorescence intensity in the light-adapted state and F_m is the maximum fluorescence intensity in the dark-adapted state. The values of 0.5 and 0.84 in equation (2-3) are the fraction of absorbed light reaching PSII, and the leaf absorptance, respectively. To quantify the speed of photosynthetic induction, the cumulative CO_2 fixation during the first 10 minutes of the photosynthetic induction (CCF_{10}) was calculated as follows (Soleh *et al*., 2017);

$$CCF_{10} = \int_0^{10} A_t \, dt \quad (2\text{-}6)$$

where A_t is the temporal CO_2 assimilation rate recorded every two minutes during a high light period. The cumulative water loss during the first 10 minutes of the photosynthetic induction (CWL_{10}) was also calculated as follows;

$$CWL_{10} = \int_0^{10} T_t \, dt \quad (2\text{-}7)$$

where T_t is the temporal transpiration rate recorded every two minutes during a high light period.

The light-saturated CO_2 assimilation rate under steady state (A_{sat}) was measured as photosynthetic capacity. Leaf chamber was controlled at PPFD of 1500 μmol photons m^{-2} s^{-1}, T_{air} of 30°C, CO_2R of 400 μmol mol^{-1} and RH of 55-70%. Three plants from each genotype were selected for A_{sat} measurements.

2.2.3 Leaf nitrogen contents

Leaf nitrogen contents per leaf area (*LNC*) were quantified as a related trait to CO_2 fixation. The leaves used for the measurement of photosynthetic induction were sampled for the quantification of *LNC*. Area of the leaf tissues was measured with LI-3100 (Li-Cor Biosciences, Lincoln, NE, USA), and then the leaf tissues were dried at 80°C more than 72 hours, weighed and coarsely ground. The nitrogen content was determined by Kjeldahl digestion followed by an indophenol assay (Vickery, 1946).

2.2.4 Statistical analysis

The values of all parameters were averaged between individual plants of each genotype and the standard error was calculated. The Tukey–Kramer multiple comparison test was used to compare the means. The relationship between several parameters was evaluated according to the Pearson correlation coefficient. All analyses were performed using Microsoft Excel (Microsoft, Redmond, WA) and the R software (R Core Team, 2018).

2.3 Results

2.3.1 Photosynthetic response to a stepwise increase in light intensity

Dynamics of leaf photosynthesis during the induction response varied significantly among the 59 rice genotypes (Fig. 2.1). All parameters, except for the C_i and *NPQ*, gradually increased after high light irradiation. Whereas C_i gradually decreased after high light irradiation. *NPQ* increased rapidly during the first two minutes after high light irradiation, and then gradually increased or decreased depending on genotypes. Overall, the genotypes which displayed superior responses of *A* tended to have relatively high g_s, A^*, *T*, *ETR* and low *NPQ*

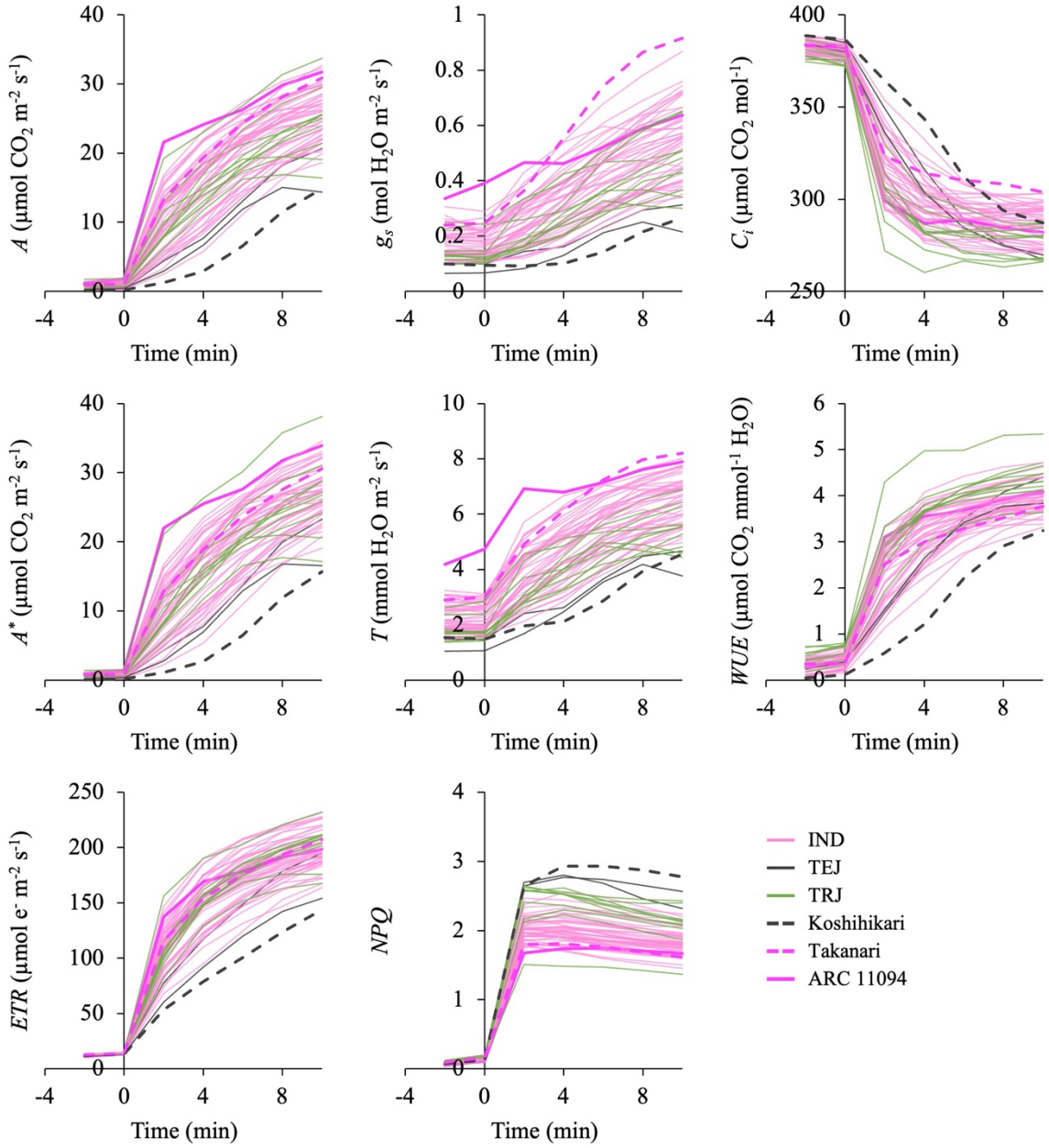

Fig. 2.1. Time courses of photosynthetic parameters in response to a stepwise increase in light intensity in 59 rice genotypes. The dynamics of CO_2 assimilation rate (A), stomatal conductance (g_s), intercellular CO_2 concentration (C_i), normalized CO_2 assimilation rate to a C_i of 300 μmol mol^{-1} (A^*), transpiration rate (T), water use efficiency (WUE), photosynthetic electron transport rate around photosystem II (ETR) and non-photochemical quenching (NPQ) were measured in 59 rice genotypes. Leaf chamber was kept at an air temperature of 30°C, a reference CO_2 concentration of 400 μmol mol^{-1} and a relative humidity of 55-70%. The photosynthetic photon flux density was changed from dark to 50 μmol photons m^{-2} s^{-1} for the first 4 minutes, and then to 1500 μmol photons m^{-2} s^{-1} for the following 10 minutes. Photosynthetic parameters were recorded every 2 minutes. Pink, gray and green represent the values of genotypes in *indica* (IND), *temperate japonica* (TEJ) and *tropical japonica* (TRJ), respectively. Gray and pink dashed lines show Koshihikari and Takanari, respectively, and pink solid line shows ARC 11094. The values were averaged between four replications of each genotype.

values. Several genotypes had a more rapid photosynthetic induction than Takanari. For instance, the *A* of ARC 11094 increased rapidly during the first two minutes in high light period, and reached 21.6 μmol CO_2 m^{-2} s^{-1} in two minutes after high light irradiation. ARC 11094 showed great g_s, A^* and *T* at initial phase of induction response, and low *NPQ* throughout high light period.

The CCF_{10} of two reference cultivars, Koshihikari and Takanari, were 3.6 mmol CO_2 m^{-2} and 12.1 mmol CO_2 m^{-2}, respectively. The highest value of CCF_{10} among WRC 57 genotypes is the 14.2 mmol CO_2 m^{-2} for ARC 11094 and approximately four fold greater than that of Koshihikari (Fig. 2.2). Three *temperate japonica* (two genotypes in WRC and Koshihikari) showed lower CCF_{10}, compared with *indica* or *tropical japonica* (Fig. 2.3). But, there was no significant difference in CCF_{10} between three major groups or between seven subpopulations based on a phylogenetic tree in Tanaka *et al*. (2020a) (Fig. 2.3).

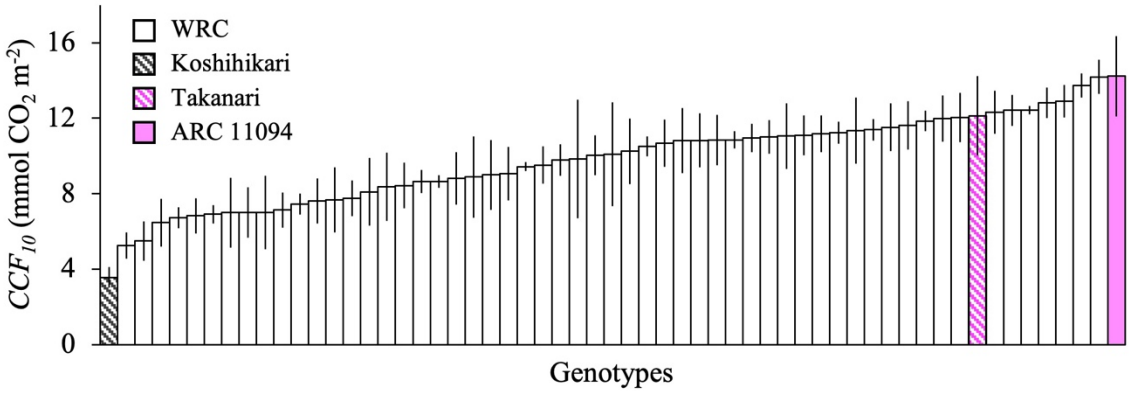

Fig. 2.2. Carbon gain during the photosynthetic induction in 59 rice genotypes. The cumulative CO_2 fixation during the first 10 minutes of the photosynthetic induction (CCF_{10}) was calculated. Gray and pink stripe bars show Koshihikari and Takanari, respectively, and pink solid bar shows ARC 11094. The values are mean ± SE (n = 4).

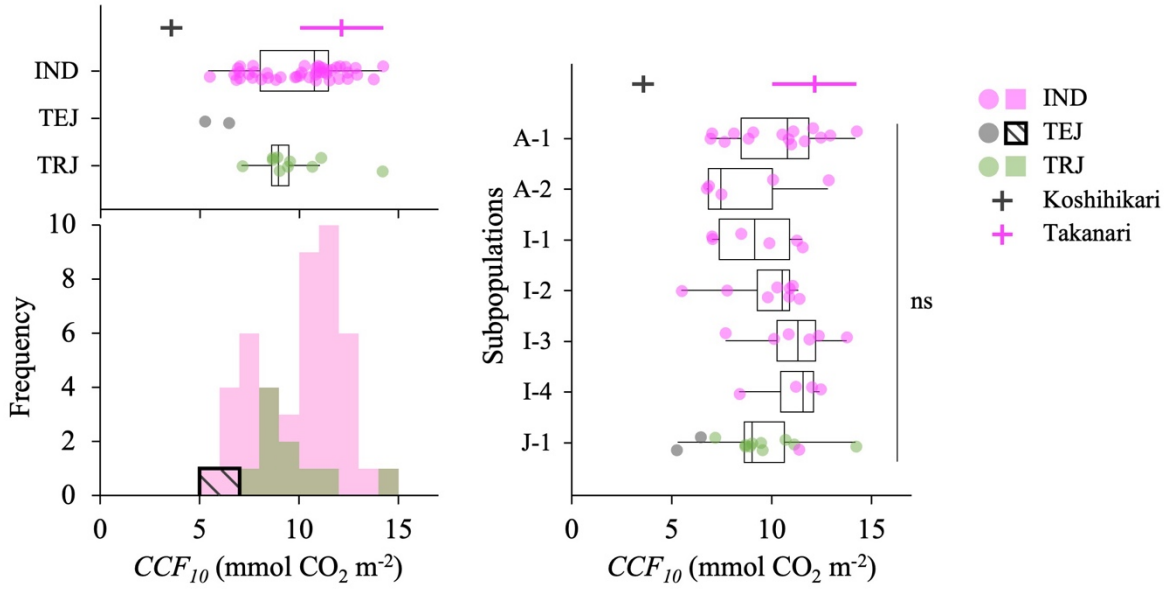

Fig. 2.3. Distribution of carbon gain during the photosynthetic induction in 57 WRC genotypes. The distribution of cumulative CO_2 fixation during the first 10 minutes of the photosynthetic induction (CCF_{10}) in 57 WRC genotypes was described as a histogram and boxplots. The 57 WRC genotypes were classified into three subspecies or seven subpopulations based on the DNA polymorphism. The histogram was generated by overlapping the distribution of *indica* (pink), *temperate japonica* (black border) and *tropical japonica* (green). Pink, gray and green dots in the boxplots represent the values of genotypes in *indica* (IND), *temperate japonica* (TEJ) and *tropical japonica* (TRJ), respectively. The values for Koshihikari and Takanari were presented by crosses in gray and pink, respectively. The vertical and horizontal bars indicate the mean values and SE, respectively. The values were obtained from Fig. 2.2. ns represents there is no significant difference at $p < 0.05$ (Tukey–Kramer multiple comparison test).

2.3.2 The relationship between photosynthetic induction and related parameters

To evaluate the relationship between photosynthetic induction and related parameters, I showed a correlation matrix among studied traits in this chapter (Fig. 2.4), then focused on several relationships and showed their scatterplots.

There was no significant correlation in CCF_{10} with days to heading after sowing (*DTH*), *LNC* and A_{sat} (Fig. 2.4, 2.5), while CCF_{10} was closely and positively correlated with A and g_s just before the transition from low to high light (A_0 and $g_{s,0}$) (Fig. 2.4, 2.6).

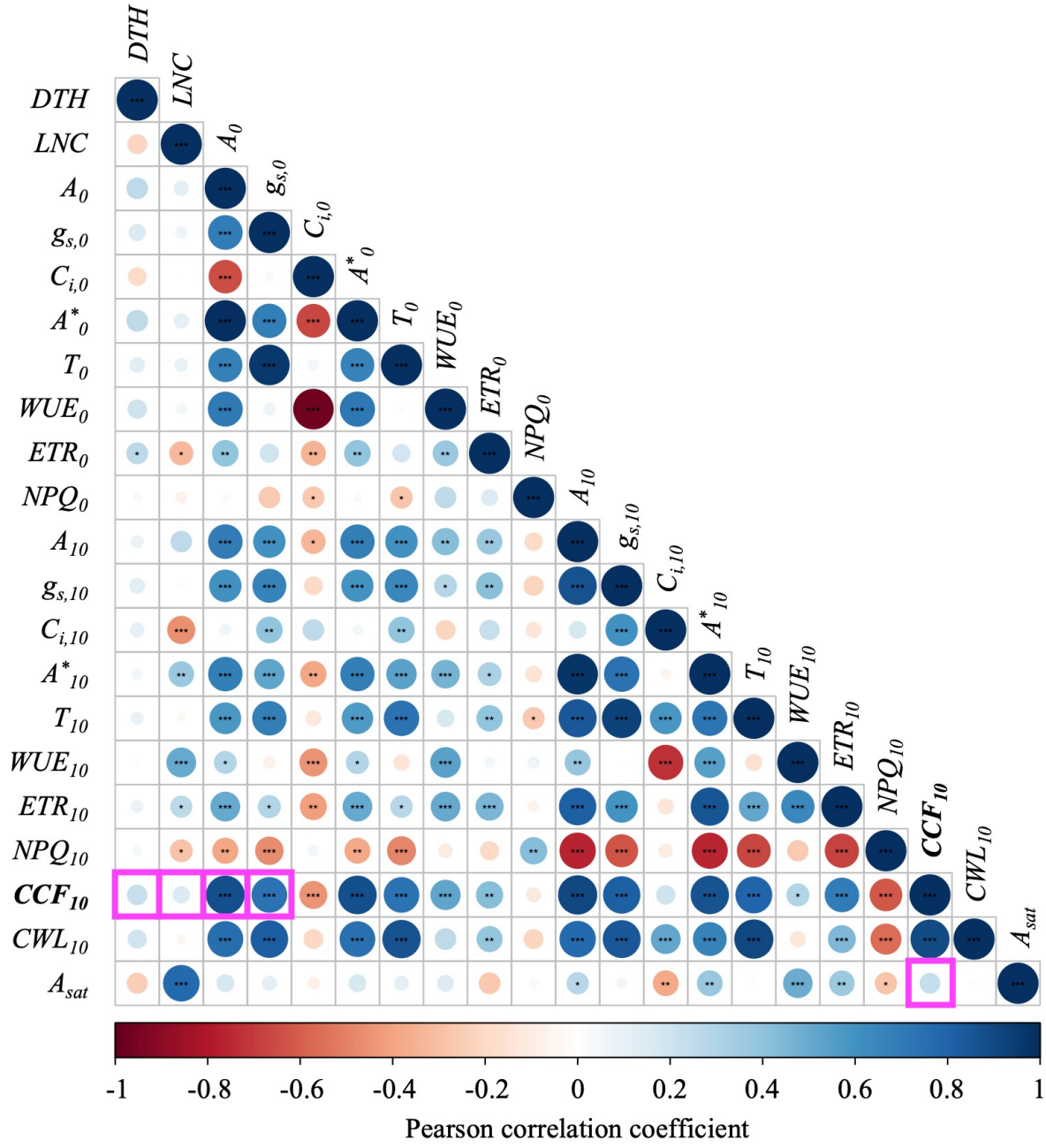

Fig. 2.4. Correlation matrix between photosynthetic induction and related parameters in 57 WRC genotypes. The correlation between days to heading after sowing (*DTH*); leaf nitrogen content per leaf area (*LNC*); the values just before the transition from low to high light or 10 minutes after high light irradiation of CO_2 assimilation rate (A_0 and A_{10}); stomatal conductance ($g_{s,0}$ and $g_{s,10}$); intercellular CO_2 concentration ($C_{i,0}$ and $C_{i,10}$); normalized CO_2 assimilation rate to a C_i of 300 µmol mol^{-1} (A^*_0 and A^*_{10}); transpiration rate (T_0 and T_{10}); water use efficiency (WUE_0 and WUE_{10}); photosynthetic electron transport rate around photosystem II (ETR_0 and ETR_{10}) and non-photochemical quenching (NPQ_0 and NPQ_{10}); cumulative CO_2 fixation during the first 10 minutes of the photosynthetic induction (CCF_{10}); cumulative water loss during the first 10 minutes of the photosynthetic induction (CWL_{10}); light-saturating CO_2 assimilation rate under steady state (A_{sat}) were analyzed. The color gradients from red to blue represent the range of Pearson correlation coefficient from -0.1 to 1.0 across 57 WRC genotypes. *, ** and *** represent a significant correlation at $p < 0.05$, 0.01 and 0.001, respectively.

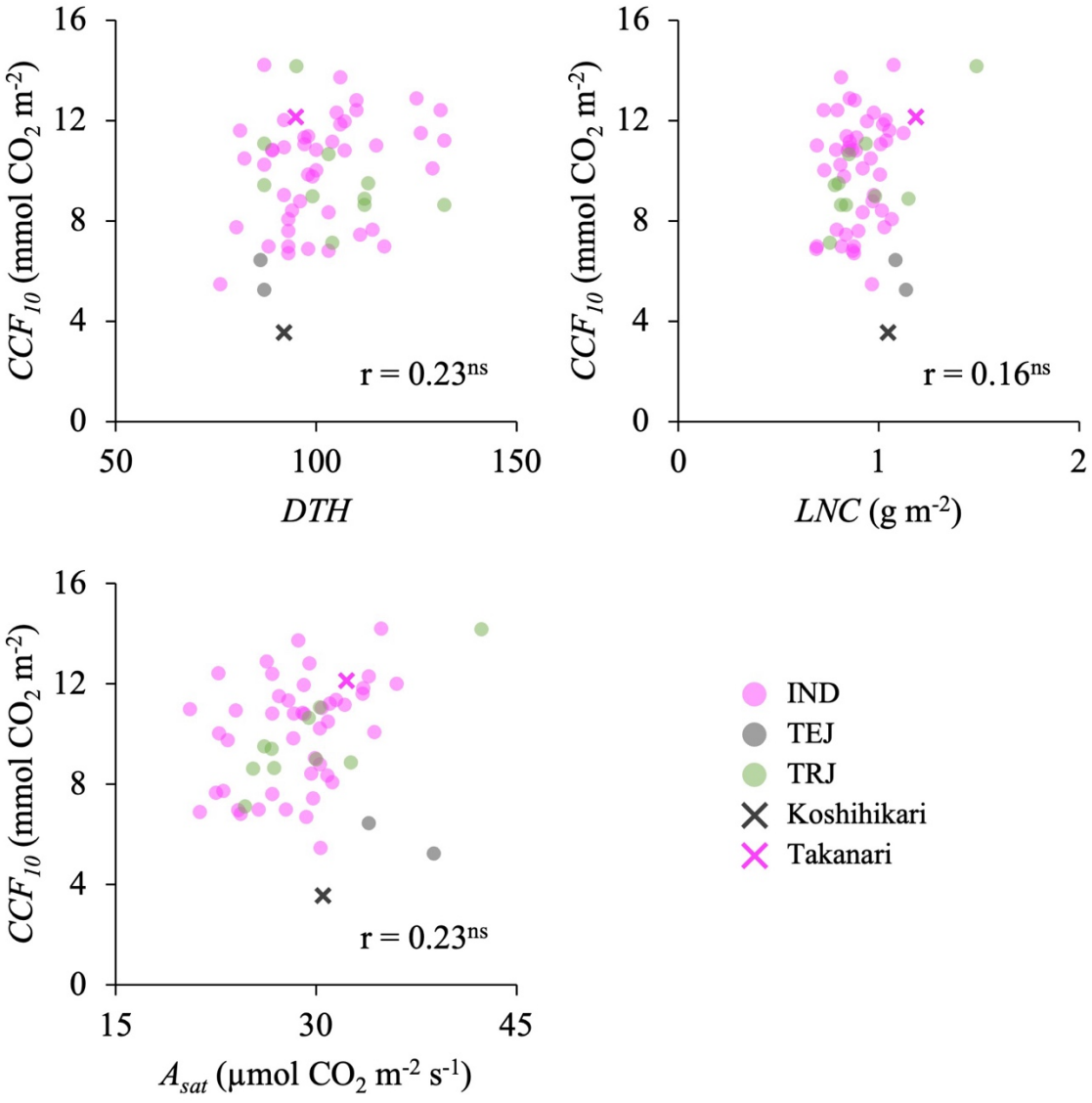

Fig. 2.5. Relationships between carbon gain during the photosynthetic induction, and heading days, leaf nitrogen contents or photosynthetic capacity. Relationships between cumulative CO_2 fixation during the first 10 minutes of the photosynthetic induction (CCF_{10}), and days to heading after sowing (*DTH*), leaf nitrogen contents per leaf area (*LNC*) or light-saturating CO_2 assimilation rate under steady state (A_{sat}) were evaluated. Pink, gray and green closed circles represent the values of genotypes in *indica* (IND), *temperate japonica* (TEJ) and *tropical japonica* (TRJ), respectively. Gray and pink cross show Koshihikari and Takanari, respectively. The values of *LNC* were averaged between four replications of each genotype, and the values of A_{sat} were averaged between three replications of each genotype. The r value was calculated among 57 WRC genotypes based on Pearson correlation coefficient. ns represents a not significant correlation at $p < 0.05$.

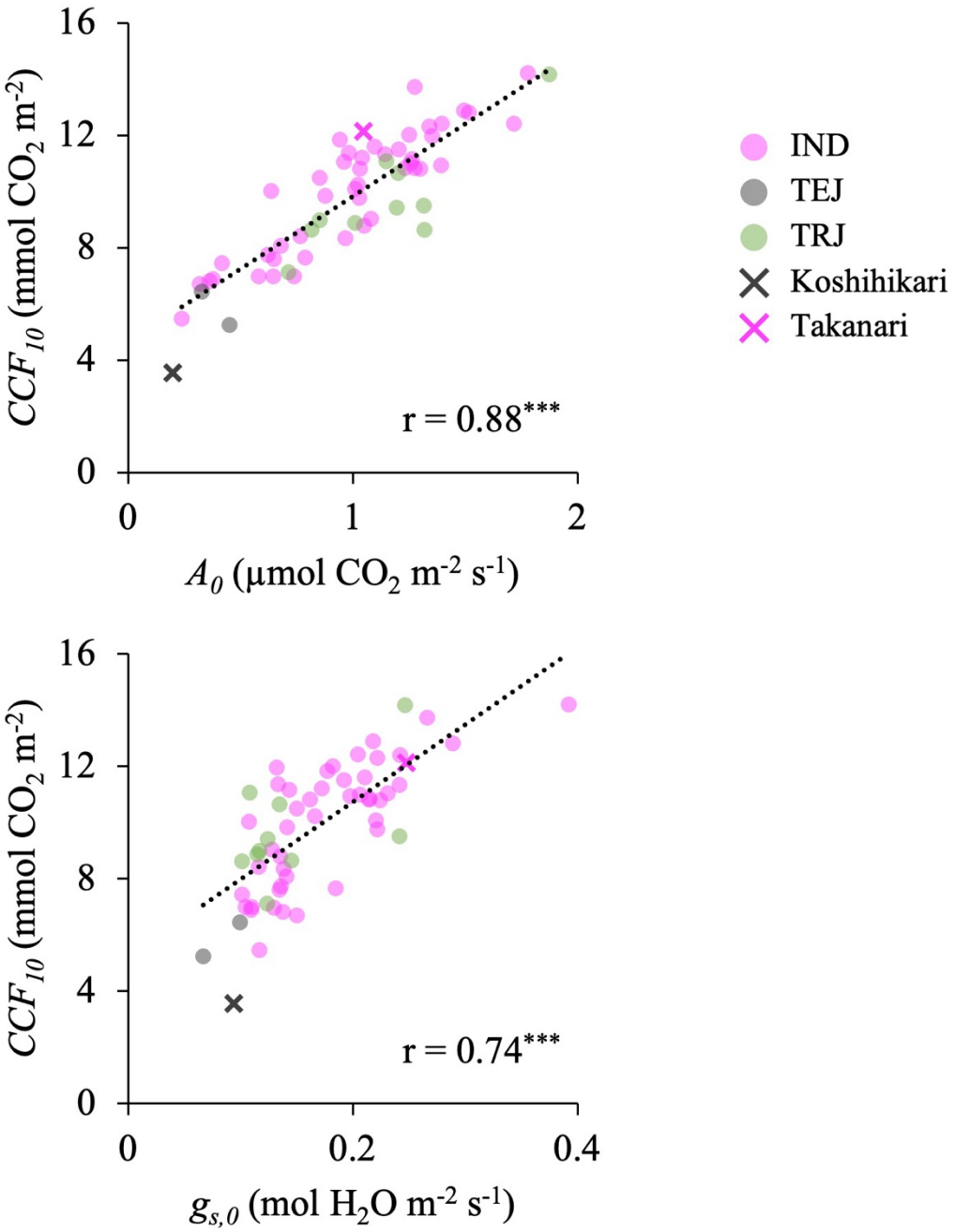

Fig. 2.6. Relationships between carbon gain during the photosynthetic induction and photosynthetic parameters just before the transition from low to high light. Relationships between cumulative CO_2 fixation during the first 10 minutes of the photosynthetic induction (CCF_{10}) and the values just before the transition from low to high light of CO_2 assimilation rate (A_0); stomatal conductance ($g_{s,0}$) were evaluated. Pink, gray and green closed circles represent the values of genotypes in *indica* (IND), *temperate japonica* (TEJ) and *tropical japonica* (TRJ), respectively. Gray and pink cross show Koshihikari and Takanari, respectively. The values were averaged between four replications of each genotype. The r value was calculated among 57 WRC genotypes based on Pearson correlation coefficient. *** represents a significant correlation at $p < 0.001$.

2.4 Discussion

2.4.1 Natural genetic variation in photosynthetic induction in rice

Previous studies have reported that photosynthetic induction varies within crops such as rice (Qu *et al*., 2016; Adachi *et al*., 2019b; Ohkubo *et al*., 2020; Acevedo-Siaca *et al*., 2020, 2021), soybean (Soleh *et al*., 2016, 2017), wheat (Faralli *et al*., 2019a; Salter *et al*., 2019) and barley (Salter *et al*., 2020). The present study showed that there is a large natural genetic variation in the photosynthetic induction in rice genotypes (Fig. 2.1, 2.2). The photosynthetic induction of Koshihikari was slow, and that of Takanari was significantly rapid among 59 rice genotypes (Fig. 2.1, 2.2). This is consistent with the previous studies (Adachi *et al*., 2019b; Ohkubo *et al*., 2020). Several genotypes in WRC displayed more rapid photosynthetic induction and larger CCF_{10} than that of Takanari (Fig. 2.1, 2.2). Notably, the speed of the photosynthetic induction in ARC 11094 was extremely fast and its CCF_{10} was approximately 4.0 and 1.2 fold greater than those of Koshihikari and Takanari, respectively (Fig. 2.1, 2.2). These results show that there is a great potential for genetic improvement of the photosynthetic induction in rice cultivars.

2.4.2 Limiting process on the natural genetic variation in photosynthetic induction

The activation of CO_2 fixation, e.g. Rubisco activation and maximum carboxylation rate (V_{Cmax}), is said to be the main factor affecting the difference in photosynthetic induction (Pearcy, 1990; Hammond *et al*., 1998; Masumoto *et al*., 2012; Yamori *et al*., 2012; Carmo-Silva and Salvucci, 2013; Kaiser *et al*., 2016; Soleh *et al*., 2016; Salter *et al*., 2019; Acevedo-Siaca *et al*., 2020, 2021b). Likewise, stomatal opening is also reported to affect the difference in CO_2 diffusion and then photosynthetic induction (Pearcy, 1990; Kaiser *et al*., 2016; Papanatsiou *et al*., 2019; Adachi *et al*., 2019b; De Souza *et al*., 2020; Yamori *et al*., 2020; Kimura *et al*., 2020).

The values of g_s and A^* in the genotypes, which showed higher CCF_{10}, increased rapidly after the transition from low to high light and was higher at 10 minutes after high light irradiation (Fig. 2.1, 2.4). This means both of CO_2 fixation and CO_2 diffusion are related to the natural genetic variation in photosynthetic induction among WRC. The detailed underlying factors in the rapid photosynthetic induction of ARC 11094 were analyzed and discussed in Chapter 3.

2.4.3 The relationship between photosynthetic induction and related traits

There is no significant relationship in CCF_{10} with *DTH* and A_{sat} (Fig. 2.4, 2.5), suggesting that the photosynthetic induction is regulated independently from the earliness of heading or photosynthetic capacity. Besides, *LNC* was not correlated with CCF_{10} (Fig. 2.4, 2.5). Although Sun *et al*. (2016) reported that the higher nitrogen contents in leaves contributed to the rapid photosynthetic induction in the specific rice cultivars, this my result implies that the variation of leaf nitrogen contents could not completely explain the natural genetic variation in photosynthetic induction in rice.

On the other hand, A_0 and $g_{s,0}$ showed significant positive correlations with CCF_{10} (Fig. 2.4, 2.6). Previous studies have demonstrated the stomatal conductance under low light influenced the photosynthetic response to a following rapid increase in light intensity (Bai *et al*., 2008; Soleh *et al*., 2017; Wachendorf & Küppers, 2017a,b). Higher stomatal density and smaller stomatal size have been reported to be advantageous for the response of stomatal conductance to fluctuating light (Faralli *et al*., 2019b; Sakoda *et al*., 2020b; Xiong *et al*., 2022a). Meanwhile, Zhang *et al*. (2019) suggested smaller stomata do not always result in the rapid stomatal response to a high light irradiation. The effect of stomatal conductance under low light on photosynthetic induction and the effect of stomatal morphology on stomatal kinetics under fluctuating light remain to be further investigated.

2.4.4 Conclusion

In conclusion in Chapter 2, I clarified the large natural genetic variation in photosynthetic induction in rice. This variation has a potential to improve the carbon gain and crop productivity under field environments. Photosynthetic induction and capacity are thought to have the different regulating mechanisms, suggesting they could be improved independently. This would enable to broaden the choices in a breeding strategy with manipulating the leaf photosynthesis.

Chapter 3

Physiological factors underlying on the rapid photosynthetic induction in rice

3.1 Introduction

Photosynthetic induction is typically limited by CO_2 diffusion from the atmosphere into the carboxylation site and CO_2 fixation in the carboxylation site (Pearcy, 1990; Kaiser *et al*., 2016). The CO_2 fixation in plant photosynthesis is catalyzed by Rubisco. Regulation of content or activity in Rubisco activase affected CO_2 fixation via Rubisco activation state under fluctuating light, but lesser at steady state (Masumoto *et al*., 2012; Yamori *et al*., 2012; Carmo-Silva and Salvucci, 2013). Dynamic A-C_i curve analysis, which is the time-course A-C_i curve analysis during photosynthetic induction, revealed V_{Cmax} was a major limiting factor to A during photosynthetic induction (Soleh *et al*., 2016; Taylor and Long, 2017; Salter *et al*., 2019; Acevedo-Siaca *et al*., 2020, 2021b). The efficiency of CO_2 diffusion from the atmosphere into the carboxylation site can be further separated into the stomatal conductance and mesophyll conductance. The stomatal and mesophyll conductance are the gas diffusion efficiency from the atmosphere to the intercellular airspaces and from the intercellular airspaces to chloroplast stroma, respectively. Stomatal conductance was reported to impose a greater limitation to the CO_2 diffusion than mesophyll conductance for most phase of photosynthetic induction (Sakoda *et al*., 2021). Stomatal conductance is determined by stomatal morphology or a single stoma behaviour. *STOMAGEN*-overexpressing mutants showed higher stomatal density and smaller stomatal size, and thus rapid stomatal opening in response to a stepwise increase in light intensity than wild type (Sakoda *et al*., 2020b). The large stomatal aperture of a single stoma contributed to the great stomatal conductance under fluctuating light (Papanatsiou *et al*., 2019;

Yamori *et al*., 2020; Kimura *et al*., 2020).

Water relations in plants also affects stomatal conductance through leaf water potential and stomatal aperture under field environments (Hirasawa *et al*., 1992). Stomatal aperture is observed to close with hydroactive stomatal response when the water potential of the leaf declines (Glinka, 1971; DeMichele & Sharpe, 1973; Buckley, 2019). The plants exhibiting such water-conserving behaviour are categorized as isohydric plants (Tardieu & Simonneau, 1998), and Taylaran *et al*. (2011) reported that the large root water uptake ability contributed to great stomatal conductance through the leaf water status under steady state conditions in rice. On the other hand, anisohydric plants allow for leaf water potential to decrease, maintaining higher stomatal conductance under drought conditions (Moshelion *et al*., 2015). However, the relationship between the difference of isohydric and anisohydric strategies and photosynthetic induction remains unclear.

ARC 11094 has the extremely rapid photosynthetic induction among 59 rice genotypes I measured in Chapter 2. Stomatal dynamics of ARC 11094 in response to a stepwise increase in light intensity was distinct from those of other rice genotypes. Considering the relationship between stomatal dynamics and water status (Kaiser *et al*., 2017; Sakoda *et al*., 2021), it was hypothesized that the stomatal characteristics of ARC 11094 were different from those of other rice genotypes, in terms of plant water use. Therefore, this genotype is regarded as a useful plant material to understand underlying mechanisms on the rapid photosynthetic induction, especially stomatal dynamics, in rice.

In Chapter 3, I focused on the rapid photosynthetic induction in ARC 11094, with two reference genotypes; Koshihikari and Takanari. I evaluated the stomatal morphology and behaviour, and water relations in plants as factors related to the CO_2 diffusion. In addition, the maximum rates of Rubisco carboxylation, electron transport, and biochemical characteristics

of the leaves were measured as factors related to CO_2 fixation. I also examined diurnal changes in the gas exchange rate in a field-mimicked environment. I discussed the mechanisms underlying rapid photosynthetic induction and the relationship between water use strategy and photosynthetic induction in rice through these analyses.

3.2 Materials and Methods

3.2.1 Plant materials and cultivation procedures

The seeds of ARC 11094 (ssp. *indica*), Takanari (ssp. *indica*) and Koshihikari (ssp. *temperate japonica*) were sown in nursery boxes filled with artificial soil on 19 April 2019, 21 April 2020 and 27 April 2021. The seedlings were transplanted to 2 L plastic pots filled with paddy soil (alluvial loam) at 28, 24 and 23 days after sowing in 2019, 2020 and 2021, respectively. Fertilizer and water management were followed as Chapter 2. These plants were measured at approximately three months after sowing.

To investigate the photosynthetic characteristics under changing osmotic potential, the three genotypes were cultivated in a greenhouse with the LED light source in an experimental field at the Graduate School of Agriculture, Kyoto University, Japan (35°2 'N, 135°47' E, 65 m altitude). Plants were cultivated in 2 L plastic pots with paddy soil (alluvial loam) and were measured at 47-49 days after sowing. The basal fertilizer (0.16 g N, 0.13 g P_2O_5 and 0.15 g K_2O) and the additional fertilizer 0.05 g N were applied to each pot. The environment in the greenhouse was set at a photoperiod of 13 h, a PPFD of 800 μmol photons m^{-2} s^{-1}, and an air temperature of 28/20°C day/night.

A field experiment was performed in 2020 to evaluate crop productivity in the three genotypes. Sowing and transplanting date were same as a pot experiment. For yield measurements, a plot of 10 by 6 plants was established with three replications per each genotype.

The amount of basal fertilizer was 60 kg N, 47 kg P_2O_5 and 56 kg K_2O per a hectare. The amount of additional fertilizer was 40 kg N, 31 kg P_2O_5 and 37 kg K_2O per a hectare and applied at the middle of July. Weeds, diseases and insects were strictly controlled, and the field was fully irrigated throughout the growing season.

3.2.2 Gas exchange rate measurements

Gas exchange rates at steady and non-steady states in the uppermost fully expanded leaves were measured with three portable gas exchange analyzers, LI-6800 (Li-Cor Biosciences, Lincoln, NE, USA). For the measurement of gas exchange rate at steady state, condition of the leaf chamber was set to PPFD of 1500 μmol photons m^{-2} s^{-1} (90% of red light and 10% of blue light), T_{air} of 30°C, CO_2R of 400 μmol mol^{-1} and RH of 55-70%. A, g_s, C_i, A^*, T and WUE were recorded.

The response of A to C_i under steady state was obtained under the aforementioned conditions except for CO_2R, which was increased to 100, 200, 300, 400, 600 and 800 μmol mol^{-1}. The A-C_i curves were analyzed using the equations of Farquhar *et al*. (1980) with the "Plantecophys" package in R (bilinear fitting method; Duursma, 2015) to estimate V_{Cmax} and the maximum electron transport rate (J_{max}). The parameters were normalized to 25°C during the fitting process based on Bernacchi *et al*. (2001).

To observe the photosynthetic dynamics under non-steady state, plants were placed in the dark room from the previous evening until the measurement. The PPFD was changed from 0 μmol photons m^{-2} s^{-1} to 50 μmol photons m^{-2} s^{-1} for 10 minutes and then 1500 μmol photons m^{-2} s^{-1} for 90 minutes (Fig. 3.1). The ratio of red-blue LED light sources was kept at 90:10. The photosynthetic parameters were recorded every 10 seconds. A dynamic A-C_i curve analysis was conducted based on previous studies (Soleh *et al*., 2016; Taylor & Long, 2017). At first, the

leaves were adapted to the steady state at PPFD of 1500 µmol photons m^{-2} s^{-1}, T_{air} of 30°C, CO_2R of 400 µmol mol^{-1} and RH of 55-70%. Subsequently, the cycle of 50 µmol photons m^{-2} s^{-1} for 30 minutes and 1500 µmol photons m^{-2} s^{-1} for 10 minutes was repeated at CO_2R values of 100, 200, 300, 400, 600 and 800 µmol mol^{-1}. As described above, I obtained the dynamics of V_{Cmax} and J_{max} from the A-C_i curves fitted to the data for every 10 seconds interval.

Diurnal changes in gas exchange rates in a field-mimicked environment were measured using two LI-6400 (Li-Cor Biosciences, Lincoln, NE, USA). Overnight dark-adapted leaves were clamped within leaf chambers, and the PPFD and T_{air} used in Ohkubo *et al*. (2020) (Fig. 3.1) was replicated for 12 hours. Photosynthetic parameters at a CO_2R of 400 µmol mol^{-1} were recorded every 10 seconds.

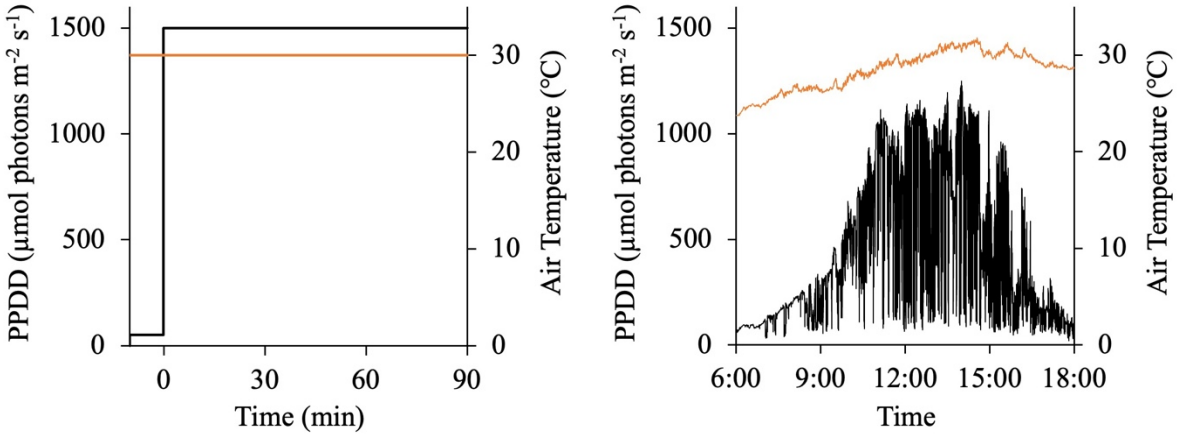

Fig. 3.1. Conditions in the leaf chamber at the measurement of photosynthetic dynamics. Photosynthetic responses to a step increase in light intensity (left) were measured. The value of photosynthetic photon flux density (PPFD) was changed from 0 µmol photons m^{-2} s^{-1} to 50 µmol photons m^{-2} s^{-1} for 10 minutes, and then to 1500 µmol photons m^{-2} s^{-1} for the following 90 minutes, and air temperature was constant at 30°C. The measurement of diurnal changes of photosynthesis was conducted under field-mimicked environment (right). The values of PPFD and air temperature observed in rice canopy were replicated every 10 seconds for 12 hours.

3.2.3 Leaf nitrogen, Rubisco and chlorophyll contents

The uppermost expanded leaves were sampled at 7-8 a.m. to evaluate leaf nitrogen,

Rubisco and chlorophyll contents. The quantification of *LNC* was followed in Chapter 2. The quantification of Rubisco contents per leaf area and chlorophyll contents per leaf area (*Chl a+b*) was performed as described in Sakoda *et al*. (2020a). A leaf tissue of 1.5 cm^2 was collected, frozen immediately with liquid nitrogen and then stored at -80°C until further use. The leaf tissue was homogenised using a cold mortar and pestle in an extraction buffer containing 50 mM 4-(2-hydroxyethyl)-1-piperazineethanesulfonic acid (HEPES)-KOH, 5 mM $MgCl_2$, 1 mM Na_2 ethylenediaminetraacetic acid (EDTA), 0.1% (w/v) polyvinyl pyrrolidine (PVPP), 0.05% (v/v) Triton X-100, 5% glycerol, 4 mM amino-n-caproic acid, 0.8 mM benzamidine-HCl, and 5 mM dithiothreitol (DTT) at pH 7.4 with a small amount of quartz sand. A 200 µl aliquot was separated for chlorophyll quantification. The homogenate was then centrifuged at 14,500× *g* for five minutes at 4°C. The supernatant was then used for Rubisco quantification. The Rubisco content was quantified spectrophotometrically by formamide extraction of the bands corresponding to the large and small subunits of Rubisco separated by SDS-PAGE (Makino *et al*., 1986) using bovine serum albumin as the standard protein. The chlorophyll content extracted using 80% acetone was quantified spectrophotometrically as a following equation (Porra *et al*. 1989);

$$Chl\ a+b = 17.67(A^{646.6} - A^{750}) + 7.12(A^{663.6} - A^{750}) \quad (3\text{-}1)$$

where the unit of *Chl a+b* is µg ml^{-1}, and $A^{646.6}$, $A^{663.6}$ and A^{750} are the absorbance of the solutions at 646.6, 663.6 and 750 nm, respectively.

3.2.4 Stomatal morphology

Stomatal morphology (stomatal density: *SD*, and guard cell length: *GCL*) were quantified as related traits to CO_2 diffusion. Replicas of the adaxial and abaxial leaf surfaces used for gas exchange measurements were prepared using Suzuki's Universal Method of

Printing. These replicas were observed at 100-fold magnification using an optical microscope (CX31 and DP21; Olympus, Tokyo, Japan), and three microscopic images were obtained for each replica. The *SD* and *GCL* for each leaf was the sum and average of both surfaces, respectively. Additionally, specific stomatal conductance was calculated by dividing g_s by *SD* to evaluate the contribution of a single stoma to g_s, following Ohsumi *et al*. (2007).

3.2.5 Water relations in plants

The leaf water potential (*LWP*) under steady state was measured by the pressure chamber method using Model670 (PMS Instrument Co., Albany, OR). The leaves were adapted to high light intensity (1500 μmol photons m^{-2} s^{-1}) for sufficient time before the measurement. Whole-plant hydraulic conductance (K_{plant}) was calculated using the following equation, based on Hirasawa (1991);

$$K_{plant} = -T_{steady}/LWP \qquad (3\text{-}2)$$

where T_{steady} indicates *T* measured under steady state.

The exudation rate per plant (*E*), total, root and shoot dry weights, and root/shoot ratio were measured to evaluate root activity. I cut the shoots of plants placed in the dark or after 10 min of irradiation with a PPFD of 50 μmol photons m^{-2} s^{-1} using a razor blade at 15 cm above the soil surface. Exudates were collected in pre-weighed cotton covered with plastic bags to prevent water loss by evaporation. After collection for 30 min, the volume was calculated based on the difference in the weight of cotton. The roots and shoots of the plants were washed with water carefully. All the samples were dried at 80°C for more than 72 hours and then weighed. I calculated the normalized *E* to root dry weight (*E*/*Root*) to remove the effects of differences in individual growth.

3.2.6 Photosynthetic response to changing osmotic potential

To characterize the photosynthetic response to leaf water deficit, I observed dynamics of g_s under varying osmotic potential. Leaves were cut below the collar, then immediately cut again when immersed in the water to avoid the cavitation, and arranged with water using 15 ml tubes. The leaves were clamped within the leaf chamber of LI-6800, which was set at a PPFD of 1500 μmol photons m^{-2} s^{-1}, an T_{air} of 30°C, a CO2R concentration of 400 μmol mol^{-1}, and a RH of 55-70%. After stabilization of photosynthesis, 1% (w/v) polyethylene glycol (PEG)-4000 was added until the final concentration of the PEG-4000 to 0.1% (w/v) is achieved and the solution was stirred gently. Photosynthetic parameters were recorded every 10 seconds when the osmotic potential changed.

3.2.7 Crop productivity of the plants grown under the field

At the plant maturity stage, 10 plants were harvested per each plot for the measurement of grain yield and yield components. The grain yield was adjusted to 14% moisture. Yield components, i.e., the panicle number per square meter, spikelet number per panicle, filled grain ratio and 1000-grain weight, were determined. Filled grain was selected with water, and 1000-grain weight was adjusted to 14% moisture. Simultaneously, above ground biomass and harvest index were measured.

3.2.8 Statistical analysis

The values of all parameters were averaged between individual plants of each genotype and the standard error was calculated. The Tukey–Kramer multiple comparison test was used to compare the means. All analyses were performed using Microsoft Excel (Microsoft, Redmond, WA) and the R software (R Core Team, 2018).

3.3 Results

3.3.1 Gas exchange rates at steady and non-steady state

First, A_{sat} and the other photosynthetic parameters (g_s, C_i, A^*, T and WUE) under steady state ($g_{s,steady}$, $C_{i,steady}$, A^*_{steady}, T_{steady} and WUE_{steady}) were measured. The A_{sat} of ARC 11094, Takanari and Koshihikari were 26.1, 29.2 and 22.5 μmol CO_2 m^{-2} s^{-1}, respectively (Table 3.1). ARC 11094 and Takanari showed greater $g_{s,steady}$ than Koshihikari, but $C_{i,steady}$ of Takanari was similar to that of Koshihikari (Table 3.1). Therefore, the A^*_{steady} of Takanari tended to be greater than those of ARC 11094 and Koshihikari (Table 3.1). The T_{steady} of ARC 11094 and Takanari was higher than that of Koshihikari, and ARC 11094 showed lower WUE_{steady} than those of Takanari and Koshihikari (Table 3.1).

Table 3.1. Photosynthetic parameters and water relations in plants under steady state. Steady state values of light-saturating CO_2 assimilation rate (A_{sat}), stomatal conductance ($g_{s,steady}$), intercellular CO_2 concentration ($C_{i,steady}$), normalized CO_2 assimilation rate to a C_i of 300 μmol mol^{-1} (A^*_{steady}), transpiration rate (T_{steady}) and water use efficiency (WUE_{steady}) were measured with LI-6800 at a photosynthetic photon flux density of 1500 μmol photons m^{-2} s^{-1}, a reference CO_2 concentration of 400 μmol mol^{-1}, an air temperature of 30°C and a relative humidity of 55-70%. Leaf water potential (LWP) was evaluated immediately after the photosynthetic measurement under steady state with the pressure chamber method. Whole plant hydraulic conductance (K_{plant}) was calculated using the values of T_{steady} and LWP. Values are mean ± SE (n = 4). Lower-case letters represent significant differences among genotypes at $p < 0.05$ (Tukey-Kramer multiple comparison test).

Parameters	ARC 11094		Takanari		Koshihikari	
A_{sat} (μmol CO_2 m^{-2} s^{-1})	26.1 ± 1.3	ab	29.2 ± 1.8	a	22.5 ± 1.9	b
$g_{s,steady}$ (mol H_2O m^{-2} s^{-1})	0.51 ± 0.03	a	0.47 ± 0.04	a	0.33 ± 0.03	b
$C_{i,steady}$ (μmol CO_2 mol^{-1})	287 ± 3	a	263 ± 4	b	258 ± 2	b
A^*_{steady} (μmol CO_2 m^{-2} s^{-1})	27.4 ± 1.6		33.4 ± 2.2		26.1 ± 2.2	
T_{steady} (mmol H_2O m^{-2} s^{-1})	7.1 ± 0.2	a	6.7 ± 0.4	a	5.3 ± 0.4	b
WUE_{steady} (μmol CO_2 $mmol^{-1}$ H_2O)	3.7 ± 0.1	b	4.4 ± 0.1	a	4.3 ± 0.1	a
LWP (MPa)	-0.60 ± 0.12		-0.40 ± 0.06		-0.33 ± 0.04	
K_{plant} (mmol H_2O m^{-2} s^{-1} MPa^{-1})	13.2 ± 2.5		17.6 ± 3.6		17.7 ± 1.5	

Next, I investigated the response of the photosynthetic parameters to high light irradiation. After step increases in light intensity, A of ARC 11094 and Takanari increased more rapidly than that of Koshihikari (Fig. 3.2). The time to reach 80% of the maximum A after high light irradiation ($T_{80,A}$) in ARC 11094, Takanari, and Koshihikari were 4.3, 6.8 and 32.0 minutes, respectively (Fig. 3.2). However, the values of A in the dark (dark respiration rate; R_d) and just before the transition from low to high light (A_0), and the maximum values during induction response (A_{max}), and the time to reach 50% of A_{max} after high light irradiation ($T_{50,A}$) were not significantly different among all the genotypes (Fig. 3.2; Table 3.2). A^* in the dark and just before the transition from low to high light (A^*_{dark}, A^*_0), the maximum values of g_s and A^* during induction response ($g_{s,max}$, A^*_{max}), and the time to reach 50% of A^*_{max} after high light irradiation ($T_{50,A*}$) also showed no significant differences. The g_s in the dark ($g_{s,dark}$), the time to reach 50% of $g_{s,max}$ after high light irradiation ($T_{50,gs}$) and the time to reach 80% of $g_{s,max}$ and A^*_{max} after high light irradiation ($T_{80,gs}$ and $T_{80,A*}$) were higher or shorter in ARC 11094 and Takanari than Koshihikari (Fig. 3.2; Table 3.2). In ARC 11094 and Takanari, g_s just before the transition from low to high light ($g_{s,0}$) tended to be higher than that in Koshihikari ($p = 0.057$; Table 3.2). The values of g_s, A^*, and T in ARC 11094 and Takanari increased more rapidly and were higher than those in Koshihikari under both of low and high light periods (Fig. 3.2). C_i was also higher in ARC 11094 and Takanari than in Koshihikari under high light period (Fig. 3.2). In contrast, the *WUE* of Koshihikari was higher than those of ARC 11094 and Takanari after high light irradiation (Fig. 3.2).

PPFD in the rice canopy fluctuated drastically and affected all photosynthetic parameters (Fig. 3.1, 3.3). ARC 11094 had greater A, g_s, A^*, and T values than Koshihikari throughout the day (Fig. 3.3). Takanari had higher A, g_s and T than Koshihikari during most of the day, but slightly lower than Koshihikari in the late afternoon (Fig. 3.3). C_i of Takanari tended

to be higher, and the *WUE* of ARC 11094 and Takanari tended to be lower than that of Koshihikari in the morning (Fig. 3.3).

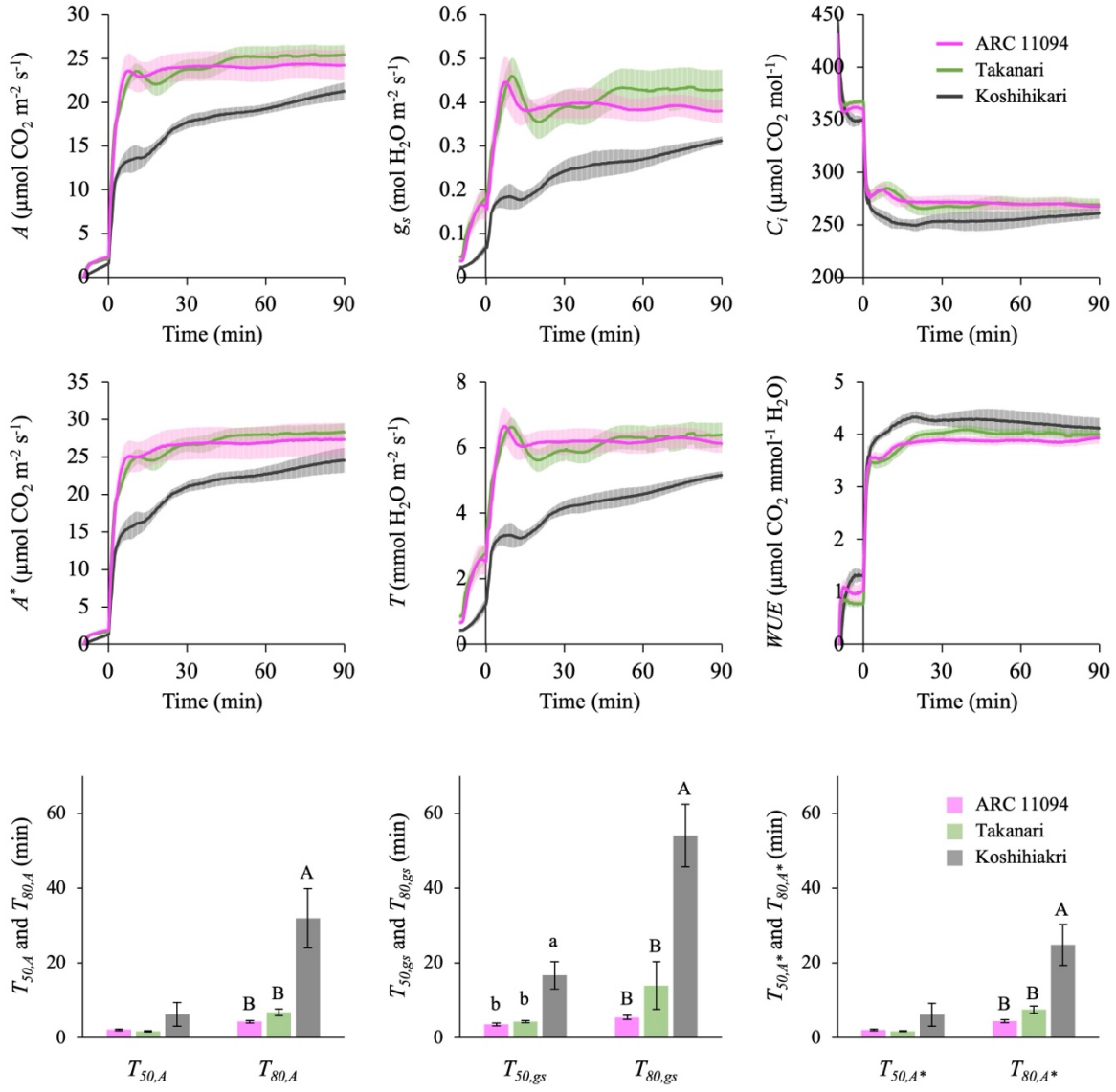

Fig. 3.2. Time courses of photosynthetic parameters in response to changes in light intensity. The dynamics of CO_2 assimilation rate (A), stomatal conductance (g_s), intercellular CO_2 concentration (C_i), normalized CO_2 assimilation rate to a C_i of 300 μmol mol^{-1} (A^*), transpiration rate (T) and water use efficiency (WUE) were measured. Leaf chamber was kept at an air temperature of 30°C, a reference CO_2 concentration of 400 μmol mol^{-1} and a relative humidity of 55-70%. The photosynthetic photon flux density was changed from dark to 50 μmol photons m^{-2} s^{-1} for the first 10 minutes, and then to 1500 μmol photons m^{-2} s^{-1} for the following 90 minutes. Photosynthetic parameters were recorded every 10 seconds. Time to reach 50% or 80% of the maximum values during induction response after high light irradiation was calculated in A, g_s and A^* ($T_{50,A}$, $T_{50,gs}$, $T_{50,A*}$, $T_{80,A}$, $T_{80,gs}$ and $T_{80,A*}$). Pink, green and gray show ARC 11094, Takanari and Koshihikari, respectively. Values are mean ± SE (n = 4-5). Letters represent significant differences among genotypes at $p < 0.05$ (Tukey-Kramer multiple comparison test).

Table 3.2. Photosynthetic characteristics under non-steady state. The values of CO_2 assimilation rate, stomatal conductance and normalized CO_2 assimilation rate to a C_i of 300 μmol mol^{-1} at dark (dark respiration rate; R_d, $g_{s,dark}$, A^*_{dark}), just before the transition from low to high light (A_0, $g_{s,0}$, A^*_0), and the maximum values during induction response (A_{max}, $g_{s,max}$, A^*_{max}) were estimated from Fig. 3.2. Values are mean ± SE (n = 4-5). Lower-case letters represent significant differences among genotypes at $p < 0.05$ (Tukey-Kramer multiple comparison test).

Parameters	ARC 11094		Takanari		Koshihikari	
R_d (μmol CO_2 m^{-2} s^{-1})	0.88 ± 0.03		0.83 ± 0.1		0.87 ± 0.14	
A_0 (μmol CO_2 m^{-2} s^{-1})	2.26 ± 0.19		2.11 ± 0.19		1.53 ± 0.19	
A_{max} (μmol CO_2 m^{-2} s^{-1})	24.9 ± 1.8		25.9 ± 0.9		21.2 ± 1.0	
$g_{s,dark}$ (mol H_2O m^{-2} s^{-1})	0.036 ± 0.005	ab	0.046 ± 0.006	a	0.023 ± 0.002	b
$g_{s,0}$ (mol H_2O m^{-2} s^{-1})	0.16 ± 0.03		0.18 ± 0.03		0.07 ± 0.01	
$g_{s,max}$ (mol H_2O m^{-2} s^{-1})	0.47 ± 0.05		0.49 ± 0.05		0.32 ± 0.01	
A^*_{dark} (μmol CO_2 m^{-2} s^{-1})	-0.61 ± 0.02		-0.59 ± 0.06		-0.58 ± 0.09	
A^*_0 (μmol CO_2 m^{-2} s^{-1})	1.89 ± 0.17		1.73 ± 0.16		1.31 ± 0.17	
A^*_{max} (μmol CO_2 m^{-2} s^{-1})	27.4 ± 2.2		28.4 ± 1.1		24.6 ± 1.6	

3.3.2 Dynamic A-C_i curve analysis and biochemical traits related to leaf photosynthesis

As CO_2R increased, *A* became higher, and the slope of the *A*-C_i curves increased with time in all genotypes (Fig. 3.4). In ARC 11094 and Takanari, the *A* responses were more rapid under each CO_2R, and the slope of the *A*-C_i curves was steeper than in Koshihikari (Fig. 3.4). The g_s of Takanari and Koshihikari showed smaller values as CO_2R increased, while initial responses of g_s during the first three minutes after high light irradiation were similar between high CO_2R (600 and 800 ppm) and ambient CO_2R (400 ppm) in ARC 11094 (Fig. 3.4).

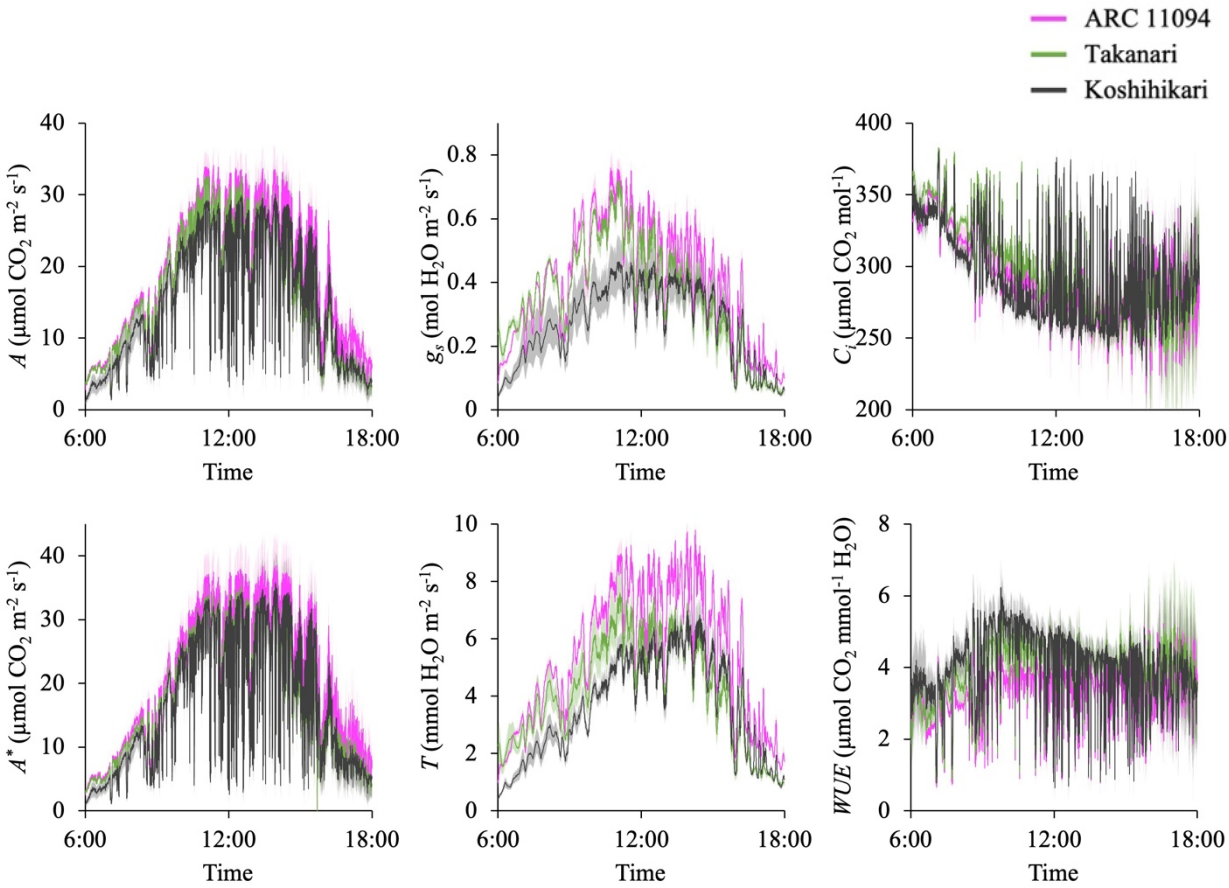

Fig. 3.3. Diurnal changes of photosynthetic parameters under field-mimicked environment. The dynamics of CO_2 assimilation rate (A), stomatal conductance (g_s), intercellular CO_2 concentration (C_i), normalized CO_2 assimilation rate to a C_i of 300 μmol mol^{-1} (A^*), transpiration rate (T) and water use efficiency (WUE) were measured. Leaf chamber was kept at a reference CO_2 concentration of 400 μmol mol^{-1}. The photosynthetic photon flux density and air temperature were changed as shown Fig. 3.1. Photosynthetic parameters were recorded every 10 seconds for 12 hours. Pink, green and gray show ARC 11094, Takanari and Koshihikari, respectively. Values are mean ± SE (n = 3).

The values of V_{Cmax} and J_{max} increased after high light irradiation for all genotypes (Fig. 3.5). The V_{Cmax} of all genotypes were not different in the initial induction phase during four minutes after high light irradiation (Fig. 3.5). J_{max} of ARC 11094 and Takanari was also high, and that of Koshihikari was low during the induction response (Fig. 3.5). But, considering the steady state values as 100%, relative V_{Cmax} and J_{max} showed no significant differences among three genotypes (Fig. 3.5).

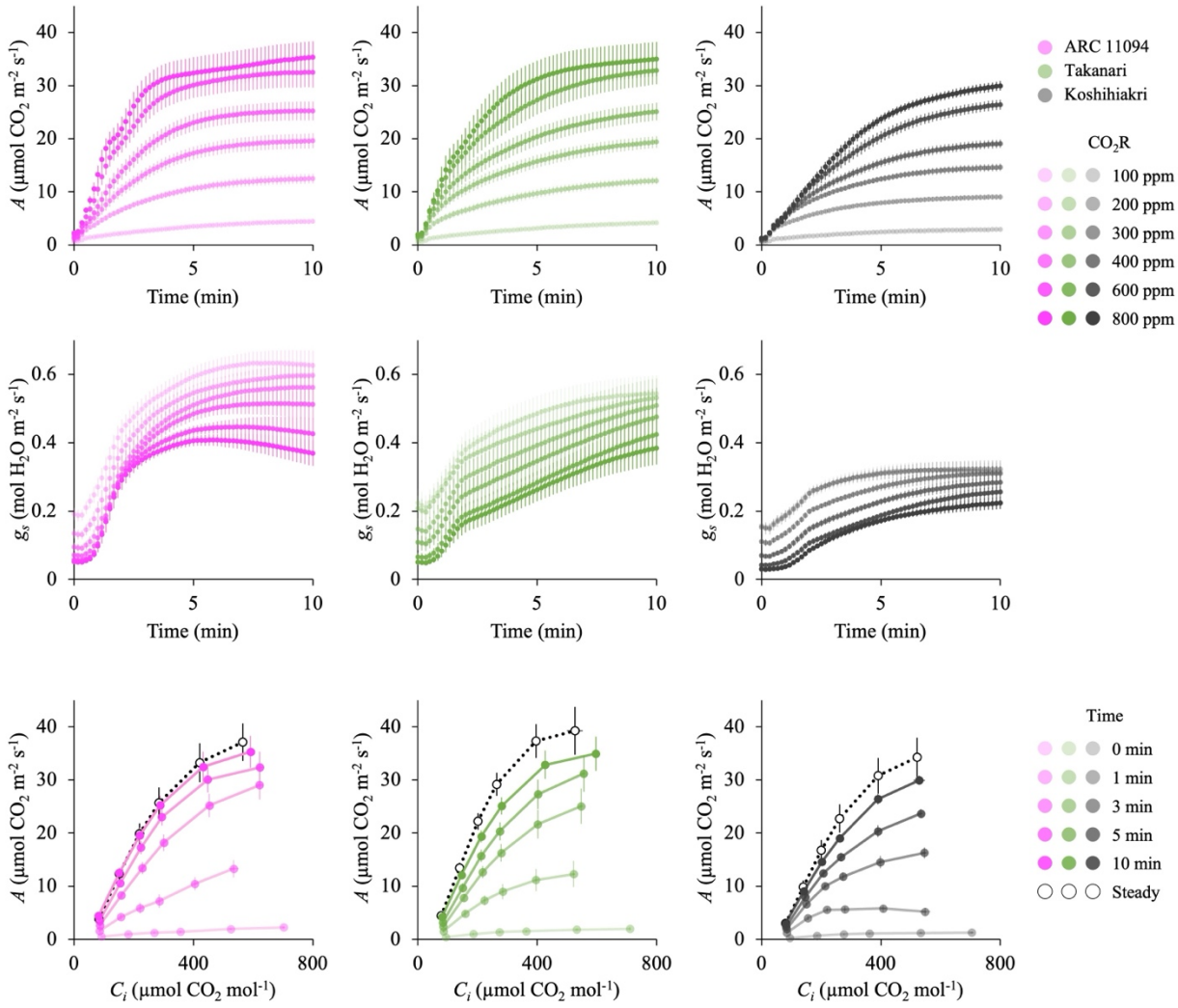

Fig. 3.4. Non-steady state photosynthesis under different CO_2 concentration. The dynamics after high light irradiation of CO_2 assimilation rate (A) and stomatal conductance (g_s) at reference CO_2 concentration of 100, 200, 300, 400, 600 and 800 μmol mol^{-1}, and A-C_i curve were evaluated. Leaf chamber was kept at an air temperature of 30°C and a relative humidity of 55-70%. Photosynthetic parameters were recorded every 10 seconds. A-C_i curve analysis under steady state was conducted independently. Pink, green and gray show ARC 11094, Takanari and Koshihikari, respectively. Values are mean ± SE (n = 4-5).

Nitrogen, Rubisco and chlorophyll contents per leaf area were investigated as traits related to CO_2 fixation. The *LNC* of ARC 11094 was significantly lower than those of Takanari and Koshihikari (Fig. 3.5). But, there were no significant differences among the three genotypes in Rubisco contents and *Chl a+b* (Fig. 3.5).

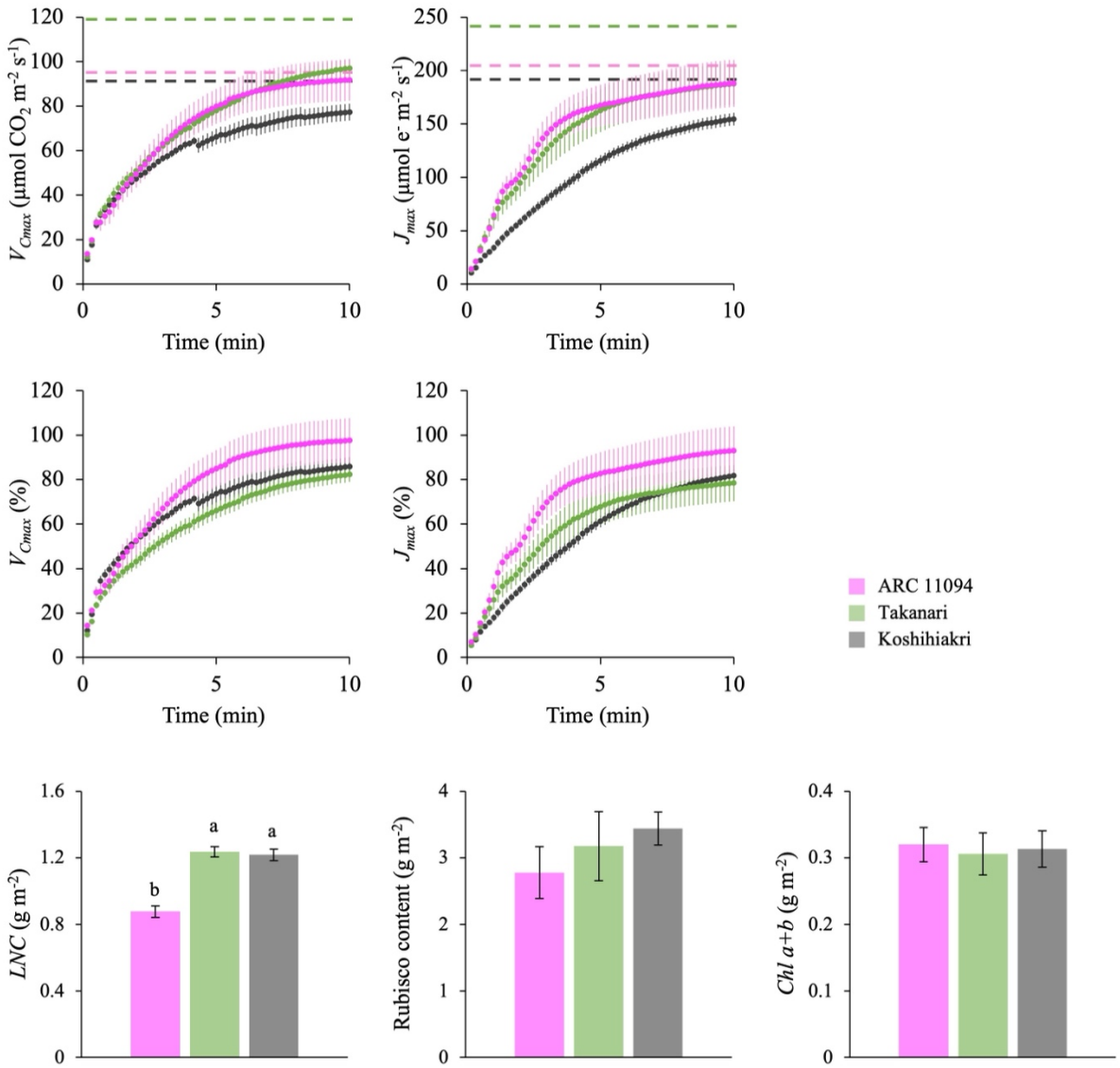

Fig. 3.5. Dynamics of limiting factors in photosynthetic induction and biochemical traits in leaves. The dynamics of the maximum rate of carboxylation (V_{Cmax}) and electron transport (J_{max}) were estimated from Fig. 3.4 and normalized to 25°C. Dashed horizontal lines indicate the values under steady state. Relative values of V_{Cmax} and J_{max} were calculated when the steady state values were considered as 100%. Contents of nitrogen (*LNC*), Rubisco and chlorophyll (*Chl a+b*) per leaf area were quantified. Pink, green and gray show ARC 11094, Takanari and Koshihikari, respectively. Values are mean ± SE (n = 4-5). Lower-case letters represent significant differences among genotypes at $p < 0.05$ (Tukey-Kramer multiple comparison test).

3.3.3 Stomatal traits and water relations

ARC 11094 and Koshihikari had similar *SD*, and Takanari had higher values than the other two genotypes (Fig. 3.6). On the other hand, the *GCL* of Takanari was the lowest, followed

in order by Koshihikari and ARC 11094 (Fig. 3.6). To estimate the contribution of a single stoma to g_s, I calculated the specific g_s. Specific g_s values of ARC 11094 were higher in Takanari and Koshihikari, and Takanari showed similar values to Koshihikari after 30 minutes of high light irradiation (Fig. 3.6).

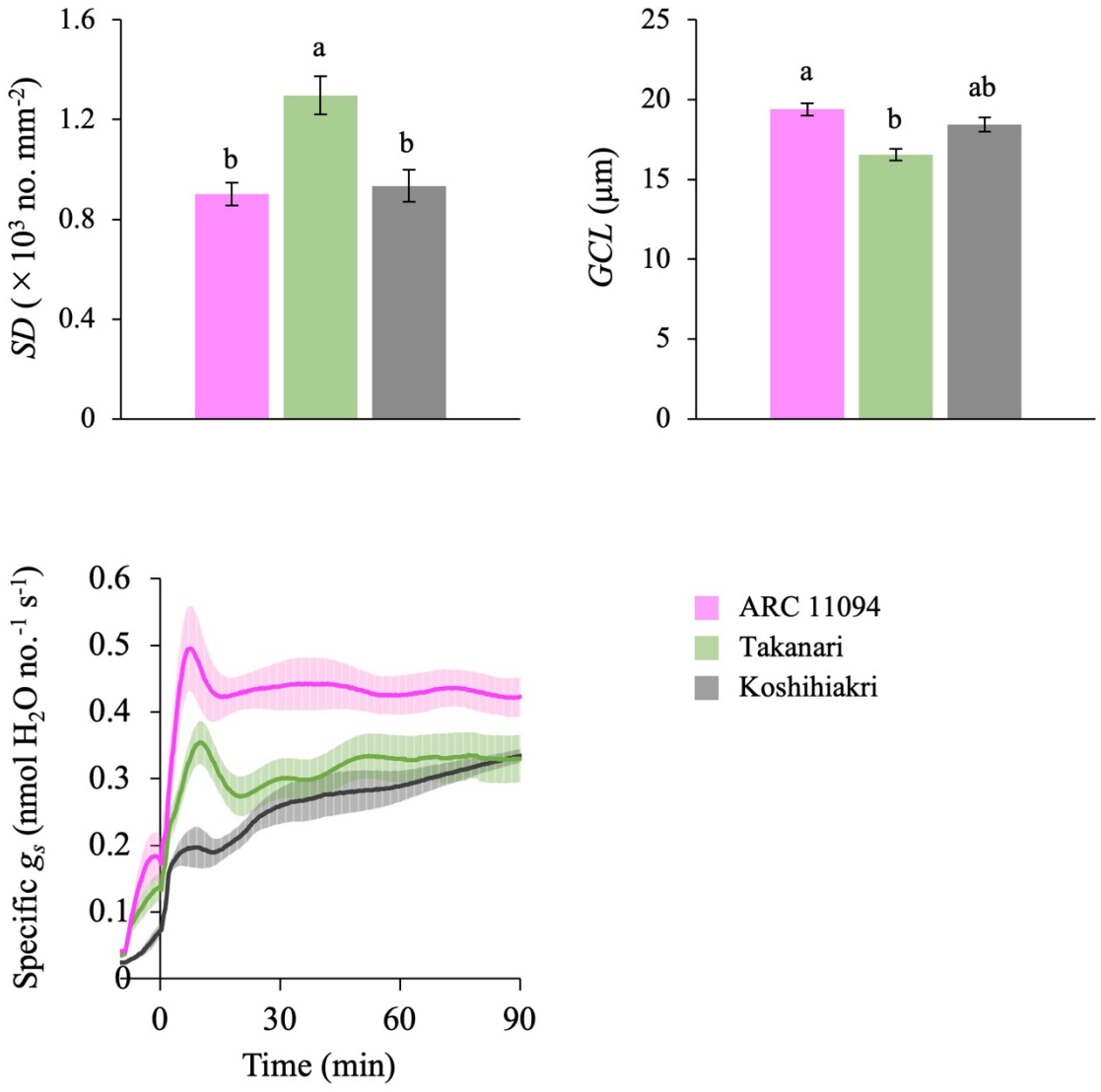

Fig. 3.6. Stomatal morphology and time courses of specific stomatal conductance to changes in light intensity. Stomatal density (*SD*) and guard cell length (*GCL*), and dynamics of specific stomatal conductance (g_s) were evaluated. Morphological traits of stomata was quantified with SUMP method. Specific g_s was calculated by dividing g_s, which was obtained from Fig. 3.2, by *SD*. Pink, green and gray show ARC 11094, Takanari and Koshihikari, respectively. Values are mean ± SE (n = 4-5). Lower-case letters represent significant differences among genotypes at $p < 0.05$ (Tukey-Kramer multiple comparison test).

The *LWP* and K_{plant} under saturating light tended to be lower in ARC 11094 than in Takanari and Koshihikari (Table 3.1). *E* and *E/Root* were measured under dark or low light for 10 minutes as an indicator of water transport efficiency from root to shoot. There was no apparent difference between the two light treatments in any genotype (Fig. 3.7). The *E* of Takanari was significantly higher than those of ARC 11094 and Koshihikari (Fig. 3.7). The *E/Root* of ARC 11094 was lower than those of Takanari and Koshihikari, and Takanari and Koshihikari showed similar values (Fig. 3.7). The total dry weight of Takanari was the highest, followed in order by Koshihikari and ARC 11094 (Fig. 3.7). Although the root dry weights of ARC 11094 and Takanari were significantly higher than that of Koshihikari, the shoot dry weight of ARC 11094 was lower than those of Takanari and Koshihikari, resulting in a remarkably higher root/shoot ratio in ARC 11094 (Fig. 3.7).

A, g_s, C_i and *T* of all genotypes showed a significant decrease approximately five minutes after the changing the osmotic potential (Fig. 3.8). However, the parameters of ARC 11094 recovered slightly and maintained higher values compared to the other two genotypes 10 minutes after the changing the osmotic potential (Fig. 3.8). On the other hand, *WUE* of all genotypes increased approximately five minutes after the changing the osmotic potential (Fig. 3.8). The increase of *WUE* in ARC 11094 was less than those in Takanari and Koshihikari (Fig. 3.8). A^* did not show apparent differences among genotypes (Fig. 3.8).

3.3.4 Yield and yield components

Grain yield of Takanari was greater than that of Koshihikari (Fig. 3.9). Panicle number per square meter was lower and spikelet number per panicle was higher in Takanari than Koshihikari, but the differences in above ground biomass, harvest index, filled grain ratio and

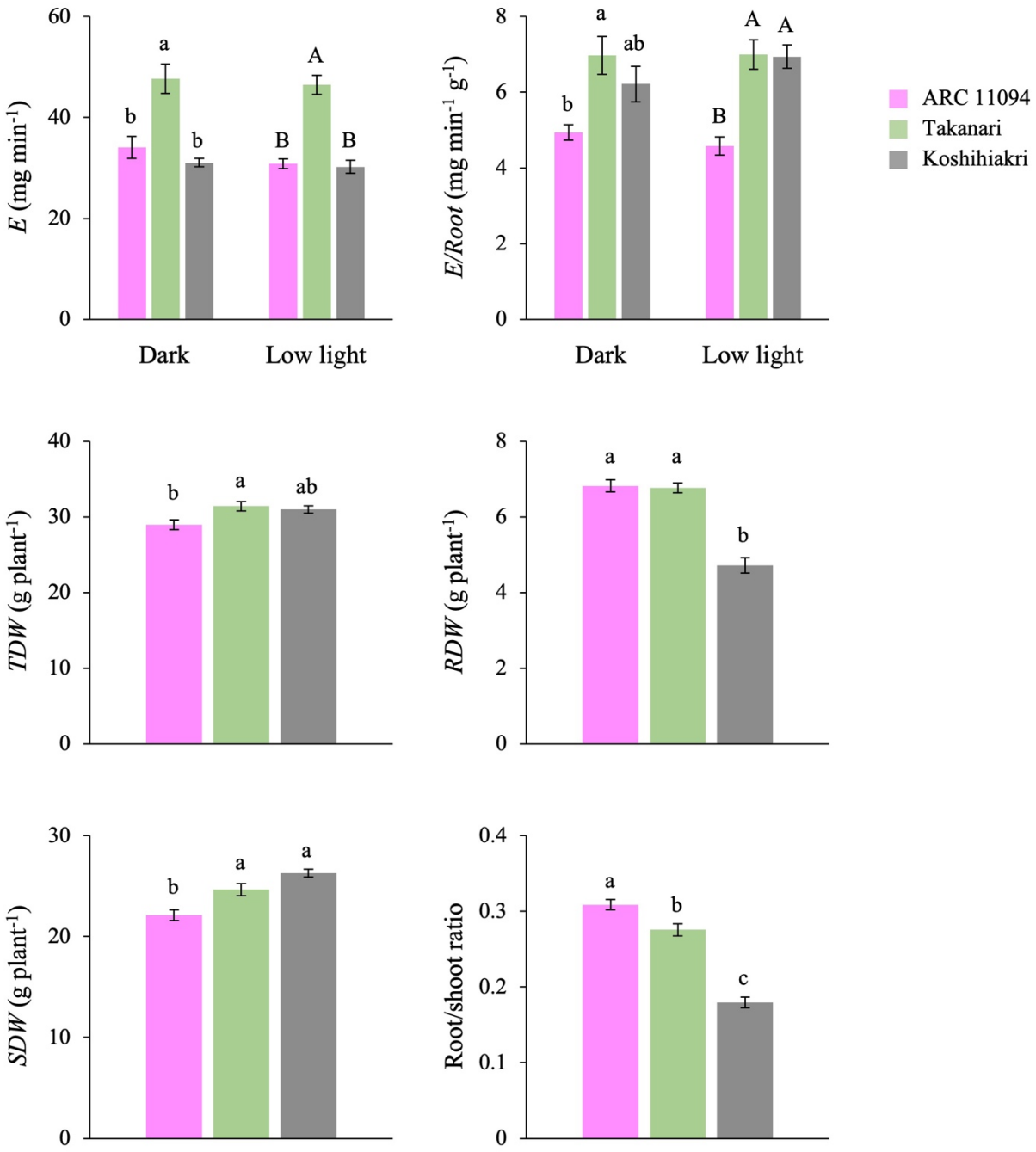

Fig. 3.7. Water uptake of the whole root system. Exudation rate per plant (*E*), normalized *E* to the root dry weight (*E/Root*), total, root or shoot dry weight and root/shoot ratio were measured. Exudates were collected for 30 minutes after cutting, and then exudation rates were calculated. Left and right in the graphs of *E* and *E/Root* represent the values at dark or 10 minutes after low light irradiation (50 µmol photons m^{-2} s^{-1}), respectively. *E/Root* was calculated by dividing *E* by root dry weight. Pink, green and gray show ARC 11094, Takanari and Koshihikari, respectively. Values are mean ± SE (n = 4 or 8). Letters represent significant differences among genotypes at $p < 0.05$ (Tukey-Kramer multiple comparison test).

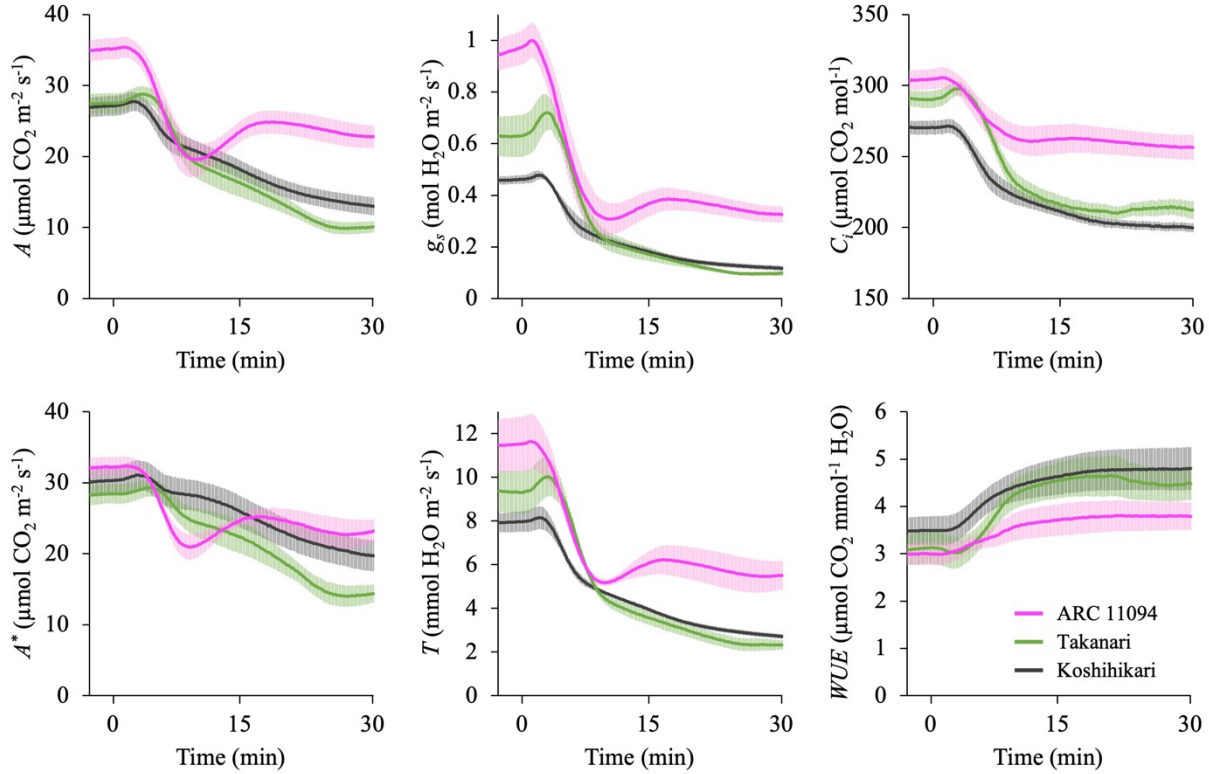

Fig. 3.8. Responses of photosynthetic parameters to osmotic stress. The dynamics of CO_2 assimilation rate (A), stomatal conductance (g_s), intercellular CO_2 concentration (C_i), normalized CO_2 assimilation rate to a C_i of 300 μmol mol^{-1} (A^*), transpiration rate (T) and water use efficiency (WUE) in response to changing osmotic potential were measured. Leaf chamber was kept at a photosynthetic photon flux density of 500 μmol photons m^{-2} s^{-1}, an air temperature of 30°C, a reference CO_2 concentration of 400 μmol mol^{-1} and a relative humidity of 55-70%. Photosynthetic parameters were recorded every 10 seconds when osmotic potential was changed with polyethylene glycol. Pink, green and gray show ARC 11094, Takanari and Koshihikari, respectively. Values are mean ± SE (n = 6).

1000-grain weight between Takanari and Koshihikari were not significant (Fig. 3.9). ARC 11094 showed significantly lower values in all parameters, except for panicle number per square meter, and higher value in panicle number per square meter than Takanari and Koshihikari (Fig. 3.9).

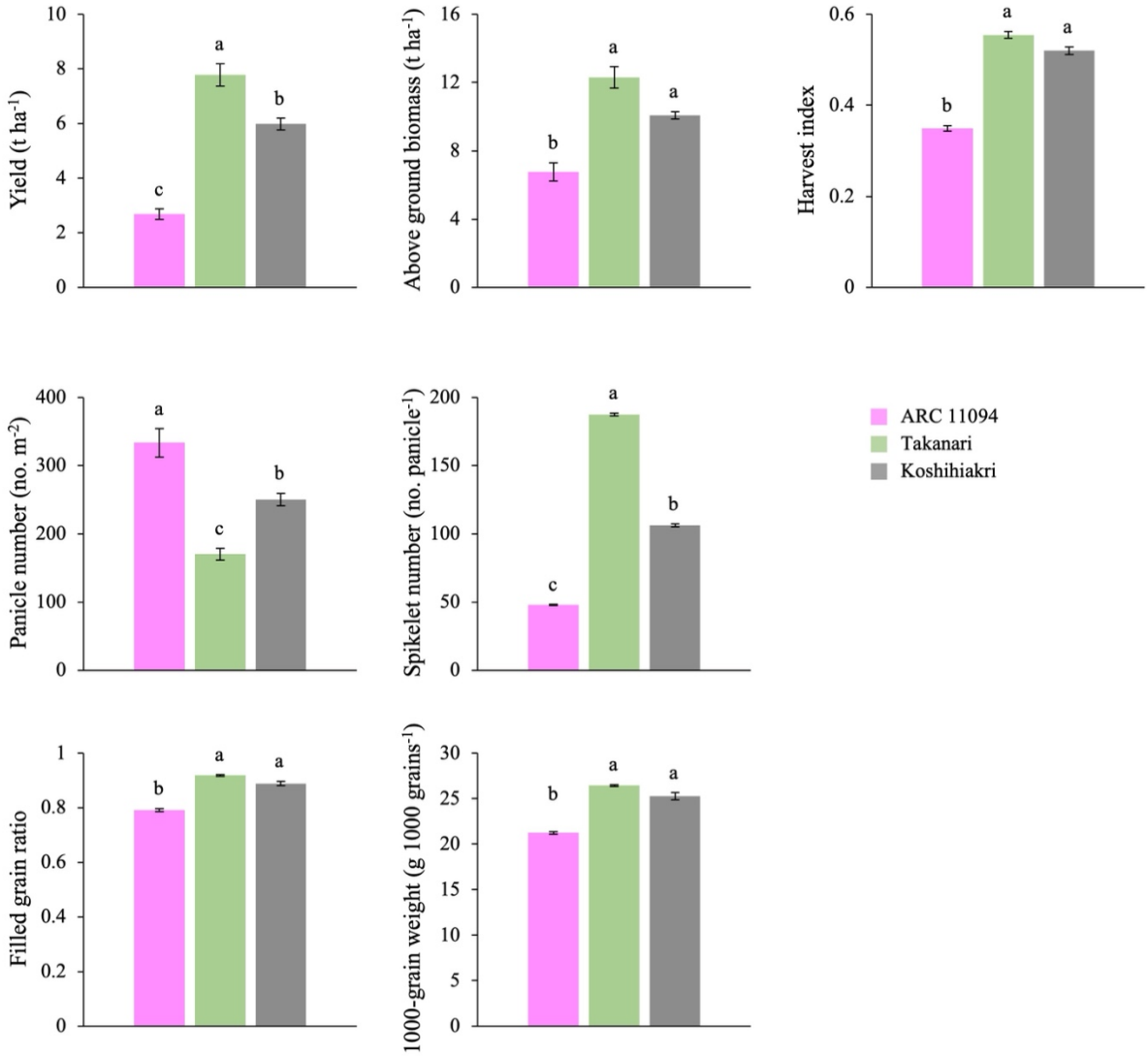

Fig. 3.9. Yield and yield components of plants grown under field. Grain yield, above ground biomass, harvest index, panicle number per square meter, spikelet number per panicle, filled grain ratio and 1000-grain weight were evaluated. These traits were measured at the maturity stage from ten plants with three replications. Filled grain was selected with water, and grain yield and 1000-grain weigh were adjusted to 14% moisture. Pink, green and gray show ARC 11094, Takanari and Koshihikari, respectively. Values are mean ± SE (n = 3). Lower-case letters represent significant differences among genotypes at $p < 0.05$ (Tukey-Kramer multiple comparison test).

3.4 Discussion

3.4.1 ARC 11094 and Takanari showed a rapid photosynthetic induction

ARC 11094 and Takanari showed a more rapid photosynthetic induction than

Koshihikari did. A^* and g_s demonstrated higher values in ARC 11094 and Takanari than in Koshihikari during the induction response (Fig. 3.2), suggesting that both of CO_2 diffusion and CO_2 fixation are more efficient in ARC 11094 and Takanari than Koshihikari. I investigated the dynamics of V_{Cmax} and J_{max}, *LNC*, Rubisco contents and *Chl a+b* as related traits to A^*, efficient CO_2 fixation in ARC 11094 and Takanari could not be explained by the differences in these parameters among the three genotypes. The other traits, such as Rubisco activation state or nitrogen distribution in leaves, might be different among the three genotypes, however, further investigation would be need to clarify the underlying mechanisms on the efficient CO_2 fixation in ARC 11094 and Takanari.

3.4.2 Stomatal morphology or single stomatal behaviour were related to the photosynthetic induction

The stomatal morphology was distinct among the three genotypes (Fig. 3.6). Takanari had a higher stomatal density and smaller stomatal size than ARC 11094 and Koshihikari (Fig. 3.6). These characteristics in Takanari have been reported to be advantageous for the response of g_s to fluctuating light (Faralli *et al*., 2019b; Sakoda *et al*., 2020b; Xiong *et al*., 2022a). The stomatal morphology of ARC 11094 was similar to that of Koshihikari (Fig. 3.6). Therefore, the contribution of a single stoma to g_s, such as stomatal aperture or pore depth, was significant in ARC 11094 compared to Takanari and Koshihikari (Fig. 3.6). Altogether, high g_s during the induction response is related to stomatal morphology in Takanari, but single stomatal behaviour in ARC 11094.

3.4.3 Greater root activity contributed to the rapid photosynthetic induction in Takanari

Root water uptake ability can affect leaf photosynthesis through leaf water potential

and g_s (Hirasawa, 1991; Taylaran *et al*., 2011). I investigated the exudation rate as parameters related to root activity. The *E* of Takanari was superior to that of Koshihikari under dark and low light conditions, which was attributed to the greater root mass (Fig. 3.7). These results are consistent with those of Taylaran *et al*. (2011) and imply that root activity contributes to the rapid response of g_s to a step increase in light intensity in Takanari. In ARC 11094, the root mass was similar to that in Takanari, resulting in the highest root/shoot ratio (Fig. 3.7). However, K_{plant} under high light intensity and *E/Root* under both of dark and low light conditions were lower in ARC 11094 than those in Takanari and Koshihikari (Table 3.1; Fig. 3.7). Since ARC 11094 could not utilise the large root mass efficiently, the water supply from roots to leaves was insufficient against large g_s, and the *LWP* under saturating light was low in ARC 11094 (Table 3.1). Taken together, great root activity due to large root mass would support the rapid stomatal response to high light in Takanari, while the response in ARC 11094 could not be explained in terms of water supply from roots to leaves.

3.4.4 Anisohydric stomatal behaviour contributed to the rapid photosynthetic induction in ARC 11094

Why can ARC 11094 realize the great g_s under the non-steady state even though water supply from roots to leaves is not efficient? In general, leaf water deficit induces hydroactive stomatal closure (Glinka, 1971; DeMichele & Sharpe, 1973; Buckley, 2019). Koshihikari showed a temporary setback of g_s during photosynthetic induction, which would be attributable to hydroactive stomatal closure (Fig. 3.2). However, Takanari did not demonstrate such a setback because of the great root activity (Fig. 3.2, 3.7). This stomatal behaviour of Koshihikari and Taknarari resemble the characteristics in isohydric plants (Tardieu & Simonneau, 1998; Moshelion *et al*., 2015). In contrast to Koshihikari and Takanari, ARC 11094 maintained higher

g_s after changing the osmotic potential (Fig. 3.8). This result indicates stomata of ARC 11094 is relatively unsusceptible to low leaf water potential compared to Takanari and Koshihikari, and has similar characteristics to those of anisohydric plants. Altogether, ARC 11094 may realize the rapid response of g_s to high light irradiation because of the anisohydirc stomatal behaviour. The dynamics of g_s probably caused by anisohydric characteristics was observed under field-mimicked environment. ARC 11094 showed maintained high g_s even late afternoon when leaf water potential declines, though g_s of Takanari decreased to near Koshihikari (Fig. 3.3).

These anisohydric characteristics may contribute to the rapid photosynthetic induction and significant carbon gain under field environments; however, the plant biomass production was low in ARC 11094 (Fig. 3.7, 3.9). Similar phenomena have been observed in previous studies using *slow anion channel-associated 1* (*slac1*) deficit rice or *STOMAGEN*-overexpressing *Arabidopsis* (Tanaka *et al*., 2013; Sakoda *et al*., 2020b; Yamori *et al*., 2020) and they discussed the possibility of adverse effects of water loss to plant biomass production. Considering these studies and the low *LWP* in ARC 11094 (Table 3.1), the limited water supply from roots to leaves compared with the transpiration from leaves may be one of the factors related to the low biomass in ARC 11094. However, anisohydric plants are reported to exhibit high biomass production under ample water supply in *Populus* genus (Attia *et al*., 2015). These results suggest that optimising the water balance at the whole-plant level, depending on the environments or objectives, is also important for enhancing biomass production by utilising the photosynthetic induction. Isohydric and anisohydric stomatal behaviours are thought to be related to abscisic acid biosynthesis or aquaporin expression (Gallé *et al*., 2013; Moshelion *et al*., 2015; Shelden *et al*., 2017); however, the detailed mechanism remains unclear.

3.4.5 Stomatal dynamics under dark and low light irradiation

Previous reports have shown that g_s immediately before high light irradiation is essential for subsequent photosynthetic induction (Soleh *et al*., 2017; Wachendorf & Küppers, 2017a,b). In the present study, ARC 11094 and Takanari showed significantly greater $g_{s,dark}$ than Koshihikari. The varietal order was consistent in $g_{s,0,}$ although it was not statistically significant (p = 0.057) (Fig. 3.2; Table 3.2). The *SLAC1* or *open stomata 1* (*OST1*) contributes to stomatal closure in response to abscisic acid and high CO_2 (Xue *et al*., 2011). The deficient mutants of these genes showed higher $g_{s,dark}$ than wild-type plants in *Arabidopsis* (Kimura *et al*., 2020) and could be regarded as anisohydric in that they maintain stomata open irrespective of water loss. In addition, the stomatal response induced by blue light occurs and is saturated under low light intensity (<5-10 μmol photons m^{-2} s^{-1}; Shimazaki *et al*., 2007; Matthews *et al*., 2020; Lawson & Matthews, 2020). Therefore, the sensitivity of stomata to abscisic acid, high CO_2 or blue light may be related to the high $g_{s,dark}$ or $g_{s,0}$ in ARC 11094 and Takanari. In ARC 11094, especially, initial stomatal responses to high light irradiation under high CO_2 concentration (600 and 800 ppm) were similar to that under ambient CO_2 concentration (400 ppm) (Fig. 3.4). This result supports the hypothesis that ARC 11094 has similar behaviour to *slac1* or *ost1* deficient mutant, or anisohydric plants on the stomatal response to increases in light intensity. If the genetic factors and molecular mechanisms for the rapid photosynthetic induction of ARC 11094 are elucidated, a suitable approach to improve stomatal characteristics can be devised.

3.4.6 Conclusion

In conclusion in Chapter 3, I characterized the physiological underlying factors on natural genetic variation of photosynthetic induction using three rice genotypes. ARC 11094 and Takanari showed more efficient CO_2 diffusion during the induction response than

Koshihikari. The efficient CO_2 diffusion in Takanari was related to stomatal density, stomatal size and root mass. The efficient CO_2 diffusion of ARC 11094 was related to stomatal aperture or pore depth. Additionally, ARC 11094 showed the anisohydric stomatal behaviour and maintained stomatal opening under water-insufficient conditions in leaves. As shown in the present thesis, there are various strategies for rapid photosynthetic induction, and ARC 11094 has the unique mechanism for stomatal response to fluctuating light environments in terms of water relations. Understanding and combining these characteristics could lead to further rapid photosynthetic induction and improve crop productivity in field environments.

Chapter 4

Differences in photosynthetic induction among rice subspecies and the related ecophysiological factors

4.1 Introduction

Photosynthetic induction is thought to be important for not only crop carbon gain but also plant adaptation to various environments under field conditions. In Chapter 2, I found the possibility that the *temperate japonica* has a slow photosynthetic induction compared with *indica* and *tropical japonica* (Fig. 2.3). Qu *et al*. (2016) described that there would be differences of stomatal dynamics under fluctuating light conditions between rice subpopulations; *aromatic*, *aus*, *indica*, *temperate japonica* and *tropical japonica*. The details of the differences have to be elucidated for utilizing the natural genetic variation of photosynthetic induction in future breeding programs.

Rice Core Collection of Japanese Landraces (JRC) developed by Ebana *et al*. (2008) is consist of 5 *indica*, 33 *temperate japonica* and 12 *tropical japonica* genotypes, and a suitable tool to understand the rice adaptation in northern areas. I thought that investigation of the natural genetic variation in photosynthetic induction among JRC and a combined-analysis with both of the results in WRC (Chapter 2) and JRC unveil the difference in photosynthetic induction between rice subspecies; *indica*, *temperate japonica* and *tropical japonica*. In addition, I also considered the results of measurement by the author conducted with 166 *temperate japonica* rice cultivars developed in Japan.

In Chapter 4, I investigated the natural genetic variation in photosynthetic induction among 50 JRC genotypes with two reference cultivars; Koshihikari and Takanari. Firstly, I

evaluated the overall trends about the photosynthetic induction and other related traits in only JRC as similar to Chapter 2. Then, I discussed the difference in photosynthetic induction between rice subspecies.

4.2 Materials and Methods

4.2.1 Plant materials and cultivation procedures

I used 50 genotypes of JRC with two reference cultivars: Koshihikari and Takanari. The 50 genotypes of JRC is consist of 5 *indica*, 33 *temperate japonica* and 12 *tropical japonica*, and the genetic diversity in JRC seems smaller than that in WRC (Ebana *et al*., 2007; Tanaka *et al*., 2020b). Koshihikari is a popular rice cultivar in Japan and classified into *temperate japonica*. Takanari is a high-yielding rice cultivar and classified into *indica*, and has superior photosynthetic response to fluctuating light than Koshihikari (Adachi *et al*., 2019b; Ohkubo *et al*., 2020; Chapter 2 in the present thesis). Seeds of all genotypes were sown in nursery boxes on 27 April 2021 and the seedlings were transplanted into 2 L plastic pots filled with alluvial loam soil on 19 May 2021. Four plants of each genotype were grown at an experimental field in the Graduate School of Agriculture, Kyoto University, Japan. Fertilizer and water management were followed as Chapter 2.

4.2.2 Gas exchange rate and chlorophyll fluorescence measurements

Gas exchange rate and chlorophyll fluorescence in response to a stepwise increase in light intensity were measured simultaneously with three portable gas exchange analyzers, LI-6800 (Li-Cor Biosciences, Lincoln, NE, USA) in the morning at 59-63 days after sowing. The uppermost fully expanded leaf was selected from four plants per genotype for the measurement of photosynthetic induction and capacity. To observe the photosynthetic induction, plants were

placed in the dark room from the previous evening until the measurement. Condition of the leaf chamber was set to T_{air} of 30°C, CO_2R of 400 µmol mol^{-1} and RH of 55-70%. The PPFD was set to 50 µmol photons m^{-2} s^{-1} (low light) for the first four minutes, and was changed to 1500 µmol photons m^{-2} s^{-1} (high light) for the following 10 minutes. *A*, g_s, C_i, A^*, *T* and *WUE* were recorded every 10 seconds, and *ETR* and *NPQ* were recorded every two minutes. The calculation of A^*, *WUE*, *ETR*, *NPQ*, CCF_{10} and CWL_{10} were conducted following the method in Chapter 2.

The A_{sat} was measured as photosynthetic capacity at 55 days after sowing. Leaf chamber was controlled at PPFD of 1500 µmol photons m^{-2} s^{-1}, T_{air} of 30°C, CO_2R of 400 µmol mol^{-1} and RH of 55-70%. Four plants from each genotype were selected for A_{sat} measurements.

4.2.3 Leaf nitrogen and chlorophyll contents

LNC and *Chl a+b* were quantified as related traits to CO_2 fixation. The leaves used for the measurement of photosynthetic induction were cut at the collar for quantification of *LNC, Chl a+b* and stomatal morphology (described below). A 0.5 cm^2 leaf tissue was apart from each leaf for *Chl a+b*, and the other part of leaf was used for stomatal morphology, and then for *LNC*. The quantification of *LNC* was conducted following the method in Chapter 2. To extract the chlorophyll, the leaf tissues were soak into 1.5 ml N,N-dimethylformamide (DMF) over 24 hours. The calculation of *Chl a+b* was conducted as follows (Porra *et al*. 1989);

$$Chl\ a + b = 17.67(A^{646.8} - A^{750}) + 7.12(A^{663.8} - A^{750}) \quad (4\text{-}1)$$

where the unit of *Chl a+b* is µg ml^{-1}, and $A^{646.8}$, $A^{663.8}$ and A^{750} are the absorbance of the solutions at 646.8, 663.8 and 750 nm, respectively.

4.2.4 Stomatal morphology

Stomatal morphology (*SD* and *GCL*) were quantified as related traits to CO_2 diffusion. Preparation and observation of replicas of the adaxial and abaxial leaf surfaces were conducted following the method in Chapter 3, and one microscopic image was obtained for each replica. The *SD* and *GCL* for each leaf was the sum and average of both surfaces, respectively.

4.2.5 Biomass production

All plants of 50 JRC genotypes were sampled at 64-65 days after sowing. After removing the roots, samples were dried at 80°C more than 72 hours and then weighed as shoot dry weight (*SDW*).

4.2.6 Statistical analysis

The values of all parameters were averaged between individual plants of each genotype and the standard error was calculated. The Tukey–Kramer multiple comparison test was used to compare the means. The relationship between several parameters was evaluated according to the Pearson correlation coefficient. All analyses were performed using Microsoft Excel (Microsoft, Redmond, WA) and the R software (R Core Team, 2018). In a combined-analysis with WRC and JRC, all parameters were normalized, considering the values of Koshihikari in each year as 1. Steel–Dwass test was used to compare the means between subspecies using the normalized parameters. Principal component analysis (PCA) was performed on the normalized parameters in WRC and JRC using the prcomp function in the 'stats' package in R software.

4.2.7 An extra measurement of photosynthetic induction with 166 temperate japonica

We measured the photosynthetic induction in 166 *temperate japonica* rice cultivars, which have been cultivated with a certain share or used as parents of popular cultivars in Japan.

Six replications of each cultivar were grown at an experimental field in the College of Agriculture, Ibaraki University, Japan. Other cultivation managements were similar to the above.

Measurement of photosynthetic induction was conducted with eight portable gas exchange analyzers, LI-6400 (Li-Cor Biosciences, Lincoln, NE, USA) in the morning at 56-62 days after sowing. The PPFD of leaf chambers was set to 50 μmol photons m^{-2} s^{-1} (low light) for the first five minutes, and was changed to 1500 μmol photons m^{-2} s^{-1} (high light) for the following 10 minutes. Other conditions of leaf chambers were similar to above. Photosynthetic parameters (A, g_s, C_i, A^*, T and WUE) were recorded every five seconds.

4.3 Results

4.3.1 Difference of photosynthetic induction among genotypes in JRC

Overall trend of photosynthetic dynamics in response to high light irradiation was similar to the results in Chapter 2; that is, the genotypes which displayed superior responses of A tended to have relatively high g_s, A^*, T, ETR and low NPQ values (Fig. 4.1). Koshihikari showed a slow photosynthetic induction and its CCF_{10} value was 2.8 mmol CO_2 m^{-2}, while Takanari showed a rapid photosynthetic induction and its CCF_{10} values were 10.3 mmol CO_2 m^{-2} (Fig. 4.1, 4.2). The dynamics of photosynthetic parameters and the CCF_{10} differed between genotypes, and the lowest or highest values of CCF_{10} among 50 JRC genotypes were 0.12 mmol CO_2 m^{-2} for Aikoku or 10.7 mmol CO_2 m^{-2} for Meguromochi, respectively (Fig. 4.2). Meguromochi was an only genotype, which showed greater CCF_{10} than Takanari. Although the ranges of the three subspecies overlapped with each other, the mean CCF_{10} of *temperate japonica* was significantly lower than those of *indica* and *tropical japonica* (Fig. 4.3).

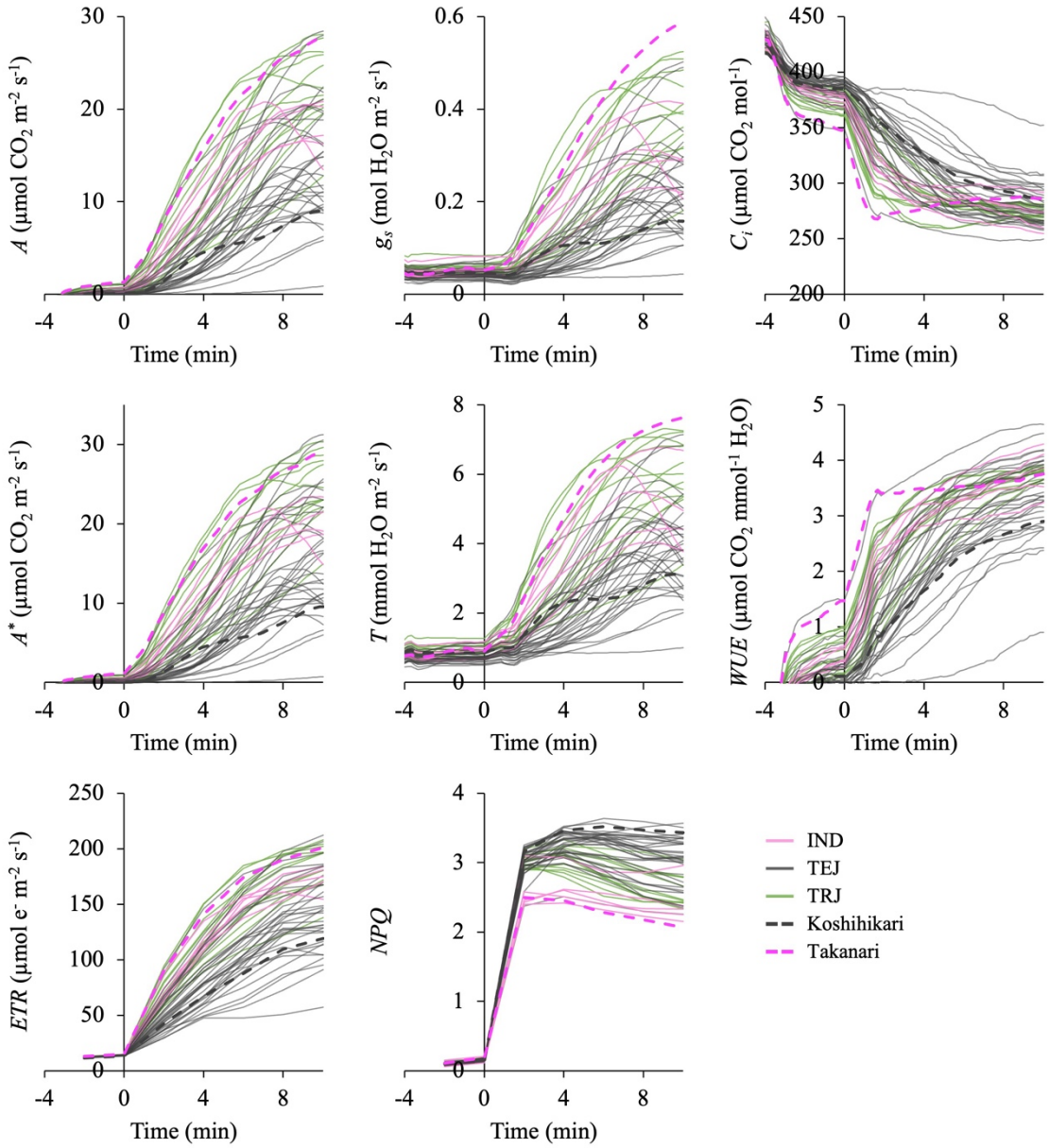

Fig. 4.1. Time courses of photosynthetic parameters in response to a stepwise increase in light intensity in 52 rice genotypes. The dynamics of CO_2 assimilation rate (A), stomatal conductance (g_s), intercellular CO_2 concentration (C_i), normalized CO_2 assimilation rate to a C_i of 300 μmol mol^{-1} (A^*), transpiration rate (T), water use efficiency (WUE), photosynthetic electron transport rate around photosystem II (ETR) and non-photochemical quenching (NPQ) were measured in 52 rice genotypes. Leaf chamber was kept at an air temperature of 30°C, a reference CO_2 concentration of 400 μmol mol^{-1} and a relative humidity of 55-70%. The photosynthetic photon flux density was changed from dark to 50 μmol photons m^{-2} s^{-1} for the first 4 minutes, and then to 1500 μmol photons m^{-2} s^{-1} for the following 10 minutes. Gas exchange rate (A, g_s, C_i, A^*, T and WUE) or chlorophyll fluorescence parameters (ETR and NPQ) were recorded every 10 seconds or 2 minutes, respectively. Pink, gray and green represent the values of genotypes in *indica* (IND), *temperate japonica* (TEJ) and *tropical japonica* (TRJ), respectively. Gray and pink dashed lines show Koshihikari and Takanari, respectively. The values were averaged between four replications of each genotype.

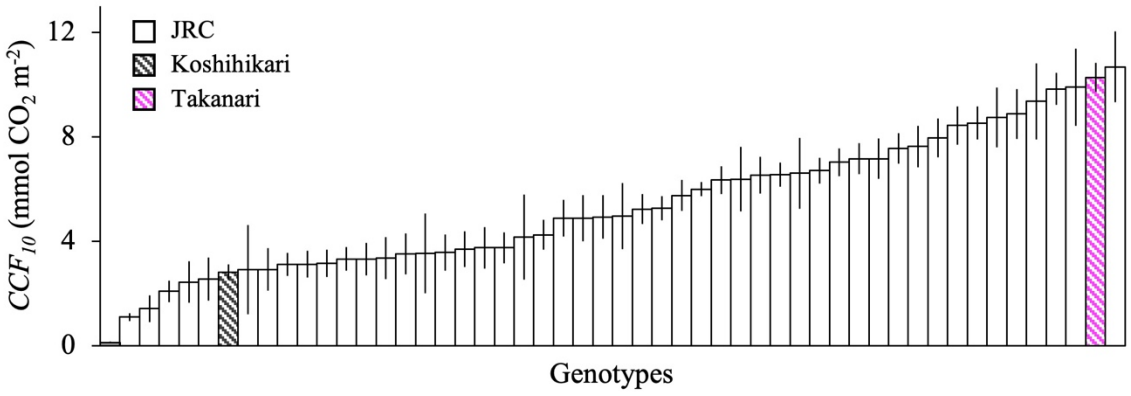

Fig. 4.2. Carbon gain during the photosynthetic induction in 52 rice genotypes. The cumulative CO_2 fixation during the first 10 minutes of the photosynthetic induction (CCF_{10}) was calculated. Gray and pink stripe bars show Koshihikari and Takanari, respectively. The values are mean ± SE (n = 4).

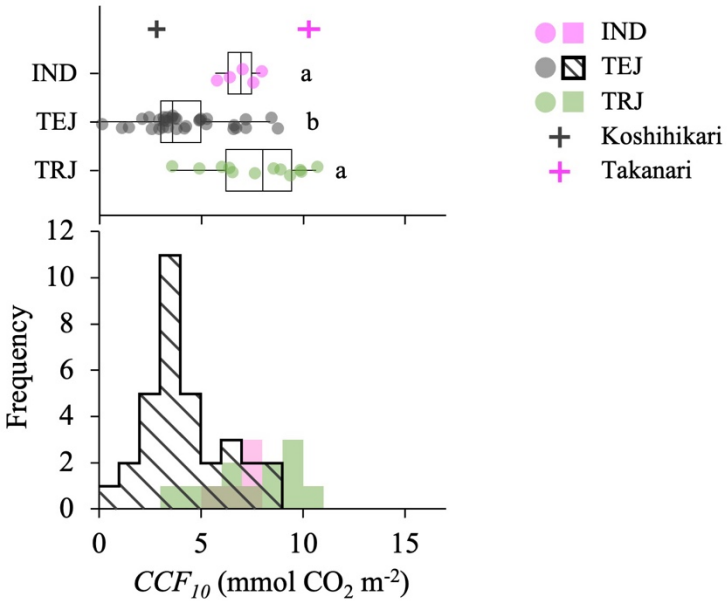

Fig. 4.3. Distribution of carbon gain during the photosynthetic induction in JRC genotypes. The distribution of cumulative CO_2 fixation during the first 10 minutes of the photosynthetic induction (CCF_{10}) in 50 JRC genotypes was described as a histogram and boxplot. The histogram was generated by overlapping the distribution of *indica* (pink), *temperate japonica* (black border) and *tropical japonica* (green). Pink, gray and green dots in the boxplot represent the values of genotypes in *indica* (IND), *temperate japonica* (TEJ) and *tropical japonica* (TRJ), respectively. The values for Koshihikari and Takanari were presented by crosses in gray and pink, respectively. The vertical and horizontal bars indicate the mean values and SE, respectively. The values were obtained from Fig. 4.2. Lower-case letters in the boxplot represent significant differences between subspecies at $p < 0.05$ (Tukey–Kramer multiple comparison test).

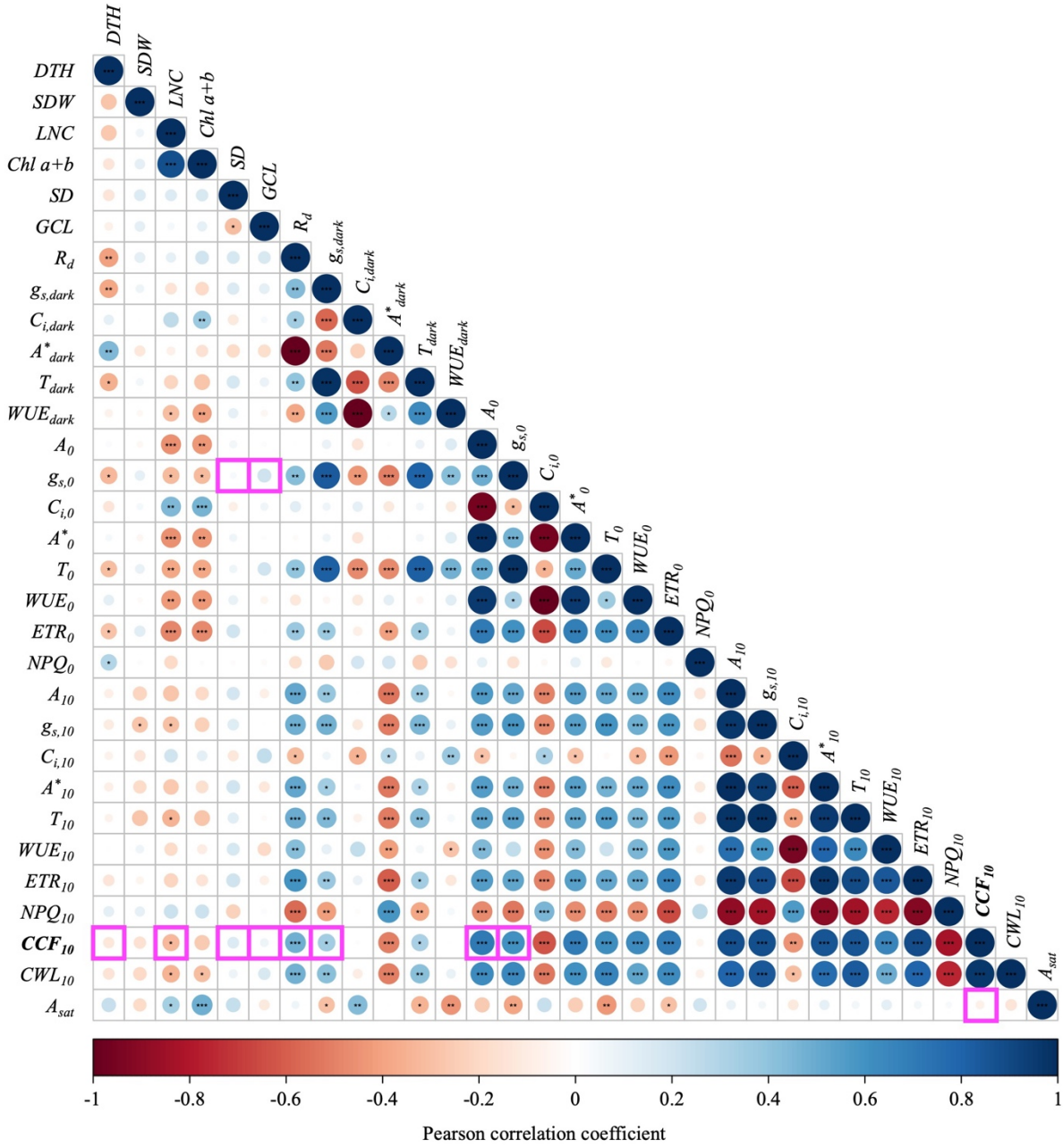

Fig. 4.4. Correlation matrix between photosynthetic induction and related parameters in 50 JRC genotypes. The correlation between days to heading after sowing (*DTH*); shoot dry weight (*SDW*); leaf nitrogen content per leaf area (*LNC*); chlorophyll contents per leaf area (*Chl a+b*); stomatal density (*SD*); guard cell length (*GCL*); the values under dark, just before the transition from low to high light or 10 minutes after high light irradiation for CO_2 assimilation rate (dark respiration rate; R_d, A_0 and A_{10}); stomatal conductance ($g_{s,dark}$, $g_{s,0}$ and $g_{s,10}$); intercellular CO_2 concentration ($C_{i,dark}$, $C_{i,0}$ and $C_{i,10}$); normalized CO_2 assimilation rate to a C_i of 300 µmol mol^{-1} (A^*_{dark}, A^*_0 and A^*_{10}); transpiration rate (T_{dark}, T_0 and T_{10}); water use efficiency (WUE_{dark}, WUE_0 and WUE_{10}); photosynthetic electron transport rate around photosystem II (ETR_{dark}, ETR_0 and ETR_{10}) and non-photochemical quenching (NPQ_{dark}, NPQ_0 and NPQ_{10}); cumulative CO_2 fixation during the first 10 minutes of the photosynthetic induction (CCF_{10}); cumulative water loss during the first 10 minutes of the photosynthetic induction (CWL_{10}); light-saturating CO_2 assimilation rate under steady state (A_{sat}) were analyzed. The color gradients from red to blue represent the range of Pearson correlation coefficient from -0.1 to 1.0 across 50 JRC genotypes. *, ** and *** represent a significant correlation at $p < 0.05$, 0.01 and 0.001, respectively.

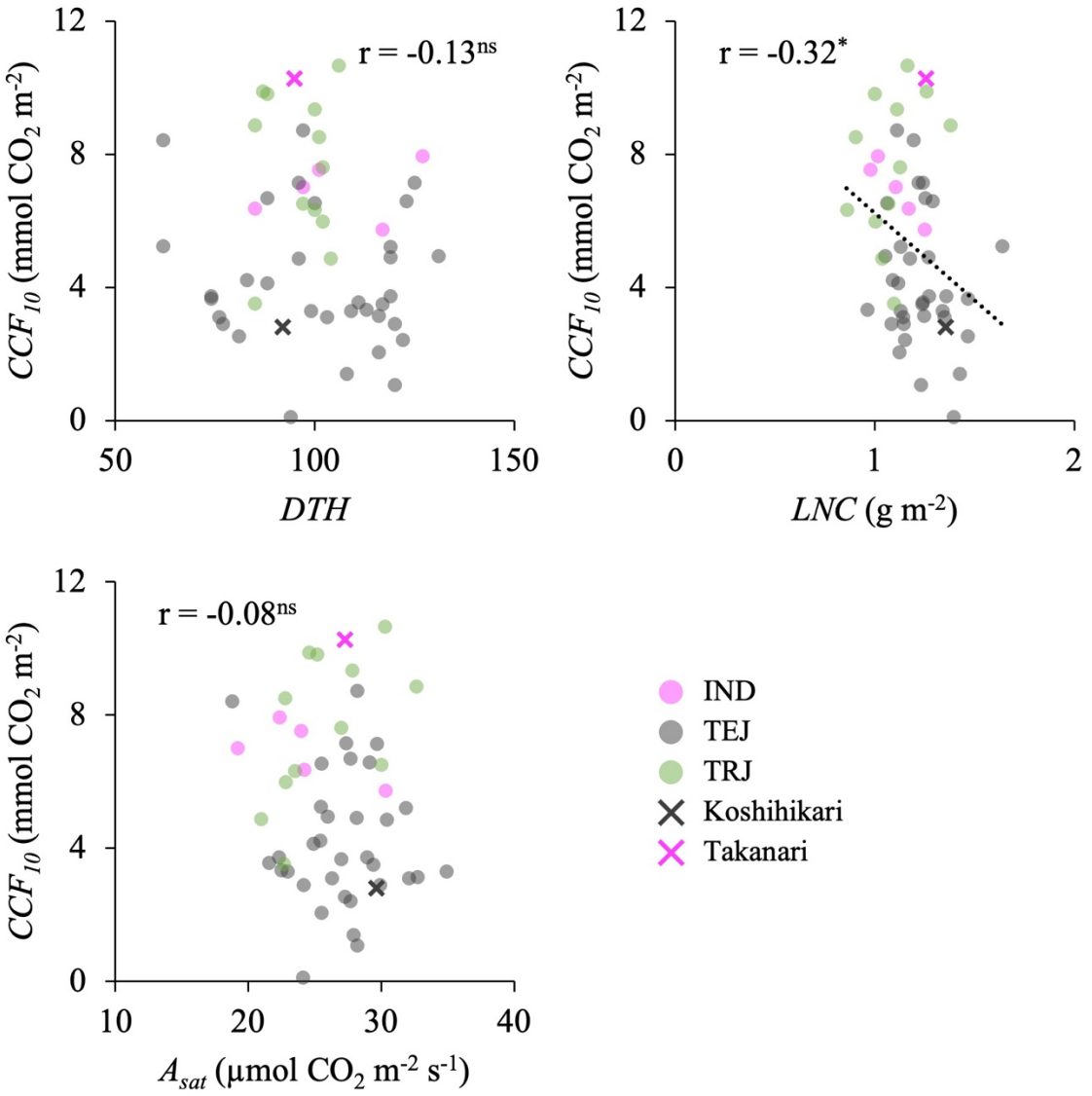

Fig. 4.5. Relationships between carbon gain during the photosynthetic induction, and heading days, leaf nitrogen contents or photosynthetic capacity. Relationships between cumulative CO_2 fixation during the first 10 minutes of the photosynthetic induction (CCF_{10}), and days to heading after sowing (*DTH*), leaf nitrogen contents per leaf area (*LNC*) or light-saturating CO_2 assimilation rate under steady state (A_{sat}) were evaluated. Pink, gray and green closed circles represent the values of genotypes in *indica* (IND), *temperate japonica* (TEJ) and *tropical japonica* (TRJ), respectively. Gray and pink cross show Koshihikari and Takanari, respectively. The values of *LNC* were averaged between four replications of each genotype, and the values of A_{sat} were averaged between three replications of each genotype. The r value was calculated among 50 JRC genotypes based on Pearson correlation coefficient. * represents a significant correlation at $p < 0.05$ and ns represents a not significant correlation at $p < 0.05$.

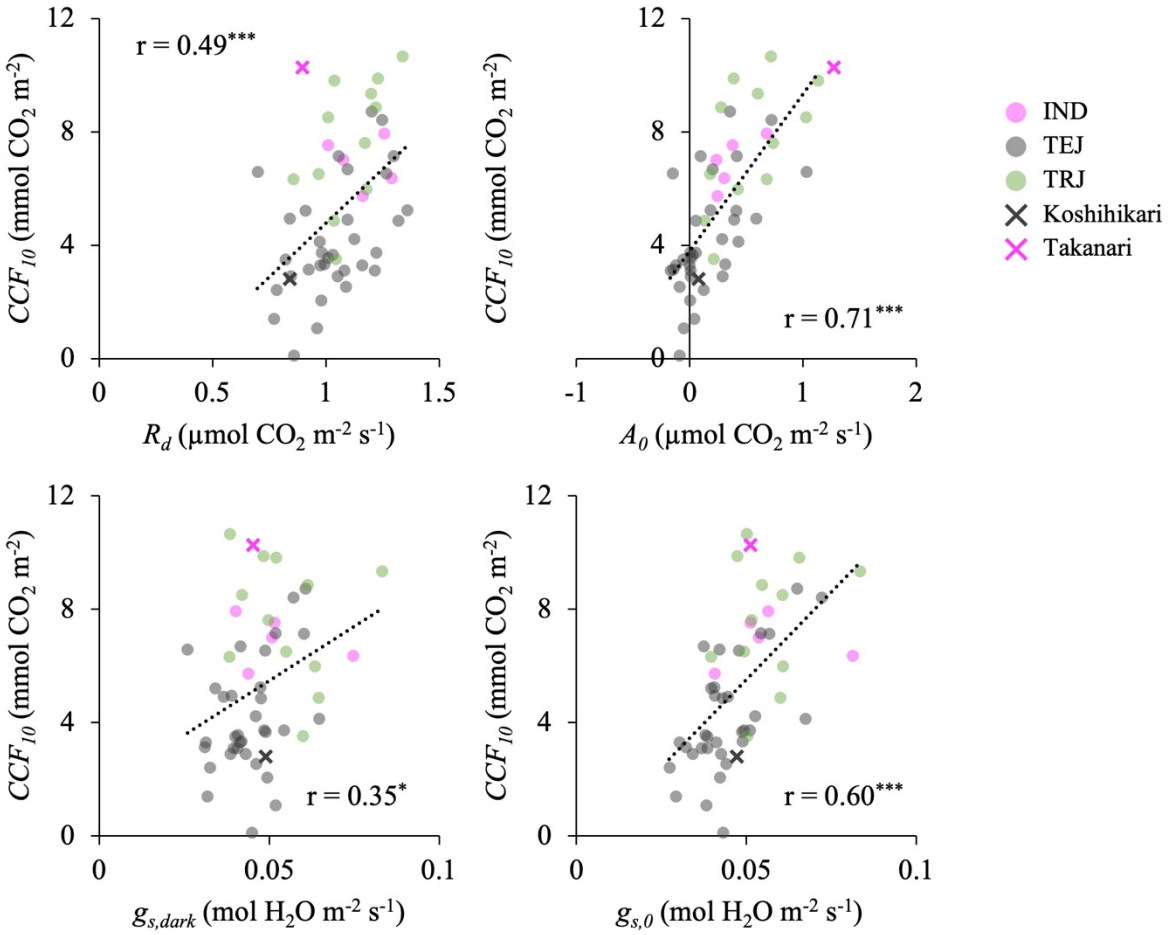

Fig. 4.6. Relationships between carbon gain during the photosynthetic induction and photosynthetic parameters under dark or just before the transition from low to high light. Relationships between cumulative CO_2 fixation during the first 10 minutes of the photosynthetic induction (CCF_{10}) and the values under dark or just before the transition from low to high light in CO_2 assimilation rate (dark respiration rate; R_d, A_0) and stomatal conductance ($g_{s,dark}$, $g_{s,0}$) were evaluated. Pink, gray and green closed circles represent the values of genotypes in *indica* (IND), *temperate japonica* (TEJ) and *tropical japonica* (TRJ), respectively. Gray and pink cross show Koshihikari and Takanari, respectively. The values were averaged between four replications of each genotype. The r value was calculated among 50 JRC genotypes based on Pearson correlation coefficient. *, *** represents a significant correlation at $p < 0.05$, $p < 0.001$.

4.3.2 The relationship between photosynthetic induction and related parameters in JRC

As similar to Chapter 2, I showed a correlation matrix among studied traits in this chapter to evaluate the relationship between photosynthetic induction and related parameters (Fig. 4.4), then focused on several relationships and showed their scatterplots.

There was no significant correlation in CCF_{10} with *DTH*, *LNC* and A_{sat} (Fig. 4.4, 4.5),

while CCF_{10} was positively correlated with R_d, A_0, $g_{s,dark}$ and $g_{s,0}$ (Fig. 4.4, 4.6). Both of *SD* and *GCL* did not show significant correlations with CCF_{10} and $g_{s,0}$ (Fig. 4.4, 4.7).

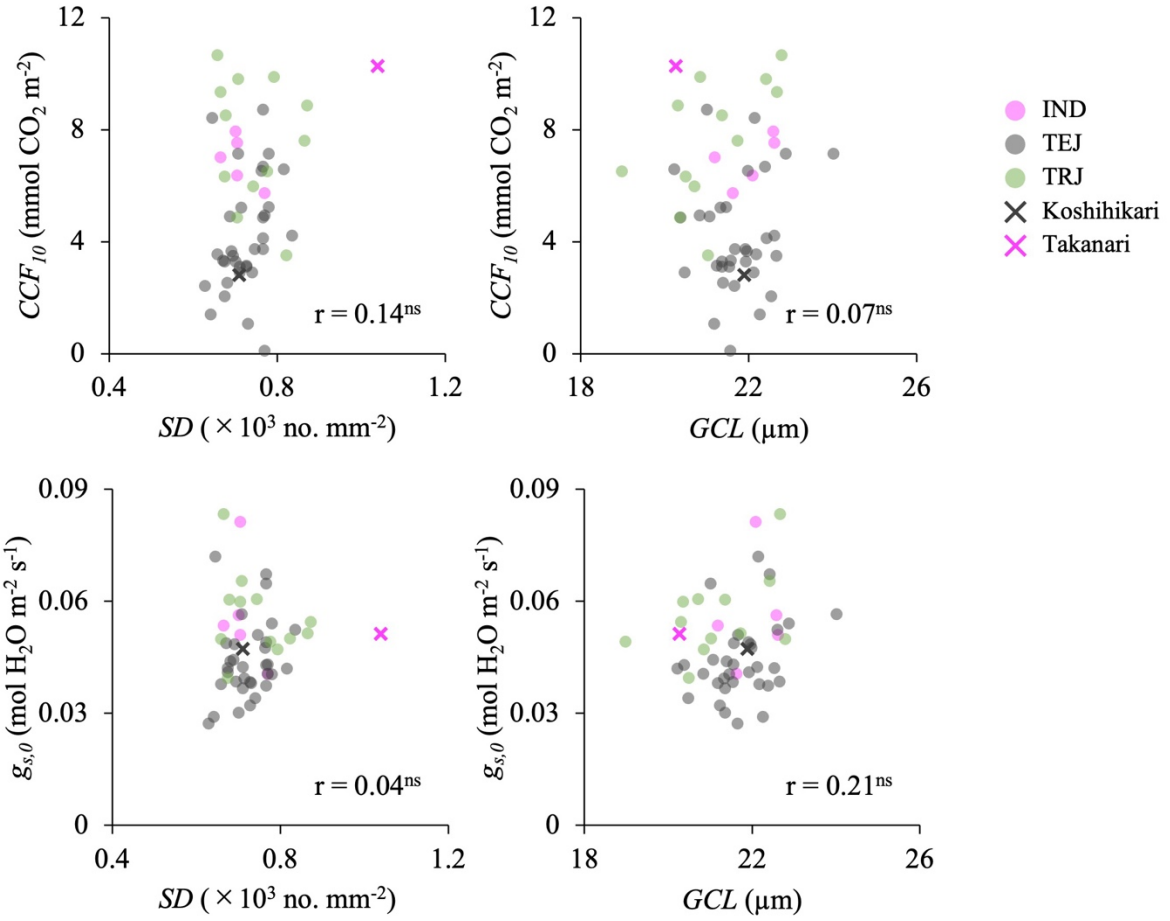

Fig. 4.7. Relationships between photosynthetic induction and stomatal morphology. Relationships between cumulative CO_2 fixation during the first 10 minutes of the photosynthetic induction (CCF_{10}), stomatal conductance just before the transition from low to high light ($g_{s,0}$), and stomatal density (*SD*) or guard cell length (*GCL*) were evaluated. Pink, gray and green closed circles represent the values of genotypes in *indica* (IND), *temperate japonica* (TEJ) and *tropical japonica* (TRJ), respectively. Gray and pink cross show Koshihikari and Takanari, respectively. The values were averaged between four replications of each genotype. The r value was calculated among 50 JRC genotypes based on Pearson correlation coefficient. ns represents a not significant correlation at $p < 0.05$.

4.3.3 Difference in photosynthesis among rice subspecies

I investigated the difference of photosynthesis between *indica*, *temperate japonica* and

tropical japonica with the combined-analysis on 57 WRC and 50 JRC genotypes. The distribution of A_{sat} was similar among rice subspecies and there was no significant difference (Fig. 4.8). Most *temperate japonica* genotypes showed lower CCF_{10} and CWL_{10}, and the mean value in *temperate japonica* were significantly lower than those in *indica* and *tropical japonica* (Fig. 4.8).

I performed a PCA to visualize the difference of photosynthetic induction between rice subspecies. The first principal component (PC1) explained 47.3% of the variance and the second principal component (PC2) explained 13.3% of the variance (Fig. 4.9). Most genotypes in *indica* and *tropical japonica* showed higher PC1 scores, while most *temperate japonica* showed lower PC1 scores (Fig. 4.9). The range of PC2 scores in *temperate japonica* and *tropical japonica* were similar, but *indica* showed lower PC2 scores than those of other two subspecies (Fig. 4.9). ARC 11094, which had a most rapid photosynthetic induction among 107 rice genotypes, was located with low PC1 score and high PC2 score (Fig. 4.9). Aikoku, which had a slowest photosynthetic induction among 107 rice genotypes, was located with low PC1 and PC2 scores (Fig. 4.9).

4.3.4 Photosynthetic induction 166 temperate japonica rice cultivars developed in Japan

There is a variation in the photosynthetic induction among 166 *temperate japonica* rice cultivars developed in Japan. The range of CCF_{10} in 166 *temperate japonica* rice cultivars skewed to lower compared with the range of CCF_{10} in 57 WRC or 50 JRC genotypes. The CCF_{10} in 166 *temperate japonica* rice cultivars showed correlation weakly and negatively with release year of the cultivars.

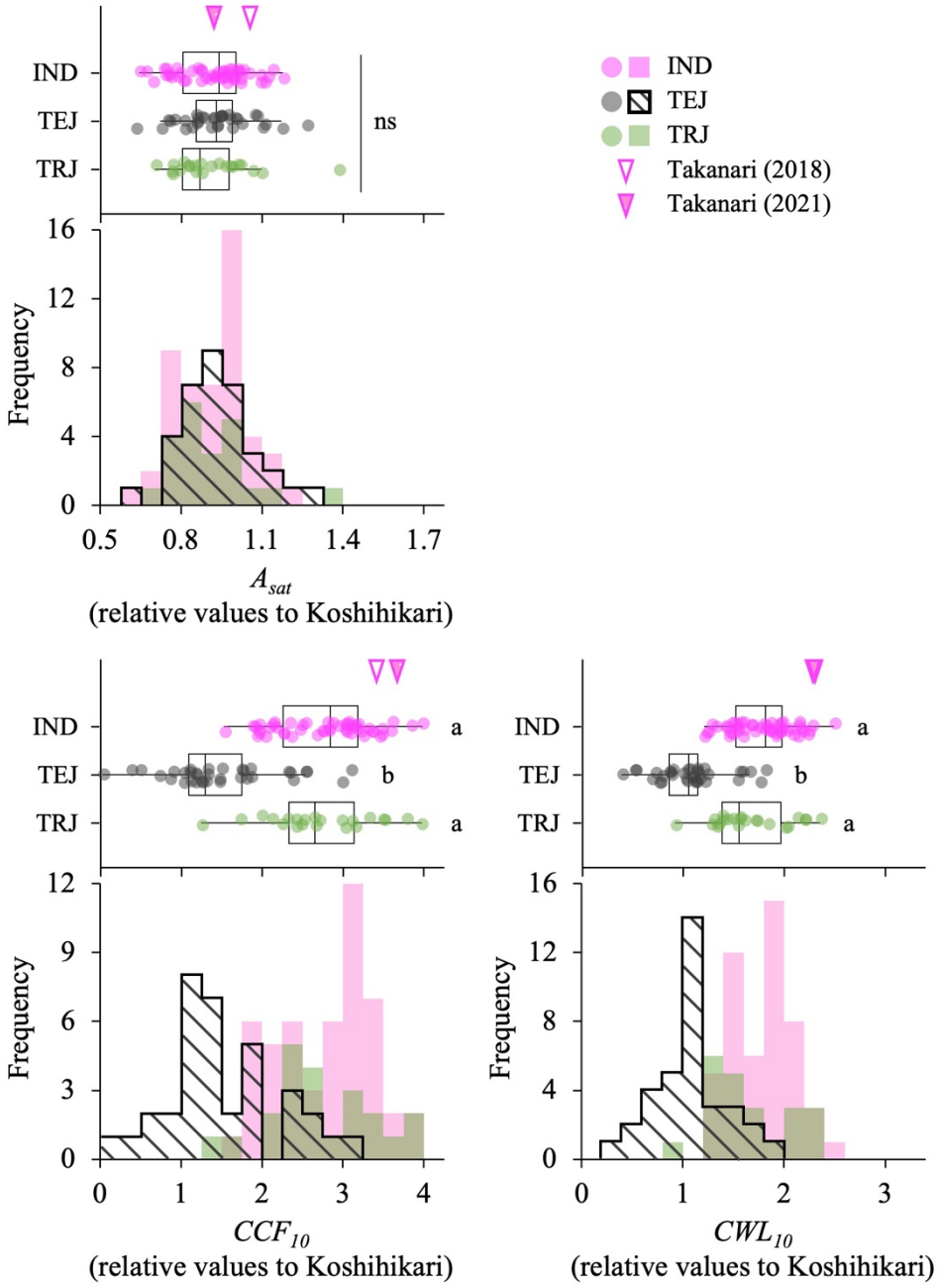

Fig. 4.8. Differences of photosynthesis under steady and non-steady state between rice subspecies. The distributions of light-saturating CO_2 assimilation rate under steady state (A_{sat}), cumulative CO_2 fixation during the first 10 minutes of the photosynthetic induction (CCF_{10}) and cumulative water loss during the first 10 minutes of the photosynthetic induction (CWL_{10}) in 107 rice genotypes were described as a histogram and boxplot. All parameters were normalized, considering the value of Koshihikari as 1. The histogram was generated by overlapping the distribution of *indica* (pink), *temperate japonica* (black border) and *tropical japonica* (green). Pink, gray and green dots in the boxplots represent the values of genotypes in *indica* (IND), *temperate japonica* (TEJ) and *tropical japonica* (TRJ), respectively. Inverted triangles represent the values of Takanari. Lower-case letters in the boxplots represent significant differences between subspecies at $p < 0.05$ (Steel–Dwass test).

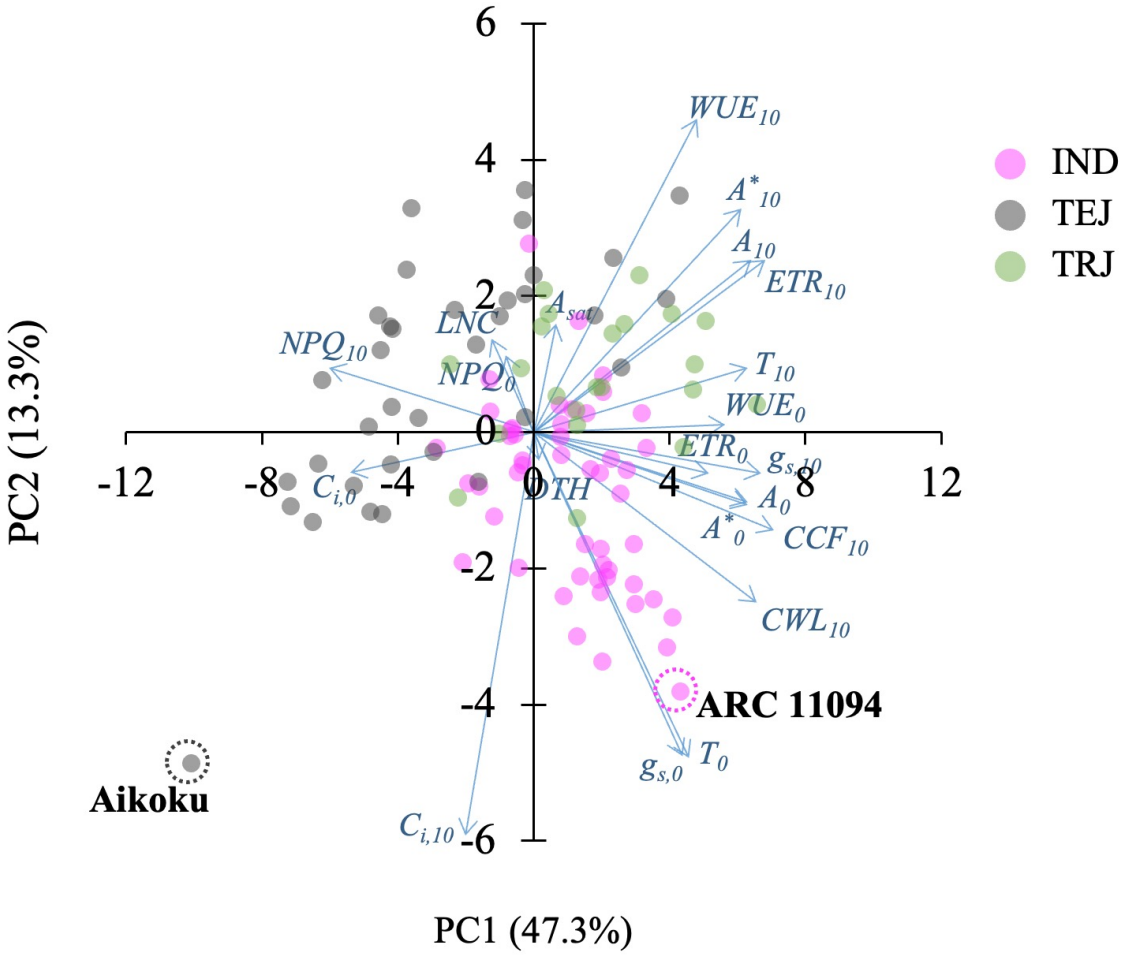

Fig. 4.9. Principal component analysis among normalized parameters. The principal component analysis was conducted among normalized values of the studied traits; days to heading after sowing (*DTH*); leaf nitrogen content per leaf area (*LNC*); the values just before the transition from low to high light or 10 minutes after high light irradiation of CO_2 assimilation rate (A_0 and A_{10}); stomatal conductance ($g_{s,0}$ and $g_{s,10}$); intercellular CO_2 concentration ($C_{i,0}$ and $C_{i,10}$); normalized CO_2 assimilation rate to a C_i of 300 µmol mol^{-1} (A^*_0 and A^*_{10}); transpiration rate (T_0 and T_{10}); water use efficiency (WUE_0 and WUE_{10}); photosynthetic electron transport rate around photosystem II (ETR_0 and ETR_{10}) and non-photochemical quenching (NPQ_0 and NPQ_{10}); cumulative CO_2 fixation during the first 10 minutes of the photosynthetic induction (CCF_{10}); cumulative water loss during the first 10 minutes of the photosynthetic induction (CWL_{10}); light-saturating CO_2 assimilation rate under steady state (A_{sat}). Pink, gray and green dots in the graph represent the values of genotypes in *indica* (IND), *temperate japonica* (TEJ) and *tropical japonica* (TRJ), respectively. The blue allows represent the eigenvectors. The first and second principal components (PC1 and PC2) accounted for 47.3% and 13.3% of the variance, respectively.

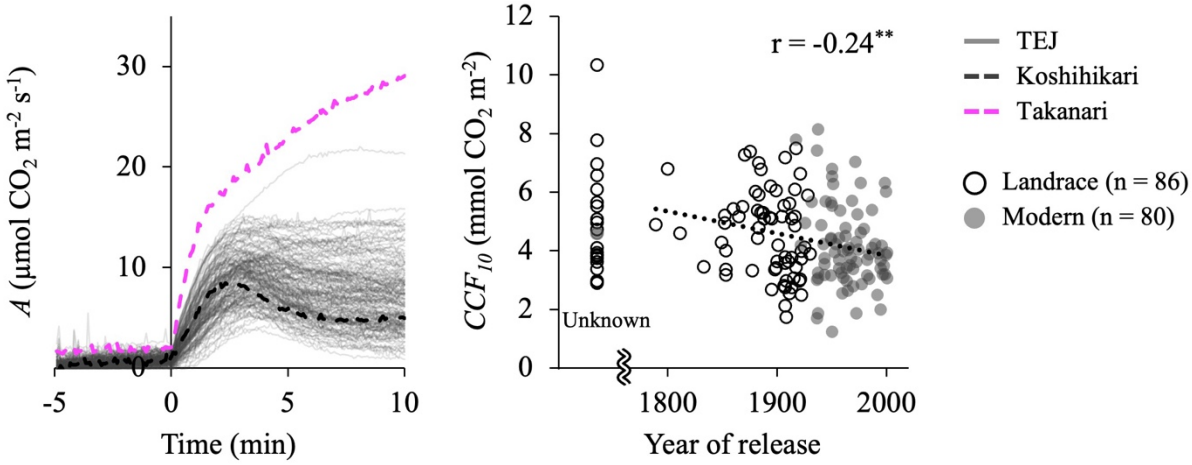

Fig. 4.10. Natural genetic variation of photosynthetic induction and the relationship with release year in 166 *temperate japonica* rice cultivars. The dynamics of CO_2 assimilation rate (A) in response to high light irradiation and the relationship between cumulative CO_2 fixation during the first 10 minutes of the photosynthetic induction (CCF_{10}) and release year in 166 *temperate japonica* rice cultivars were analyzed. Leaf chamber was kept at an air temperature of 30°C, a reference CO_2 concentration of 400 μmol mol^{-1} and a relative humidity of 55-70%. The photosynthetic photon flux density was changed from dark to 50 μmol photons m^{-2} s^{-1} for the first 5 minutes, and then to 1500 μmol photons m^{-2} s^{-1} for the following 10 minutes. A were recorded every 5 seconds. Gray and pink dashed lines in left graph show Koshihikari and Takanari, respectively. Open and close circles in right graph represent landrace and modern cultivars, respectively. The values were averaged between six replications of each genotype. The r value was calculated among 145 *temperate japonica* rice cultivars based on Pearson correlation coefficient. ** represents a significant correlation at $p < 0.01$.

4.4 Discussion

4.4.1 Natural genetic variation in photosynthetic induction and related traits in JRC

The significant natural genetic variation in photosynthetic induction was found in JRC (Fig. 4.1, 4.2). Takanari showed the rapid photosynthetic induction and Koshihikari showed the slow photosynthetic induction (Fig. 4.1, 4.2), which is consistent with the previous studies (Adachi *et al.*, 2019b; Ohkubo *et al.*, 2020; Chapter 2 and 3 in the present thesis). Similar relationships to Chapter 2 were observed in the present chapter about CCF_{10}, *DTH*, *LNC*, A_{sat}, A_0 and $g_{s,0}$ (Fig. 4.4, 4.5, 4.6). In other words, photosynthetic induction is regulated independently from the earliness of heading or photosynthetic capacity, the effect of leaf

nitrogen to photosynthetic induction is limited, and photosynthesis under low light influences the following photosynthetic induction.

In addition to the above, I evaluated the effect of photosynthesis under dark (R_d and $g_{s,dark}$) and stomatal morphology (*SD* and *GCL*) to photosynthetic induction. Surprisingly, CCF_{10} and R_d were positively correlated (Fig. 4.6). It is known that R_d is effected by the intercellular carbohydrate concentration (Ascon-Bieto *et al*., 1983; Azcon-Bieto & Osmond, 1983; Noguchi *et al*., 1996) or the ratio of ADP to ATP (Noguchi *et al*., 1996), but the detailed relationship with photosynthetic induction is unclear in the present study. Correlation between CCF_{10} and $g_{s,dark}$ was relatively weak than that between CCF_{10} and $g_{s,0}$ (Fig. 4.6). This implies the importance of the stomatal sensitivity to low light irradiation for the rapid photosynthetic induction. The relationship between stomatal morphology and the response of g_s to fluctuating light have been discussed in many previous studies (Faralli *et al*., 2019b; Zhang *et al*., 2019; Sakoda *et al*., 2020b; Xiong *et al*., 2022a). In my results, both of *SD* and *GCL* were not significantly correlated to CCF_{10} and $g_{s,0}$. Therefore, the effect of stomatal morphology on $g_{s,0}$ and following photosynthetic induction would be limited for variation among divergent genotypes or different depend on each genotype.

4.4.2 Differences in photosynthetic induction among rice subspecies and the related factors

Photosynthetic capacity was not different between rice subspecies, however, photosynthetic induction in *temperate japonica* was significantly slower than those of *indica* and *tropical japonica* (Fig. 4.3, 4.8). Slow photosynthetic induction in *temperate japonica* resulted in a decrease of carbon gain but suppressing the water loss (Fig. 4.8). Generally, there is a trade-off between CO_2 uptake and water loss via stomatal opening. The rice genotypes in *temperate japonica* may put importance to reduce water loss rather than to increase carbon gain

under fluctuating light conditions. During the rice cultivation process, ancient *japonica* firstly developed from a specific population of the wild rice species (*Oryza rufipogon* Griff.). And then, the ancient *japonica* further developed into *tropical japonica* and *temperate japonica*, while *indica* was developed from crosses between the ancient *japonica* and local wild rice (Huang *et al*., 2012). Thus, there may have been natural or artificial selections, in terms of photosynthetic induction, during the emergence of *temperate japonica*. Besides, there may be different mechanisms in photosynthetic induction between *indica* and *tropical japonica* because the range of PC2 scores were different between the two subspecies (Fig. 4.9).

4.4.3 Differences in photosynthetic induction among rice cultivars developed during the modern breeding in Japan

Photosynthetic induction have not been accelerated, or rather deaccelerated gradually during the rice modern breeding in Japan since 1800s (Fig. 4.10). To visualize where inherited genetic factors in the slow photosynthetic induction of Koshihikari came from, the breeding history of Koshihikari was shown in Fig. 4.11. The ancestors of Koshihikari: Shinriki, Aikoku, Ginbouzu and Kyoto-asahi, which were widely cultivated in Japan during its Meiji to Taisho Era, showed slower photosynthetic induction among *temperate japonica*. Notably, Aikoku had significantly low CCF_{10} and was conspicuously distinct from other genotypes in PCA (Fig. 4.2, 4.9). Koshihikari and its relatives occupied the top five cultivars and approximately 65% of rice cultivation area in Japan at 2016. These imply that the factors related to the slow photosynthetic induction have been inherited from the popular rice cultivars in early modern breeding (i.e. Shinriki, Aikoku, Ginbouzu and Kyoto-asahi) to Koshihikari and its relatives, and spread throughout Japan. Interestingly, Hinode, a parent rice cultivar of Kyoto-asahi, was categorized to *tropical japonica* and showed a rapid photosynthetic induction. These two cultivars may be

helpful materials to understand the ecophysiological significance or mechanisms of the slow photosynthetic induction in *temperate japonica*.

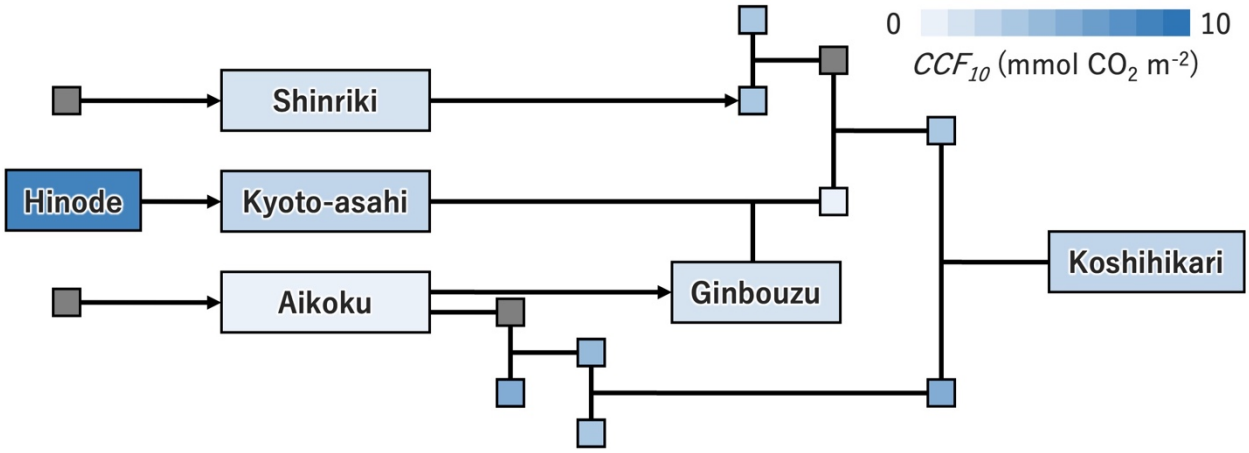

Fig. 4.11. Breeding history of a popular rice cultivar in Japan, Koshihikari. The blue gradient shows the values of CCF_{10}. Black represents the cultivars which were not used for the present thesis. Shinriki, Kyoto-asahi, Aikoku, Ginbouzu and Koshihikari are classified into *temperate japonica*, but Hinode is classified into *tropical japonica*.

4.4.4 Conclusion

In conclusion in Chapter 4, I investigated the difference of photosynthetic induction between rice subspecies. The photosynthetic induction in *temperate japonica* was slower than those in *indica* and *tropical japonica*, and *indica* and *tropical japonica* may have different mechanisms underlying photosynthetic induction. There is a possibility that photosynthetic induction in *temperate japonica* have been gradually deaccelerated during the rice modern breeding in Japan. A deeper understanding of the ecophysiological significance or mechanisms of the slow photosynthetic induction in *temperate japonica* has to be elucidated for the improvement of photosynthetic induction and then enhancement of crop productivity under field environments.

Chapter 5

General Discussion

Crop productivity need to be increased due to growing world population. The response of leaf photosynthesis to a stepwise increase in light intensity, photosynthetic induction, is regarded as a key trait for enhancing carbon gain and then plant biomass production under fluctuating light conditions (Taylor & Long, 2017; Tanaka *et al*., 2019). The aim of the present study is to clarify the natural genetic variation in photosynthetic induction and related factors in untapped genetic resources in rice, and then contribute to improvement of photosynthetic dynamics and consequently crop productivity under field environments.

5.1 Natural genetic variation in photosynthetic induction in rice and the room of improvement

I investigated the photosynthetic induction of totally 274 rice genotypes: 57 WRC genotypes, 50 JRC genotypes, 166 *temperate japonica* cultivars developed in Japan, and a high-yielding cultivar, Takanari. The values of CCF_{10} ranged from 0.12 mmol CO_2 m^{-2} of Aikoku to 14.2 mmol CO_2 m^{-2} of ARC 11094. Several genotypes showed a more rapid photosynthetic induction and higher CCF_{10} than Takanari. The photosynthetic induction have not been accelerated during the modern rice breeding in Japan, and the most popular rice cultivar in Japan, Koshihikari, showed a slow photosynthetic induction and low CCF_{10}. These suggest that there is a large room for improvement of photosynthetic induction in many rice cultivars in Japan.

The natural genetic variation in the photosynthetic induction in rice was not related to

the earliness of heading. Therefore, the photosynthetic induction can be improved without major changes in crop management practices. Besides, photosynthetic induction and capacity seemed to be regulated independently, which is consistent with a previous study in soybean (Soleh *et al*., 2017). Improvement of photosynthetic induction could be realized in combination with the conventional manipulation of photosynthetic capacity.

I found the various underlying physiological factors on the rapid photosynthetic induction in ARC 11094 and Takanari. The rapid photosynthetic induction in Takanari was resulted from high stomatal density, small stomatal size, and great root activity through large root mass. On the other hand, the rapid photosynthetic induction in ARC 11094 was attributable to a single stoma behaviour and anisohydric characteristics. Photosynthetic induction would be further improved by combining or pyramiding such mechanisms.

To optimize the photosynthetic dynamics under field environment, we should consider the secondary effects by the manipulation of photosynthetic induction, such as a trade-off between CO_2 uptake and water loss via stomatal opening. Anisohydric stomatal behaviour in ARC 11094 contributed to the rapid photosynthetic induction and great carbon gain under field-mimicked environment, but had adverse effects of water loss to plant biomass production. Additionally, *temperate japonica* had slower photosynthetic induction than *indica* and *tropical japonica*, resulted in a decrease of carbon gain but suppressing water loss. The rice genotypes in *temperate japonica* may put importance to reduce water loss rather than to increase carbon gain under fluctuating light conditions. Therefore, efficient stomatal response to fluctuating light with suppressing the water loss would be a desirable trait for improvement of photosynthetic induction and thus crop productivity.

5.2 Next step for the improvement of photosynthetic induction

Through the present thesis, I clarified the natural genetic variation and the underlying ecophysiological factors in photosynthetic induction in rice. As a next step for the genetic improvement of photosynthetic induction, we have to identify the causal quantitative trait loci (QTLs) or genes. Salter *et al*. (2020) identified a QTL related to the dynamic photosynthesis by QTL mapping analysis in barley. However, it seems difficult to improve photosynthetic induction separately from photosynthetic capacity, because the QTL was detected in the analysis for photosynthetic rate under steady state, too. The other genetic studies in the photosynthetic induction using genetic resources have not been reported so far.

Recently, we identified a QTL related to the varietal differences in photosynthetic induction between Koshihikari and Takanari, using chromosome segment substitution lines (CSSLs) derived from this two cultivars. Identification of the causal gene and analysis of the function in the QTL have been conducted, and now it is thought to affect the root water uptake ability. The DNA sequence of the QTL region in ARC 11094 resembles to that in Koshihikari rather than Takanari. It means that the genetic factor of the rapid photosynthetic induction in ARC 11094 differs from that in Takanari, as well as physiological factors are different. Nowadays, I tried to identify the QTL related to the rapid photosynthetic induction in ARC 11094 by QTL-seq using an BC_1F_2 population derived from ARC 11094 and Koshihikari. In this QTL-seq analysis, I combines the dimension reduction of t-Distributed Stochastic Neighbor Embedding (t-SNE; van der Maaten & Hinton, 2008) to detect time-depended genetic factors. Accomplishment of this analysis would be helpful for a deeper understanding about the molecular mechanisms in photosynthetic induction. Furthermore, it is possible to conduct genome wide association study (GWAS) in WRC, JRC, or 166 *temperate japonica* rice cultivars developed in Japan, respectively, because the whole genome sequencing was already performed in each panel (Tanaka *et al*., 2020a,b; Yano *et al*., 2016). The genetic improvement of

photosynthetic induction and development of rice cultivars possessing an efficient photosynthetic induction would be enabled through these genetic analysis.

5.3 Future perspectives in the present thesis

The global climate has been drastically changed and caused the negative impacts to crop production (Iizumi *et al*., 2018). The frequency of abiotic stress, such as aridity stress, heat stress, nutrient stress and flood events, is increasing and projected to do so (Bailey-Serres *et al*., 2019). The impacts of climate change are expected to be different both in quality and in quantity at each region or site. Because a suitable approach for enhancement of the crop productivity would differ at each region or site, various strategies are need to improve the agronomical traits. Multiple mechanisms underlying photosynthetic induction have been reported, suggesting that there are many choices to improve the photosynthetic induction. In addition, combining or pyramiding several mechanisms would lead to have more choices. Furthermore, utilizing the acquired knowledge about photosynthetic capacity could further broaden the range of strategies to optimize the photosynthetic dynamics under field environments. Through these, the 'ideal' photosynthetic dynamics under field environments according to each objective or circumstance will be realized.

5.4 Conclusion

The present thesis elucidated the large natural genetic variation and substantial room of improvement in photosynthetic induction in rice. Subsequently, I determined the characteristics underlying on the rapid photosynthetic induction and that these were different depending on each rice genotype. Skewed distribution of slow photosynthetic induction in *temperate japonica* implies that the ecological significance are related to the speed of

photosynthetic induction. Further and comprehensive understanding of leaf photosynthesis in response to fluctuating light conditions will be required to optimize the photosynthetic dynamics under field environments for enhancement of crop productivity.

Acknowledgements

This thesis could not be completed without the support and inspiration from many people. Firstly, I would like to express my sincere gratitude to Dr. Yu Tanaka for the continuous support throughout my study. His guidance helped me in all the time of my research and writing of this thesis. I am also grateful to Dr. Tatsuhiko Shiraiwa and Dr. Tomoyuki Tanaka-Katsube for their valuable and insightful suggestions to this thesis.

I would like to extend my gratitude to Dr. Shunsuke Adachi (Tokyo University of Agriculture and Technology) for the interesting collaborative research and fruitful comments (especially for Chapter 3 and 4). A part of the experiment in Chapter 4 was conducted with the support of Dr. Naomi Asagi, Mr. Shoma Hiramatsu, Mr. Rikuo Tamaki, Ms. Airi Miyamoto (Ibaraki University), Mr. Yoshiaki Seki, Mr. Sotaro Honda (Tokyo University of Agriculture and Technology), and Dr. Makoto Matsuoka (Nagoya University).

My sincere thanks also goes to Mr. Kazuki Tanaka, Mr. Shogo Ohashi, Ms. Mina Nakahara and Mr. Hidenobu Yorioka for working together. I would like to thank all members of the Laboratory of Crop Science at Kyoto University, for their fruitful opinion, collaborative work and cheerful days.

This thesis was also supported by the Sasakawa Scientific Research Grant from the Japan Science Society, Support for Pioneering Research Initiated by the Next Generation from Japan Science and Technology Agency, and Grant-in-Aid for Japan Society for the Promotion of Science Fellows.

Finally, I never forget my special thanks to my parents, brothers and relatives, and all the friends for their support and encouragement.

References

Acevedo-Siaca, L.G., Coe, R., Quick, W.P. & Long, S.P. 2021b. Variation between rice accessions in photosynthetic induction in flag leaves and underlying mechanisms. *Journal of Experimental Botany* **72**: 1282-1294.

Acevedo-Siaca, L.G., Coe, R., Wang, Y., Kromdijk, J., Quick, W.P. & Long, S.P. 2020. Variation in photosynthetic induction between rice accessions and its potential for improving productivity. *New Phytologist* **227**: 1097-1108.

Acevedo-Siaca, L.G., Dionora, J., Laza, R., Quick, W.P. & Long, S.P. 2021a. Dynamics of photosynthetic induction and relaxation within the canopy of rice and two wild relatives. *Food and Energy Security* **10**: e286.

Adachi, S., Baptista, L.Z., Sueyoshi, T., Murata, K., Yamamoto, T., Ebitani, T., Ookawa, T. & Hirasawa, T. 2014. Introgression of two chromosome regions for leaf photosynthesis from an *indica* rice into the genetic background of a *japonica* rice. *Journal of Experimental Botany* **65**: 2049-2056.

Adachi, S., Nito, N., Kondo, M., Yamamoto, T., Arai-Sanoh, Y., Ando, T., Ookawa, T. Yano, M. & Hirasawa, T. 2011. Identification of Chromosomal Regions Controlling the Leaf Photosynthetic Rate in Rice by Using a Progeny from *Japonica* and High-yielding *Indica* Varieties. *Plant Production Science* **14**: 118-127.

Adachi, S., Tanaka, Y., Miyagi, A., Kashima, M., Tezuka, A., Toya, Y., Kobayashi, S., Ohkubo, S., Shimizu, H., Kawai-Yamada, M., Sage, R.F., Nagano, A.J. & Yamori, W. 2019b. High-yielding rice Takanari has superior photosynthetic response to a commercial rice Koshihikari under fluctuating light. *Journal of Experimental Botany* **70**: 5287-5297.

Adachi, S., Yamamoto, T., Nakae, T., Yamashita, M., Uchida, M., Karimata, R., Ichihara, N., Soda, K., Ochiai, T., Ao, R., Otsuka, C., Nakano, R., Takai, T., Ikka, T., Kondo, K., Ueda, T., Ookawa, T. & Hirasawa, T. 2019a. Genetic architecture of leaf photosynthesis in rice revealed by different types of reciprocal mapping populations. *Journal of Experimental Botany* **70**: 5131-5144.

Adachi, S., Yoshikawa, K., Yamanouchi, U., Tanabata, T., Sun, J., Ookawa, T., Yamamoto, T., Sage, R.F., Hirasawa, T. & Yonemaru, J. 2017. Fine Mapping of *Carbon Assimilation Rate 8*, a Quantitative Trait Locus for Flag Leaf Nitrogen Content, Stomatal Conductance and Photosynthesis in Rice. *Frontiers in Plant Science* **8**: 60.

Attia, Z., Domec, J.C., Oren, R., Way, D.A. & Moshelion, M. 2015. Growth and physiological responses of isohydric and anisohydric poplars to drought. *Journal of Experimental Botany* **66**: 4373-4381.

Azcon-Bieto, J. & Osmond, C.B. 1983. Relationship between Photosynthesis and Respiration: The Effect of Carbohydrate Status on the Rate of CO_2 Production by Respiration in Darkened and Illuminated Wheat Leaves. *Plant Physiology* **71**: 574-581.

Azcon-Bieto, J., Day, D.A. & Lambers, H. 1983. The regulation of respiration in the dark in wheat leaf slices. *Plant Science Letters* **32**: 313-320.

Bai, K., Liao, D., Jiang, D. & Cao, K. 2008. Photosynthetic induction in leaves of co-occurring *Fagus lucida* and *Castanopsis lamontii* saplings grown in contrasting light environments. *Trees* **22**: 449-462.

Bailey-Serres, J., Parker, J.E., Ainsworth, E.A., Oldroyd, G.E.D. & Schroeder, J.I. 2019. Genetic strategies for improving crop yields. *Nature* **575**: 109-118.

Bernacchi, C.J., Singsaas, E.L., Pimentel, C., Portis Jr, A.R. & Long, S.P. 2001. Improved temperature response functions for models of Rubisco-limited photosynthesis. *Plant, Cell and Environment* **24**: 253-259.

Buckley, T.N. 2019. How do stomata respond to water status? *New Phytologist* **224**: 21-36.

Burgess, A.J., Retkute, R., Prestom, S.P., Jensen, O.E., Pound, M.P., Pridmore, T.P. & Murchie, E.H. 2016. The 4-Dimensional Plant: Effects of Wind-Induced Canopy Movement on Light Fluctuations and Photosynthesis. *Frontiers in Plant Science* **7**: 1392.

Carmo-Silva, A.E. & Salvucci, M.E. 2013. The Regulatory Properties of Rubisco Activase Differ among Species and Affect Photosynthetic Induction during Light Transitions. *Plant Physiology* **161**: 1645-1655.

Carmo-Silva, E., Andralojc, P.J., Scales, J.C., Driever, S.M., Mead, A., Lawson, T., Raines, C.A. & Parry, M.A.J. 2017. Phenotyping of field-grown wheat in the UK highlights contribution of light response of photosynthesis and flag leaf longevity to grain yield. *Journal of Experimental Botany* **68**: 3473-3486.

Chazdon, R.L. & Pearcy, R.W. 1986. Photosynthetic responses to light variation in rainforest species. 1. Induction under constant and fluctuating light conditions. *Oecologia* **69**: 517-523.

Choquette, N.E., Ogut, F., Wertin, T.M., Montes, C.M., Sorgini, C.A., Morse, A.M., Brown, P.J., Leakey, A.D.B., Mclntyre, L.M. & Ainsworth, E.A. 2019. Uncovering hidden genetic variation in photosynthesis of field-grown maize under ozone pollution. *Global Change Biology* **25**: 4327-4338.

De Souza, A.P., Burgess, S.J., Doran, L., Hansen, J., Manukyan, L., Maryn, N., Gotarkar, D., Leonelli, L., Niyogi, K.K. & Long, S.P. 2022. Soybean photosynthesis and crop yield are improved by accelerating recovery from photoprotection. *Science* **377**: 851-854.

De Souza, A.P., Wang, Y., Orr, D.J., Carmo-Silva, E. & Long, S.P. 2020. Photosynthesis across African cassava germplasm is limited by Rubisco and mesophyll conductance at steady state, but by stomatal conductance in fluctuating light. *New Phytologist* **225**: 2498-2512.

DeMichele, D.W., & Sharpe, P.J.H. 1973. An Analysis of the Mechanics of Guard Cell Motion. *Journal of Theoretical Biology* **41**: 77-96.

Duursma, R.A. 2015. Plantecophys - An R Package for Analysing and Modelling Leaf Gas Exchange Data. *PLoS One* **10**: e0143346.

Ebana, K., Kojima, Y., Fukuoka, S., Nagamine, T. & Kawase, M. 2008. Development of mini core collection of Japanese rice landrace. *Breeding Science* **58**: 281-291.

Evans, L.T. & Fischer, R.A. 1999. Yield Potential: Its Definition, Measurement, and Significance. Crop *Science* **39**: 1544-1551.

Eyland, D., van Wesemael, J., Lawson, T. & Carpentier, S. 2021. The impact of slow stomatal kinetics on

photosynthesis and water use efficiency under fluctuating light. *Plant Physiology* **186**: 998-1012.

Faralli, M., Cockram, J., Ober, E., Wall, S., Galle, A., Rie, J.V., Raines, C. & Lawson, T. 2019a. Genotypic, Developmental and Environmental Effects on the Rapidity of g_s in Wheat: Impacts on Carbon Gain and Water-Use Efficiency. *Frontiers in Plant Science* **10**: 492.

Faralli, M., Matthews, J. & Lawson, T. 2019b. Exploiting natural variation and genetic manipulation of stomatal conductance for crop improvement. *Current Opinion in Plant Biology* **49**: 1-7.

Farquhar, G.D., von Caemmerer, S. & Berry, J.A. 1980. A Biochemical Model of Photosynthetic CO_2 Assimilation in Leaves of C_3 species. *Planta* **149**: 78-90.

Food and Agriculture Organization of the United Nations 2022. Crops and livestock products (Updated February 17, 2022).

Gallé, Á., Csiszár, J., Benyó, D., Laskay, G., Leviczky, T., Erdei, L. & Tari, I. 2013. Isohydric and anisohydric strategies of wheat genotypes under osmotic stress: biosynthesis and function of ABA in stress responses. *Journal of Plant Physiology* **170**: 1389-1399.

Glinka, Z. 1971. The Effect of Epidermal Cell Water Potential on Stomatal Response to Illumination of Leaf Discs of *Vicia faba*. *Physiologia Plantarum* **24**: 476-479.

Hammond, E.T., Andrews, T.J., Mott, K.A. & Woodrow, E. 1998. Regulation of Rubisco activation in antisense plants of tobacco containing reduced levels of Rubisco activase. *Plant Journal* **14**: 101-110.

Hedden, P. 2003. The genes of the Green Revolution. *Trends in Genetics* **19**: 5-9.

Hirasawa, T. & Ishihara, K. 1991. On Resistance to Water Transport in Crop Plants for Estimating Water Uptake Ability under Intense Transpiration. *Japanese Journal of Crop Science* **60**: 174-183.

Hirasawa, T., Tsuchida, M. & Ishihara, K. 1992. Relationship between Resistance to Water Transport and Exudation Rate and the Effect of the Resistance on the Midday Depression of Stomatal Aperture in Rice

Plants. *Japanese Journal of Crop Science* **61**: 145-152.

Hirooka, Y., Homma, K., Shiraiwa, T., Makino, Y., Liu, T., Xu, Z. & Tang, L. 2018. Yield and growth characteristics of erect panicle type rice (*Oryza sativa* L.) cultivar, Shennong265 under various crop management practices in Western Japan. *Plant Production Science* **21**: 1-7.

Hirotsu, N., Ujiie, K., Perera, I., Iri, A., Kashiwagi, T. & Ishimaru, K. 2017. Partial loss-of -function of *NAL1* alters canopy photosynthesis by changing the contribution of upper and lower canopy leaves in rice. *Scientific Reports* **7**: 15958.

Huang, X., Kurata, N., Wei, X., Wang, Z.X., Wang, A., Zhao, Q., Zhao, Y., Liu, K., Lu, H., Li, W., Guo, Y., Lu, Y., Zhou, C., Fan, D., Weng, Q., Zhu, C., Huang, T., Zhang, L., Wang, Y., Feng, L., Furuumi, H., Kubo, T., Miyabayashi, T., Yuan, X., Xu, Q., Dong, G., Zhan, Q., Li, C., Fujiyama, A., Toyoda, A., Lu, T., Feng, Q., Qian, Q., Li, J. & Han, B. 2012. A map of rice genome variation reveals the origin of cultivated rice. *Nature* **490**: 497-501.

Iizumi, T., Shiogama, H., Imada, Y., Hanasaki, N., Takikawa, H. & Nishimori, M. 2018. Crop production losses associated with anthropogenic climate change for 1981-2010 compared with preindustrial levels. *International Journal of Climatology* **38**: 5405-5417.

Jahn, C.E., Mckay, J.K., Mauleon, R., Stephens, J., McNally, K.L., Bush, D.R., Leung, H. & Leach, J.E. 2011. Genetic Variation in Biomass Traits among 20 Diverse Rice Varieties. *Plant Physiology* **155**: 157-168.

Kaiser, E., Kromdijk, J., Harbinson, J., Heuvelink, E. & Marcelis, L.F.M. 2017. Photosynthetic induction and its diffusional, carboxylation and electron transport processes as affected by CO_2 partial pressure, temperature, air humidity and blue irradiance. *Annals of Botany* **119**: 191-205.

Kaiser, E., Morales, A., Harbinson, J., Heuvelink, E., Prinzenberg, A.E. & Marcelis, L.F.M. 2016. Metabolic and diffusional limitations of photosynthesis in fluctuating irradiance in *Arabidopsis thaliana*. *Scientific Reports* **6**: 31252.

Kanemura, T., Homma, K., Ohsumi, A., Shiraiwa, T. & Horie, T. 2007. Evaluation of genotypic variation in leaf photosynthetic rate and its associated factors by using rice diversity research set of germplasm. *Photosynthesis Research* **94**: 23-30.

Kariya, K., Murata, K., Kokubo,Y., Ube, N., Ueno, K., Yabuta, Y., Teraishi, M., Okumoto, Y., Mori, N. & Ishihara, A. 2019. Variation of diterpenoid phytoalexin oryzalexin A production in cultivated and wild rice. *Phytochemistry* **116**: 112057.

Kariya, K., Ube, N., Ueno, M., Teraishi, M., Okumoto, Y., Mori, N., Ueno, K. & Ishihara, A. 2020. Natural variation of diterpenoid phytoalexins in cultivated and wild rice species. *Phytochemistry* **180**: 112518.

Kimura, H., Hashimoto-Sugimoto, M., Iba, K., Terashima, I. & Yamori, W. 2020. Improved stomatal opening enhances photosynthetic rate and biomass production in fluctuating light. *Journal of Experimental Botany* **71**: 2339-2350.

Kojima, Y, Ebana, K., Fukuok, S., Nagamine, T. & Kawase, M. 2005. Development of an RFLP-based Rice Diversity Research Set of Germplasm. *Breeding Science* **55**: 431-440.

Kromdijk, J., Głowacka, K., Leonelli, L., Gabilly, S.T., Iwai, M., Niyogi, K.K. & Long, S.P. 2016. Improving photosynthesis and crop productivity by accelerating recovery from photoprotection. *Science* **354**: 857-861.

Kursar, T.A. & Coley, P.D. 1993. Photosynthetic induction times in shade-tolerant species with long and short-lived leaves. *Oecologia* **93**: 165-170.

Lawson, T. & Matthews, J. 2020. Guard Cell Metabolism and Stomatal Function. *Annual Review of Plant Biology* **71**: 273-302.

Laza, M.R., Peng, S., Sanico, A.L., Visperas, R.M. & Akita, S. 2001. Higher Leaf Area Growth Rate Contributes to Greater Vegetative Growth of F_1 Rice Hybrids in the Tropics. *Plant Production Science* **4**: 184-188.

Li, F., Liu, W., Tang, J., Chen, J., Tong, H., Hu, B., Li, C., Fang, J., Chen, M. & Chu, C. 2010. Rice DENCE AND ERECT PANICLE 2 is essential for determining panicle outgrowth and elongation. *Cell Research* **20**: 838-849.

Long, S.P., Zhu, X.G., Naidu, S.L. & Ort, D.R. 2006. Can improvement in photosynthesis increase crop yields? *Plant, Cell and Environment* **29**: 315-330.

Makino, A., Mae, T. & Ohira, K. 1986. Colorimetric Measurement of Protein Stained with Coomassie Brilliant Blue R on Sodium Dodecyl Sulfate-Polyacrylamide Gel Electrophoresis by Eluting with Formamide. *Agricultural and Biological Chemistry* **50**: 1911-1912.

Masumoto, C., Fukayama, H., Hatanaka, T. & Uchida, N. 2012. Photosynthetic Characteristics of Antisense Transgenic Rice Expressing Reduced Levels of Rubisco Activase. *Plant Production Science* **15**: 174-182.

Matthews, J., Vialet-Chabrand, S. & Lawson, T. 2020. Role of blue and red light in stomatal dynamic behaviour. *Journal of Experimental Botany* **71**: 2253-2269.

McAusland, L., Vialet-Chabrand, S., Davey, P., Baker, N.R., Brendel, O. & Lawson, T. 2016. Effects of kinetics of light-induced stomatal responses on photosynthesis and water-use efficiency. *New Phytologist* **211**: 1209-1220.

Meinzer, F.C., Smith, D.D., Woodruff, D.R., Marias, D.E., McCulloh, K.A., Howard, A.R. & Magedman, A.L. 2017. Stomatal kinetics and photosynthetic gas exchange along a continuum of isohydric to anisohydric regulation of plant water status. *Plant, Cell and Environment* **40**: 1618-1628.

Monteith, J.L. 1977. Climate and the efficiency of crop production in Britain. *Philosophical Transactions of the Royal Society of London* **281**: 277-294.

Moshelion, M., Halperin, O., Wallach, R., Oren, R. & Way, D.A. 2015. Role of aquaporins in determining transpiration and photosynthesis in water-stressed plants: crop water-use efficiency, growth and yield. *Plant,*

Cell and Environment **38**: 1785-1793.

Naumburg, E. & Ellsworth, D.S. 2000. photosynthetic sunfleck utilization potential of understory saplings growing under elevated CO_2 in FACE. *Oecologia* **122**: 163-174.

Noguchi, K., Sonoike, K. & Terashima, I. 1996. Acclimation of Respiratory Properties of Leaves of *Spinacia oleracea* L., a Sun Species, and of *Alocasia macrorrhiza* (L.) G. Don., a Shade Species, to Changes in Growth Irradiance. *Plant and Cell Physiology* **37**: 377-384.

Norman, J.M., Miller, E.E. & Tanner, C.B. 1971. Light Intensity and Sunfleck-size Distributions in Plant Canopies. *Agronomy Journal* **63**: 743-748.

Ohkubo, S., Tanaka, Y., Yamori, W. & Adachi, S. 2020. Rice Cultivar Takanari Has Higher Photosynthetic Performance Under Fluctuating Light Than Koshihikari, Especially Under Limited Nitrogen Supply and Elevated CO_2. *Frontiers in Plant Science* **11**: 1308.

Ohsumi, A., Kanemura, T., Homma, K., Horie, T. & Shiraiwa, T. 2007. Genotypic Variation of Stomatal Conductance in Relation to Stomatal Density and Length in Rice (*Oryza sativa* L.). *Plant Production Science* **10**: 322-328.

Papanatsiou, M., Petersen, J., Henderson, L., Wang, Y., Christie, J.M. & Blatt, M.R. 2019. Optogenetic manipulation of stomatal kinetics improves carbon assimilation, water use, and growth. *Science* **363**: 1456-1459.

Pearcy, R.W. 1990. Sunflecks and Photosynthesis in Plant Canopies. *Annual Review of Plant Physiology and Plant Molecular Biology* **41**: 421-453.

Peng, J., Richard, D.E., Hartley, N.M., Murphy, G.P., Devos, K.M., Flintham, J.E., Beales, J., Fish, L.J., Worland, A.J., Pelica, F., Sudhakar, D., Christou, P., Snape, J.W., Gale, M.D. & Harberd, N.P. 1999. 'Green revolution' genes encode mutant gibberellin response modulators. *Nature* **400**: 256-261.

Peng, S. & Khushg, G.S. 2003. Four Decades of Breeding for Varietal Improvement of Irrigated Lowland

Rice in the International Rice Research Institute. *Plant Production Science* **6**: 157-164.

Porra, R.J., Thompson, W.A. & Kriedemann, P.E. 1989. Determination of accurate extinction coefficients and simultaneous equations for assaying chlorophylls *a* and *b* extracted with four different solvents: verification of the concentration of chlorophyll standards by atomic absorption spectroscopy. *Biochimica et Biophysica Acta* **975**: 384-394.

Qu, M., Hamdani, S., Li, W., Wang, S., Tang, J., Chen, Z., Song, Q., Li, M., Zhao, H., Chang, T., Chu, C. & Zhu, X. 2016. Rapid stomatal response to fluctuating light: an under-explored mechanism to improve drought tolerance in rice. *Functional Plant Biology* **43**: 727-738.

Qu, M., Zheng, G., Hamdani, S., Essemine, J., Song, Q., Wang, H., Chu, C., Sirault, X. & Zhu, X.G. 2017. Leaf Photosynthetic Parameters Related to Biomass Accumulation in a Global Rice Diversity Survey. *Plant Physiology* **175**: 248-258.

R Core Team 2018. R: A language and environment for statistical computing. R Foundation for Statistical Computing, Vienna, Austria.

Reifsnyder, W.E., Furnival, G.M. & Horowitz, J.L. 1971. Spatial and temporal distribution of solar radiation beneath forest canopies. *Agricultural Meteorology* **9**: 21-37.

Sakoda, K., Adachi, S., Yamori, W. & Tanaka, Y. 2022b. Towards improved dynamic photosynthesis in C_3 crops by utilizing natural genetic variation. *Journal of Experimental Botany* **73**: 3109-3121.

Sakoda, K., Kaga, A., Tanaka, Y., Suzuki, S., Fujii, K., Ishimoto, M. & Shiraiwa, T. 2020a. Two novel quantitative trait loci affecting the variation in leaf photosynthetic capacity among soybeans. *Plant Science* **291**: 110300.

Sakoda, K., Tanaka, Y., Long, S.P. & Shiraiwa, T. 2016. Genetic and Physiological Diversity in the Leaf Photosynthetic Capacity of Soybean. *Crop Science* **56**: 2731-2741.

Sakoda, K., Taniyoshi, K., Yamori, W. & Tanaka, Y. 2022a. Drought stress reduces crop carbon gain due

to delayed photosynthetic induction under fluctuating light conditions. *Physiologia Plantarum* **174**: e13603.

Sakoda, K., Yamori, W., Groszmann, M. & Evans, J.R. 2021. Stomatal, mesophyll conductance, and biochemical limitations to photosynthesis during induction. *Plant Physiology* **185**: 146-160.

Sakoda, K., Yamori, W., Shimada, T., Sugano, S.S., Hara-Nishimura, I. & Tanaka, Y. 2020b. Higher Stomatal Density Improves Photosynthetic Induction and Biomass Production in Arabidopsis Under Fluctuating Light. *Frontiers in Plant Science* **11**: 589603.

Salter, W.T., Li, S., Dracatos, P.M. & Barbour, M.M. 2020. Identification of quantitative trait loci for dynamic and steady-state photosynthetic traits in a barley mapping population. *AoB PLANTS* **12**: plaa063.

Salter, W.T., Merchant, A.M., Richards, R.A., Trethowan, R. & Buckley, T.N. 2019. Rate of photosynthetic induction in fluctuating light varies widely among genotypes of wheat. *Journal of Experimental Botany* **70**: 2787-2796.

Sasaki, A., Ashikari, M., Ueguchi-Tanaka, M., Itoh, H., Nishimura, A., Swapan, D., Ishiyama, K., Saito, T., Kobayashi, M., Khush, G.S., Kitano, H. & Matsuoka, M. 2002. A mutant gibberellin-synthesis gene in rice. *Nature* **416**: 701-702.

Shamim, M.J., Kaga, A., Tanaka, Y., Yamatani, H. & Shiraiwa, T. 2022. Analysis of Physiological Variations and Genetic Architecture for Photosynthetic Capacity of Japanese Soybean Germplasm. *Frontiers in Plant Science* **13**: 910527.

Shelden, M.C., Vandeleur, R., Kaiser, B.N. & Tyerman, S.D. 2017. A Comparison of Petiole Hydraulics and Aquaporin Expresson in an Anisohydric and Isohydric Cultivar of Grapevine in Response to Water-Stress Induced Cavitation. *Frontiers in Plant Science* **8**: 1893.

Shimazaki, K., Doi, M., Assmann, S.M. & Kinoshita, T. 2007. Light regulation of stomatal movement. *Annual Review of Plant Biology* **58**: 219-247.

Slattery, R.A., Walker, B.J., Weber, A.P.M. & Ort, D.R. 2018. The Impacts of Fluctuating Light on Crop

Performance. *Plant Physiology* **176**: 990-1003.

Soleh, M.A., Tanaka, Y., Kim, S.Y., Huber, S.C., Sakoda, K. & Shiraiwa, T. 2017. Identification of large variation in the photosynthetic induction response among 37 soybean [*Glycine max* (L.) Merr.] genotypes that is not correlated with steady-state photosynthetic capacity. *Photosynthesis Research* **131**: 305-315.

Soleh, M.A., Tanaka, Y., Nomoto, Y., Iwahashi, Y., Nakashima, K., Fukuda, Y., Long, S.P. & Shiraiwa, T. 2016. Factors underlying genotypic differences in the induction of photosynthesis in soybean [*Glycine max* (L.) Merr.]. *Plant, Cell and Environment* **39**: 685-693.

Sun, J., Ye, M., Peng, S. & Li, Y. 2016. Nitrogen can improve the rapid response of photosynthesis to changing irradiance in rice (*Oryza sativa* L.) plants. *Scientific Reports* **6**: 31305.

Takai, T., Adachi, S., Taguchi-Shiobara, F., Sanoh-Arai, Y., Iwasawa, N., Yoshinaga, S., Hirose, S., Taniguchi, Y., Yamanouchi, U., Wu, J., Matsumoto, T., Sugimoto, K., Kondo, K., Ikka, T., Ando, T., Kono, I., Ito, S., Shomura, A., Ookawa, T., Hirasawa, T., Yano, M., Kondo, M. & Yamamoto, T. 2013. A natural variant of *NAL1*, selected in high-yield rice breeding programs, pleiotropically increases photosynthetic rate. *Scientific Reports* **3**: 2149.

Tanaka, N., Shenton, M., Kawahara, Y., Kumagai, M., Sakai, H., Kanamori, H., Yonemaru, J., Fukuoka, S., Sugimoto, K., Ishimoto, M., Wu, J. & Ebana, K. 2020a. Whole-Genome Sequencing of the NARO World Rice Core Collection (WRC) as the Basis for Diversity and Association Studies. *Plant and Cell Physiology* **61**: 922-932.

Tanaka, N., Shenton, M., Kawahara, Y., Kumagai, M., Sakai, H., Kanamori, H., Yonemaru, J., Fukuoka, S., Sugimoto, K., Ishimoto, M., Wu, J. & Ebana, K. 2020b. Investigation of the Genetic Diversity of a Rice Core Collection of Japanese Landraces using Whole-Genome Sequencing. *Plant and Cell Physiology* **61**: 2087-2096.

Tanaka, Y., Adachi, S. & Yamori, W. 2019. Natural genetic variation of the photosynthetic induction response to fluctuating light environment. *Current Opinion in Plant Biology* **49**: 52-59.

Tanaka, Y., Sugano, S.S., Shimada, T. & Hara-Nishimura, I. 2013. Enhancement of leaf photosynthetic capacity through increased stomatal density in Arabidopsis. *New Phytologist* **198**: 757-764.

Tang, L., Gao, H., Hirooka, Y., Homma, K., Nakazaki, T., Liu,T., Shiraiwa, T. & Xu, Z. 2017. Erect panicle super rice varieties enhance yield by harvest index advantages in high nitrogen and density conditions. *Journal of Integrative Agriculture* **16**: 1467-1473.

Tardieu, F. & Simonneau, T. 1998. Variability among species of stomatal control under fluctuating soil water status and evaporative demand: modelling isohydric and anisohydric behaviours. *Journal of Experimental Botany* **49**: 419-432.

Taylaran, R.D., Adachi, S., Ookawa, T., Usuda, H. & Hirasawa, T. 2011. Hydraulic conductance as well as nitrogen accumulation plays a role in the higher rate of leaf photosynthesis of the most productive variety of rice in Japan. *Journal of Experimental Botany* **62**: 4067-4077.

Taylor, S.H. & Long, S.P. 2017. Slow induction of photosynthesis on shade to sun transitions in wheat may cost at least 21% of productivity. *Philosophical Transactions of the Royal Society B* **372**: 20160543.

Tomimatsu, H. & Tang, Y. 2012. Elevated CO_2 differentially affects photosynthetic induction response in two *Populus* species with different stomatal behavior. *Oecologia* **169**: 869-878.

Uga, Y., Ebana, K., Abe, J., Morita, S., Okuno, K. & Yano, M. 2009. Variation in root morphology and anatomy among accessions of cultivated rice (*Oryza sativa* L.) with different genetic backgrounds. *Breeding Science* **59**: 87-93.

United Nations, Department of Economic and Social Affairs, Population Division 2018. World Urbanization Prospects: The 2018 Revision, Online Edition.

United Nations, Department of Economic and Social Affairs, Population Division 2022. World Population Prospects 2022, Online Edition.

Urban, O., Košvancová, M., Marek, M.V. & Lichtenthaler, H.K. 2007. Induction of photosynthesis and

importance of limitations during the induction phase in sun and shade leaves of five ecologically contrasting tree species from the temperate zone. *Tree Physiology* **27**: 1207-1215.

van der Maaten, L. & Hinton, G. 2008. Visualizing Data using t-SNE. *Journal of Machine Learning Research* **9**: 2579-2605.

Vickery, H.B. 1946. The Early Years of the Kjeldahl Method to Determine Nitrogen. *Yale Journal of Biology and Medicine* **18**: 473-516.

Wachendorf, M. & Küppers, M. 2017a. The effect of initial stomatal opening on the dynamics of biochemical and overall photosynthetic induction. *Trees* **31**: 981-995.

Wachendorf, M. & Küppers, M. 2017b. Effects of leaf temperature on initial stomatal opening and their roles in overall and biochemical photosynthetic induction. *Trees* **31**: 1667-1681.

Wang, J., Nakazaki, T., Chen, S., Chen, W., Saito, H., Tsukiyama, T., Okumoto, Y., Xu, Z. & Tanisaka, T. 2009. Identification and characterization of the erect-pose panicle gene *EP* conferring high grain yield in rice (*Oryza sativa* L.). *Theoretical and Applied Genetics* **119**: 85-91.

Wang, L., Yang, Y., Zhang, S., Che, Z., Yuan, W. & Yu, D. 2020. GWAS reveals two novel loci for photosynthesis-related traits in soybean. *Molecular Genetics and Genomics* **295**: 705-716.

Wang, Y., Burgess, S.J., Becker, E.M. & Long, S.P. 2020. Photosynthesis in the fleeting shadows: an overlooked opportunity for increasing crop productivity? *The Plant Journal* **101**: 874-884.

Xiong, D., Douthe, C. & Flexas, J. 2018. Differential coordination of stomatal conductance, mesophyll conductance, and leaf hydraulic conductance in response to changing light across species. *Plant, Cell and Environment* **41**: 436-450.

Xiong, Z., Dun, Z., Wang, Y., Yang, D., Xiong, D., Cui, K., Peng, S. & Huang, J. 2022a. Effect of Stomatal Morphology on Leaf Photosynthetic Induction Under Fluctuating Light in Rice. *Frontiers in Plant Science* **12**: 754790.

Xiong, Z., Luo, Q., Xiong, D., Cui, K., Peng, S. & Huang, J. 2022b. Speed of light-induced stomatal movement is not correlated to initial or final stomatal conductance in rice. *Photosynthetica* **60**: 350-359.

Xue, S., Hu, H., Ries, A., Merilo, E. Kollist, H. & Schroeder, J.I. 2011. Central functions of bicarbonate in S-type anion channel activation and OST1 protein kinase in CO_2 signal transduction in guard cell. *The EMBO Journal* **30**: 1645-1658.

Yamori, W. 2016. Photosynthetic response to fluctuating environments and photoprotective strategies under abiotic stress. *Journal of Plant Research* **129**: 379-395.

Yamori, W., Kusumi, K., Iba, K. & Terashima, I. 2020. Increased stomatal conductance induces rapid changes to photosynthetic rate in response to naturally fluctuating light conditions in rice. *Plant, Cell and Environment* **43**: 1230-1240.

Yamori, W., Masumoto, C., Fukayama, H. & Makino, A. 2012. Rubisco activase is a key regulator of non-steady-state photosynthesis at any leaf temperature and, to a lesser extent, of steady-state photosynthesis at high temperature. *Plant Journal* **71**: 871-880.

Yang, W., Peng, S., Laza, R.C., Visperas, R.M. & Dionisio-Sese, M.L. 2007. Grain Yield and Yield Attributes of New Plant Type and Hybrid Rice. *Crop Science* **47**: 1393-1400.

Yano, K., Yamamoto, E., Aya, K., Takeuchi, H., Lo, P., Hu, L., Yamasaki, M., Yoshida, S., Kitano, H., Hirano, K. & Matsuoka, M. 2016. Genome-wide association study using whole-genome sequencing rapidly identifies new genes influencing agronomic traits in rice. *Nature Genetics* **48**: 927-934.

Yoshida, S. 1972. Physiological Aspects of Grain Yield. *Annual Review of Plant Physiology* **23**: 437-464.

Yuan, L. 2017. Progress in super-hybrid rice breeding. *The Crop Journal* **5**: 100-102.

Zhang, N., Berman, S.R., Joubert, D., Vialet-Chabrand, S., Marcelis, L.F.M. & Kaiser, E. 2022. Variation of Photosynthetic Induction in Major Horticultural Crops Is Mostly Driven by Differences in Stomatal Traits. *Frontiers in Plant Science* **13**: 860229.

Zhang, Q., Peng, S. & Li, Y. 2019. Increase rate of light-induced stomatal conductance is related to stomatal size in the genus *Oryza*. *Journal of Experimental Botany* **70**: 5259-5269.

Zhu, X.G., Long, S.P. & Ort, D.R. 2010. Improving Photosynthetic Efficiency for Greater Yield. *Annual Review of Plant Biology* **61**: 235-261.

Abbreviations

Symbol	Description	Unit
A	CO_2 assimilation rate	μmol CO_2 m^{-2} s^{-1}
A_0	A just before the transition from low to high light	μmol CO_2 m^{-2} s^{-1}
A^*	normalized A to a C_i of 300 μmol mol^{-1}	μmol CO_2 m^{-2} s^{-1}
A^X	absorbance of the solutions at X nm	
CCF_{10}	the cumulative CO_2 fixation during the first 10 minutes of the photosynthetic induction	mmol CO_2 m^{-2}
Chl a+b	chlorophyll contents per leaf area	g m^{-2}
C_i	intercellular CO_2 concentration	μmol mol^{-1}
CO_2R	reference CO_2 concentration in leaf chamber	μmol mol^{-1}
CWL_{10}	the cumulative water loss during the first 10 minutes of the photosynthetic induction	mol H_2O m^{-2}
DTH	days to heading after sowing	
E	exudation rate per plant	mg min^{-1}
E/*Root*	normalized *E* to root dry weight	mg min^{-1} g^{-1}
ETR	photosynthetic electron transport rate around photosystem II	μmol e^- m^{-2} s^{-1}
g_s	stomatal conductance	mol H_2O m^{-2} s^{-1}
$g_{s,dark}$	g_s under dark	mol H_2O m^{-2} s^{-1}
$g_{s,0}$	g_s just before the transition from low to high light	mol H_2O m^{-2} s^{-1}
GCL	guard cell length	μm
IND	*indica*	
J_{max}	maximum electron transport rate	μmol e^- m^{-2} s^{-1}
JRC	Rice Core Collection of Japanese Landraces	
K_{plant}	whole-plant hydraulic conductance	mmol H_2O m^{-2} s^{-1} MPa^{-1}
LNC	leaf nitrogen content per leaf area	g m^{-2}
LWP	leaf water potential	MPa

NPQ	non-photochemical quenching	
PPFD	photosynthetic photon flux density	μmol photons m^{-2} s^{-1}
R_d	dark respiration rate	μmol CO_2 m^{-2} s^{-1}
RH	relative humidity	%
Rubisco	ribulose 1,5-bisphosphate carboxylase/oxygenase	
SD	stomatal density	no. mm^{-2}
SDW	shoot dry weight	g $plant^{-1}$
T	transpiration rate	mmol H_2O m^{-2} s^{-1}
T_{air}	Air temperature in leaf chamber	°C
TEJ	*temperate japonica*	
TRJ	*tropical japonica*	
V_{Cmax}	maximum carboxylation rate of Rubisco	μmol CO_2 m^{-2} s^{-1}
WRC	World Rice Core Collection	
WUE	water use efficiency	μmol CO_2 $mmol^{-1}$ H_2O

List of Publications

(Chapter 2)

Taniyoshi, K., Tanaka, Y. & Shiraiwa, T. 2020. Genetic variation in the photosynthetic induction response in rice (*Oryza sativa* L.). *Plant Production Science* **23**: 513-521.

(Chapter 3)

Taniyoshi, K., Tanaka, Y., Adachi, S. & Shiraiwa, T. 2022. Anisohydric characteristics of a rice genotype 'ARC 11094' contribute to increased photosynthetic carbon fixation in response to high light. *Physiologia Plantarum* **174**: e13825.